ANALYSIS OF TUNNEL-DIODE RC-TRANSMISSION-LINE AMPLIFIERS

A THESIS

Presented to

The Faculty of the Graduate Division

by

Robert David Shults

In Partial Fulfillment

of the Requirements for the Degree

Doctor of Philosophy

in the School of Electrical Engineering

Georgia Institute of Technology

May, 1968

In presenting the dissertation as a partial fulfillment of the requirements for an advanced degree from the Georgia Institute of Technology, I agree that the Library of the Institute shall make it available for inspection and circulation in accordance with its regulations governing materials of this type. I agree that permission to copy from, or to publish from, this dissertation may be granted by the professor under whose direction it was written, or, in his absence, by the Dean of the Graduate Division when such copying or publication is solely for scholarly purposes and does not involve potential financial gain. It is understood that any copying from, or publication of, this dissertation which involves potential financial gain will not be allowed without written permission.

3/17/65
b

ANALYSIS OF TUNNEL-DIODE RC-TRANSMISSION-LINE AMPLIFIERS

Approved:

Dr. K. L. Su (Chairman)

Dr. B. O. Dasher

Dr. D. C. Ray

Date Approved by Chairman: May 17, 1968

DEDICATION

This thesis is dedicated to my mother and father, Eva K. and Wilbur D. Shults.

ACKNOWLEDGMENTS

I wish to express my sincere appreciation to my thesis advisor, Dr. Kendall L. Su, for his guidance, understanding, and encouragement during the course of this investigation. I also wish to thank Dr. B. J. Dasher and Dr. D. C. Ray for their constructive suggestions regarding the organization of the material and the preparation of this manuscript, and Dr. W. B. Jones, Jr. for his valuable assistance in the initial experimental work of this investigation.

Thanks are also due to the School of Electrical Engineering for continued research support, the Rich Electronic Computer Center for making available the computer time and facilities necessary for the solution of the problem, and to Scientific-Atlanta, Inc. for allowing me the time to complete the problem and for its aid in reproducing the manuscript.

Special thanks are due to my good friends Messrs. (and now Drs.) Clifford Guffee and John Scardina for their invaluable aid in the computer programming so vital to the completion of this investigation. Special thanks are also due to Miss Ina Sue Marlin for her endless patience and care in the typing of the manuscript.

Finally, I wish to express my appreciation to my wife, Maxine, for her patience, understanding, and encouragement, during the course of this investigation. To both my wife and my daughter, Stacey, I owe a great deal for the neglect and loss of "family fun" they have suffered during my tenure as a graduate student.

TABLE OF CONTENTS

TABLE OF CONTENTS (continued)

LIST OF ILLUSTRATIONS

LIST OF ILLUSTRATIONS (continued)

LIST OF ILLUSTRATIONS (continued)

LIST OF ILLUSTRATIONS (continued)

LIST OF ILLUSTRATIONS (continued)

LIST OF ILLUSTRATIONS (continued)

SUMMARY

It is the purpose of this thesis to develop an overall theory for and to demonstrate the feasibility of certain base-band negative-resistance amplifier configurations that utilize a single tunnel diode in conjunction with a uniformly distributed RC transmission line. The investigation is specifically oriented toward the integrated circuit morphologies, and the areas on which greatest attention is focused are the stability criteria for the amplifier configurations, the gain-bandwidth properties, and the techniques and considerations involved in their practical design together with experimental verification of the analytical results.

After a discussion of the two-port parameters and null properties of the transmission line, a choice is made for the two-port null network used throughout the remainder of the investigation. The Transmission, Series, and Reflection amplifiers are then defined as well as the insertion power gain (IPG) which is used to describe their performance.

The stability criteria of the amplifier configurations on both a static and dynamic (signal) basis are developed, and the relationship between the coupling mechanism and stability is discussed in detail. It is concluded that for the same degree of bias stability, a directly-coupled amplifier will exhibit higher gain for the signal components than a capacitance-coupled amplifier, and the gain exhibited by the directly-coupled amplifier will be maximum for the given degree of bias stability. For this reason, directly-coupled configurations are

employed throughout the investigation. The signal stability criteria are then established with the aid of a theorem due to Mitra, with the result that the bias and signal stability criteria are identical, and stabilizing the DC operating point completely stabilizes the circuit. In the study of the stability criteria a fundamental limitation of these negative-resistance amplifiers is found in that there is a trade-off between the conditions of high signal gain and high stability margin, where stability is taken to mean total (both static and signal) stability.

A description of the gain-bandwidth properties and design techniques associated with the various amplifiers is then given. It is shown that, theoretically, the gain-bandwidth product for these negative-resistance amplifiers can be made arbitrarily large, but this property is of limited practical value because of the gain-stability limitation discussed previously. A detailed proof of this property is given in an appendix.

In order to establish some techniques for designing these amplifiers an approximation for the half-power bandwidth is derived for each configuration. This approximate expression in each case is taken from a rational function, in the frequency variable s, that approximates the IPG-frequency response of the amplifier in the frequency range of interest. In addition, a definition of stability margin is made and related to the maximum possible gain for a given stability margin. The stability margin, Λ, is defined for each configuration by the relation

$$R_d = \left(1 + \frac{\Lambda}{100}\right) R_{eq} ,$$

where R_d is the diode resistance and R_{eq} is the equivalent DC resistance of the circuit external to the tunnel diode. The gain-stability limitations for the amplifier configurations are found to be

$$\text{Reflection:} \qquad \text{IPG}(0) \leq \left(\frac{100}{\Lambda} + 1\right)^2 ,$$

$$\text{Series:} \qquad \text{IPG}(0) \leq \left(\frac{100}{\Lambda}\right)^2 ,$$

and

$$\text{Transmission:} \qquad \text{IPG}(0) \leq \left(\frac{100}{\Lambda} + 1\right)^2 ,$$

where IPG(0) is the DC value of the insertion power gain. Thus, the results are that the Reflection and Transmission amplifiers have an identical gain-stability limitation, and it is less severe than that for the Series amplifiers.

For the Series and Transmission amplifiers (whose geometry permits a real-frequency transmission zero in the gain expression) a study was made of the rapidity of cutoff outside their passband and how this may be optimized. For the Series and Transmission configurations the cutoff properties are studied in terms of a frequency ratio defined as

$$\delta \triangleq \frac{f_{hp}}{f_{null}} ,$$

where f_{hp} is the half-power frequency, and f_{null} is the frequency of the transmission zero in the IPG-frequency response. With a frequency ratio of unity defined as the ideal case, a least upper bound is found

for each of these configurations to be

Series: $\quad 1.\ u.\ b.\ [\delta] = 0.07368\ ,$

and

Transmission: $\quad 1.\ u.\ b.\ [\delta] = 0.19458\ .$

Thus, it is found that the Transmission configurations can be made to exhibit the most rapid cutoff above the half-power frequency.

Design considerations are made for each amplifier configuration included in the investigation, and examples are worked out in order to provide experimental verification of the analytical results.

CHAPTER I

INTRODUCTION

Motivation of the Problem

In recent years many authors have been concerned with the theory and development of tunnel diode negative-resistance amplifiers. In general, most of the research to date has dealt with amplifiers employing lossless coupling networks, and these amplifiers have been either base-band (low-pass) or tuned, depending on the type and design of the coupling network.

At the same time the advances and developments made in the space technologies, integrated circuits, and related fields have caused the network designer to search for new and better methods of reducing the physical size of components and networks. In addition to exploiting new devices which show the possibility of performing some well-established function or of being employed in some innovation, the objectives of microminiature network techniques are to lower cost, increase performance and reliability, and to reduce the overall network size by orders of magnitude. One possibility of achieving these goals lies in the use of distributed-parameter circuitry composed of three or more homogeneous layers. Circuits of this type are simple to fabricate, can be made very small, and are easy to integrate with transistor circuits. As pointed out by Kaufman, the development of a distributed-parameter null device to replace the twin-T network grew out of a desire to create a tuned

amplifier in the form of a semiconductor monolith [1]. Kaufman further noted that circuits of this type, being fabricated of semiconductor materials, are physically simple thus giving rise to greater reliability. They are well suited to integrated solid-state systems and can be made very small. He cites an example of prototypes operating with null frequencies in the vicinity of 1 MHz with overall dimensions of 0.09 inch by 0.04 inch by 0.003 inch.

One of the most easily constructed distributed-parameter networks is the RC transmission line. This line may be fabricated so that its parameters are uniform, vary linearly, exponentially, trigonometrically, or hyperbolically. Su has recently investigated the properties of trigonometric and hyperbolic RC transmission lines [2], [3], and Googe has investigated the properties of the five-layered, or Double-Kelvin, line [4]. The uniform line was the earliest to be investigated and its properties are well known. Depending on its orientation as a two-port, the uniform line offers an open-circuit voltage transfer ratio whose frequency response may be base-band, high-pass, or constant. In addition, external elements may be employed so that the overall $-y_{12}(j\omega)$ or $z_{12}(j\omega)$ of the two-port may be controlled in a manner such that the voltage transfer ratio frequency response will exhibit a null at certain frequencies.

The versatility of even the simple uniform RC line and the proven performance of tunnel diodes in various types of negative-resistance amplifiers suggest that the two might be combined to form a new class of negative-resistance amplifiers in which the coupling networks are not lossless but which would be practically feasible and would find

engineering applications. It should be pointed out that the tunnel diode, due to its two-terminal simplicity, is a logical first choice for the negative-resistance device, but the results of this work could be extended in the main to cover amplifiers of this type that employ other negative-resistance devices of perhaps wider dynamic range or greater power level capability. If the device or circuit used to produce the negative resistance is voltage-controlled, then its incremental signal model will be of the same general form as that of the tunnel diode, and (except for perhaps some practical details of biasing) the work that follows could be used to describe the overall behavior of an amplifier using such a device. In addition, further motivation is provided by the fact that the analysis that follows involves the combination of distributed-parameter and lumped-constant components, and it is hoped that the techniques developed herein to cope with this situation will serve as a starting point for future investigations in which the transmission line may possess one of the more exotic tapers mentioned above.

Definition of the Problem

The purpose of this thesis is to investigate the overall theory of certain base-band negative-resistance amplifier configurations that utilize a single tunnel diode in conjunction with a uniformly distributed RC transmission line. The investigation is specifically oriented toward the integrated circuit morphologies, and the areas on which greatest attention is focused are the stability criterion for any given amplifier configuration, the gain-bandwidth properties, and the design techniques involved in shaping the insertion-power-gain frequency response together with experimental verification of the analytical results.

CHAPTER II

BASIC PRACTICAL AND THEORETICAL CONSIDERATIONS

Basic Properties of the Transmission Line

Before considering an amplifier configuration in any detail, it is convenient to note some of the basic properties of the uniform RC line and discuss the practical details of its fabrication.

In practice, with proper deposition equipment, the uniform line may be fabricated in miniature form by depositing films of conductive, dielectric, and resistive materials on a nonconducting supporting substrate. Such a fabrication is shown in Figure 2.1.

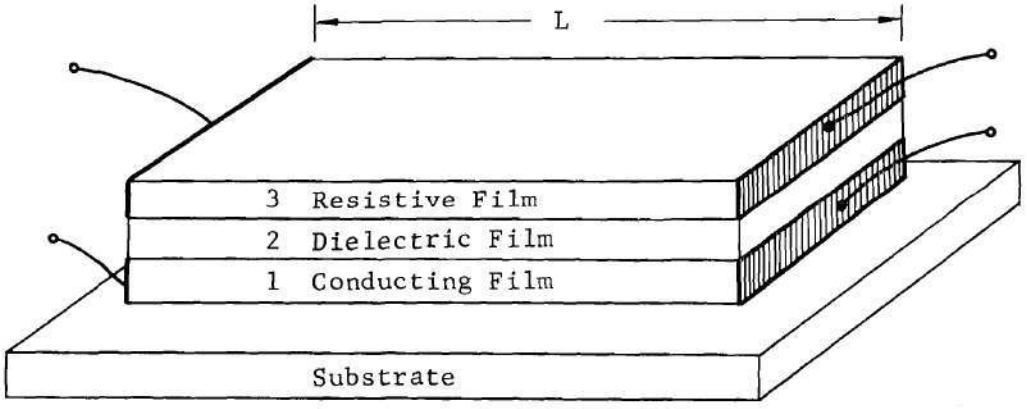

Film Fabrication of Uniform RC Lines.

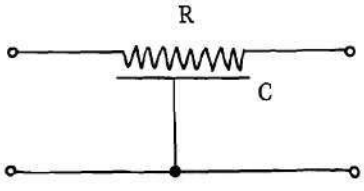

Two-Port Circuit Symbol.

$$r = \frac{\text{resistance}}{\text{unit length}} = \frac{R}{L}$$

$$c = \frac{\text{capacitance}}{\text{unit length}} = \frac{C}{L}$$

Figure 2.1 The Uniform RC Transmission Line.

Various materials may be used in the film fabrication of the uniform line. A typical example might be: Stratum 1 is a near-ideal conducting film of aluminum, Stratum 2 is a dielectric film of silicon monoxide, and the final Stratum 3 is the resistive film of nichrome. The input and output terminals are attached to Strata 1 and 3 with low-temperature indium solder. Typical parameter values with this type of construction are on the order of 50.0 ohms per square and 0.080 micro-farads per square inch, and the film fabrication of the uniform line, with the proper equipment, can be achieved very simply with high reliability and very small physical size.

In the absence of film deposition equipment it is possible to model the uniform line on an expanded scale so that prototypes may be constructed for experimental work. One method of doing this is shown in Figure 2.2.

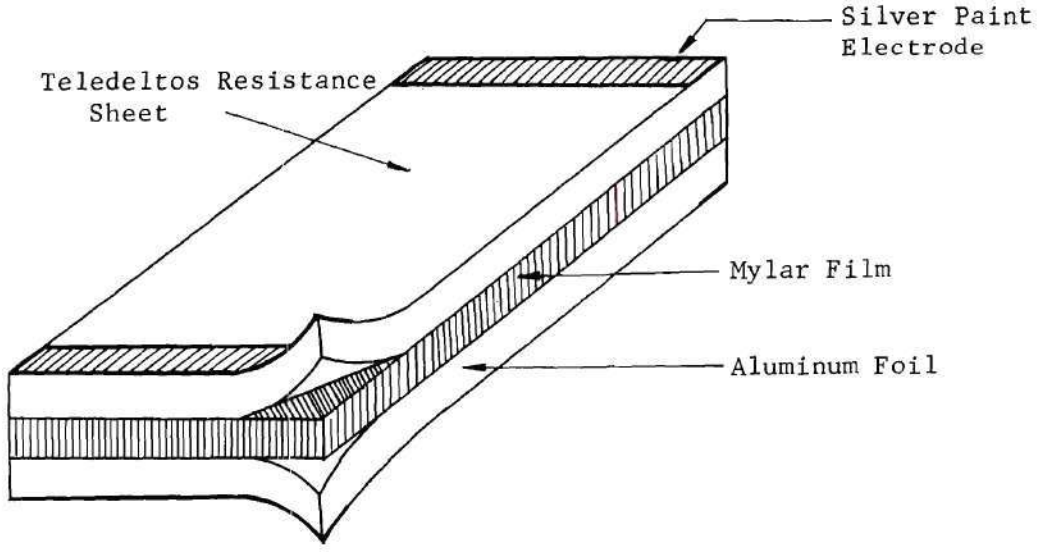

Figure 2.2 Teledeltos-Mylar Model of Uniform Line.

The Teledeltos-Mylar model is constructed by sandwiching layers of Teledeltos resistance paper, Mylar film, and aluminum or copper foil, with polystyrene cement as the bonding agent. This type of model, although usually much larger in physical size than the film fabrication, has the same type of terminal characteristics and is very simple to construct. Typical parameter values achieved in this manner are 2000 ohms per square and 300 picofarads per square inch. Since the resistance per square is fixed by the resistive coefficient of the Teledeltos paper, this type of model has a limitation in the range of RC products which can be achieved.

Another method of modeling the uniform line, the one used in the experimental work of this thesis, is similar to the Teledeltos-Mylar model. The resistance paper is replaced by a layer of conducting radio-frequency shielding paint. Depending on the spraying density, the resistive coefficient of this layer may be adjusted to values as low as 2.0 ohms per square and as high as that of the Teledeltos paper. In addition to this increased range in the resistive coefficient, another advantage of this model is that the bond between the sprayed-on resistive layer and the Mylar is much better than that of the Teledeltos model with a consequent increase in the capacitance and decrease in overall size. A typical value of the capacitance achievable is 0.005 microfarads per square inch. The range of RC products obtainable with this model makes it more useful than the Teledeltos-Mylar model.

The open-circuit impedance parameters of the uniform line when viewed as a two-port network are

$$z_{11} = z_{22} = \frac{r \coth\sqrt{srcL^2}}{\sqrt{src}} , \tag{2.1}$$

and

$$z_{12} = z_{21} = \frac{r \operatorname{csch}\sqrt{srcL^2}}{\sqrt{src}} , \tag{2.2}$$

where r and c are the resistance and capacitance per unit length, as shown in Figure 2.1, L is the length of the line, and s is the complex frequency variable, $\sigma + j\omega$. Since R = rL and C = cL, equations (2.1) and (2.2) may be rewritten as

$$z_{11} = z_{22} = \frac{R}{(a\sqrt{s})} \cdot \coth(a\sqrt{s}) , \tag{2.3}$$

and

$$z_{12} = z_{21} = \frac{R}{(a\sqrt{s})} \cdot \frac{1}{\sinh(a\sqrt{s})} , \tag{2.4}$$

where

$$a = \sqrt{RC} , \tag{2.5}$$

and R and C represent the total resistance and capacitance of the transmission line.

The transformation from open-circuit impedance parameters to short-circuit admittance parameters yields

$$y_{11} = y_{22} = \frac{(a\sqrt{s})}{R} \cdot \coth(a\sqrt{s}) , \tag{2.6}$$

and

$$y_{12} = y_{21} = -\frac{(a\sqrt{s})}{R} \cdot \operatorname{csch}(a\sqrt{s}) . \tag{2.7}$$

Since the RC line is a reciprocal device (i.e., $z_{12} = z_{21}$ and $y_{12} = y_{21}$) it may be represented, as shown in Figure 2.3, with the simple Tee and Pi networks of classical two-port theory.

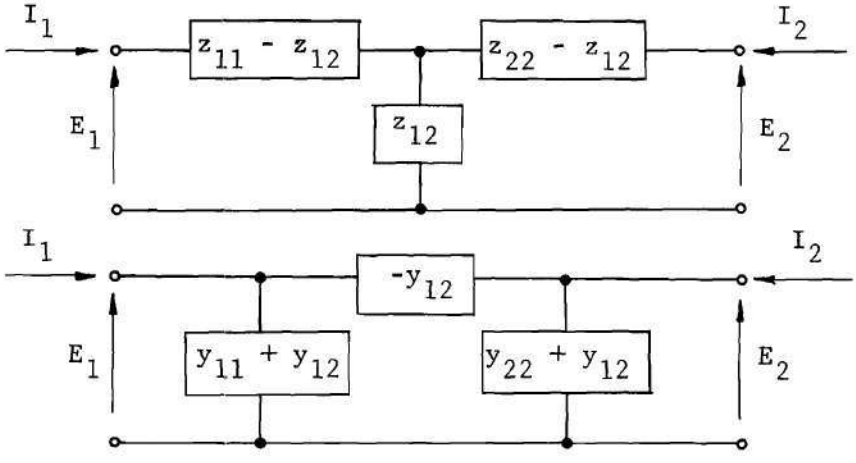

Figure 2.3 Two-Port Models of the Uniform RC Line.

The open-circuit voltage transfer ratio of the line is then

$$T_{oc}(s) = \left.\frac{E_2}{E_1}\right|_{I_2=0} = \frac{z_{12}}{z_{11}} = \frac{-y_{12}}{y_{11}} = \frac{1}{\cosh(a\sqrt{s})} . \tag{2.8}$$

The magnitude-frequency response of this transfer ratio for $s = j\omega$ is shown in Figure 2.4 and is of the base-band or low-pass type.

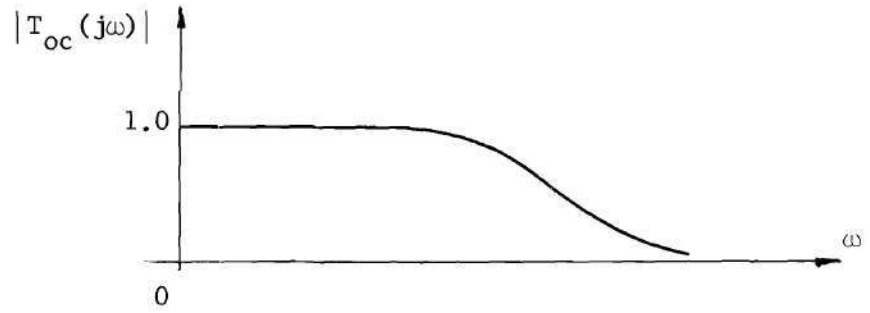

Figure 2.4 Open-Circuit Voltage Transfer Frequency Response of the Uniform RC Line.

The voltage transfer ratio can be made to exhibit real-frequency transmission zeros through the use of externally connected elements. This can be shown by investigating $z_{12}(j\omega)$ and $-y_{12}(j\omega)$ of the two-port. The polar plots of $z_{12}(j\omega)$ and $-y_{12}(j\omega)$ are shown in Figure 2.5.

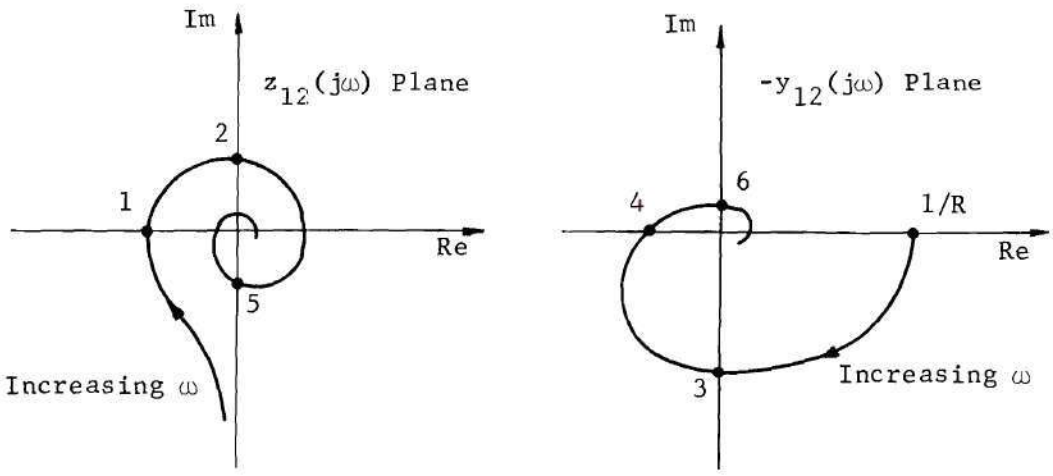

Figure 2.5 Polar Plots of $z_{12}(j\omega)$ and $-y_{12}(j\omega)$ for the Uniform RC Transmission Line Two-Port.

The polar behavior of $z_{12}(j\omega)$ shows that a transmission zero can be produced by connecting an external element in series with the two-port. In particular, a positive resistance of the proper value will produce a transmission zero at a frequency where $z_{12}(j\omega)$ is purely real and negative, such as point 1 in Figure 2.5. Likewise, a capacitor of the proper value connected in series with the two-port will produce a transmission zero at a frequency where $z_{12}(j\omega)$ is purely imaginary and positive, such as point 2 in Figure 2.5. Consideration of the polar behavior of $-y_{12}(j\omega)$ shows that real-frequency transmission zeros may be produced by connecting an external element in parallel with the two-port. A capacitor of the proper value will produce a transmission zero at a frequency where $-y_{12}(j\omega)$ is purely imaginary and negative, such as point 3 in Figure 2.5. Likewise, a positive conductance of the proper value connected in parallel with the two-port will produce a transmission zero at a frequency where $-y_{12}(j\omega)$ is purely real and negative, such as point 4 in Figure 2.5.

In any case, only elements of positive resistance (conductance) or capacitance will be considered for producing real-frequency transmission zeros. Even though it is theoretically possible to produce real-frequency transmission zeros with a series-connected or parallel-connected inductor, this method is impractical since inductance is very difficult to achieve with the present thin-film technology. In addition, the values of ω for which an inductor may be used, such as points 5 and 6 in Figure 2.5, are so high that the amplitude of the response is well below the dynamic range of interest, and a transmission zero at these frequencies would be of little practical value in shaping the frequency response.

For these reasons, inductors as null-producing elements are not considered.

In light of the foregoing discussion, any one of the two-port networks shown in Figure 2.6 will possess a voltage transfer frequency response that displays a null at some real frequency ω_n.

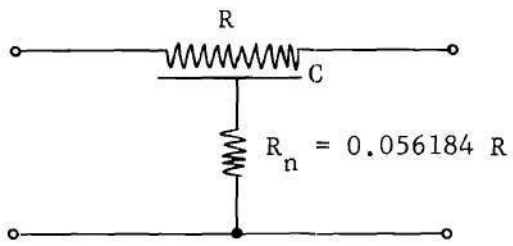

$$f_n = \frac{\omega_n}{2\pi} = \frac{1.78040}{RC}$$

(a) Series-R Nulling.

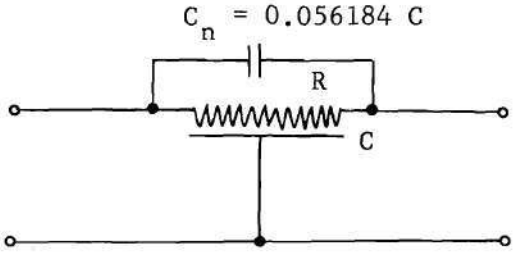

$$f_n = \frac{\omega_n}{2\pi} = \frac{1.78040}{RC}$$

(b) Parallel-C Nulling.

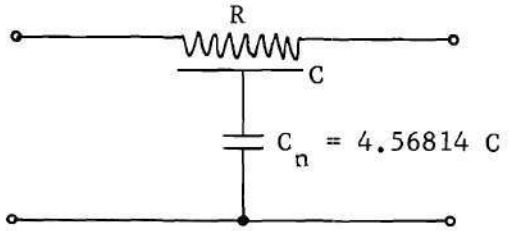

$$f_n = \frac{\omega_n}{2\pi} = \frac{4.90775}{RC}$$

(c) Series-C Nulling.

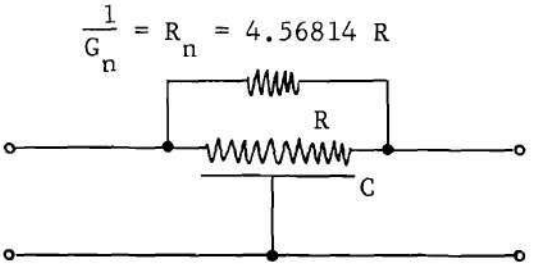

$$f_n = \frac{\omega_n}{2\pi} = \frac{4.90775}{RC}$$

(d) Parallel-R Nulling.

Figure 2.6 RC Transmission Line Two-Ports with External Null-Producing Elements.

In a practical case, the chosen coupling network will be doubly-terminated. That is, it will be inserted between a non-ideal source and a finite load resistance. In addition to the effects of the source and

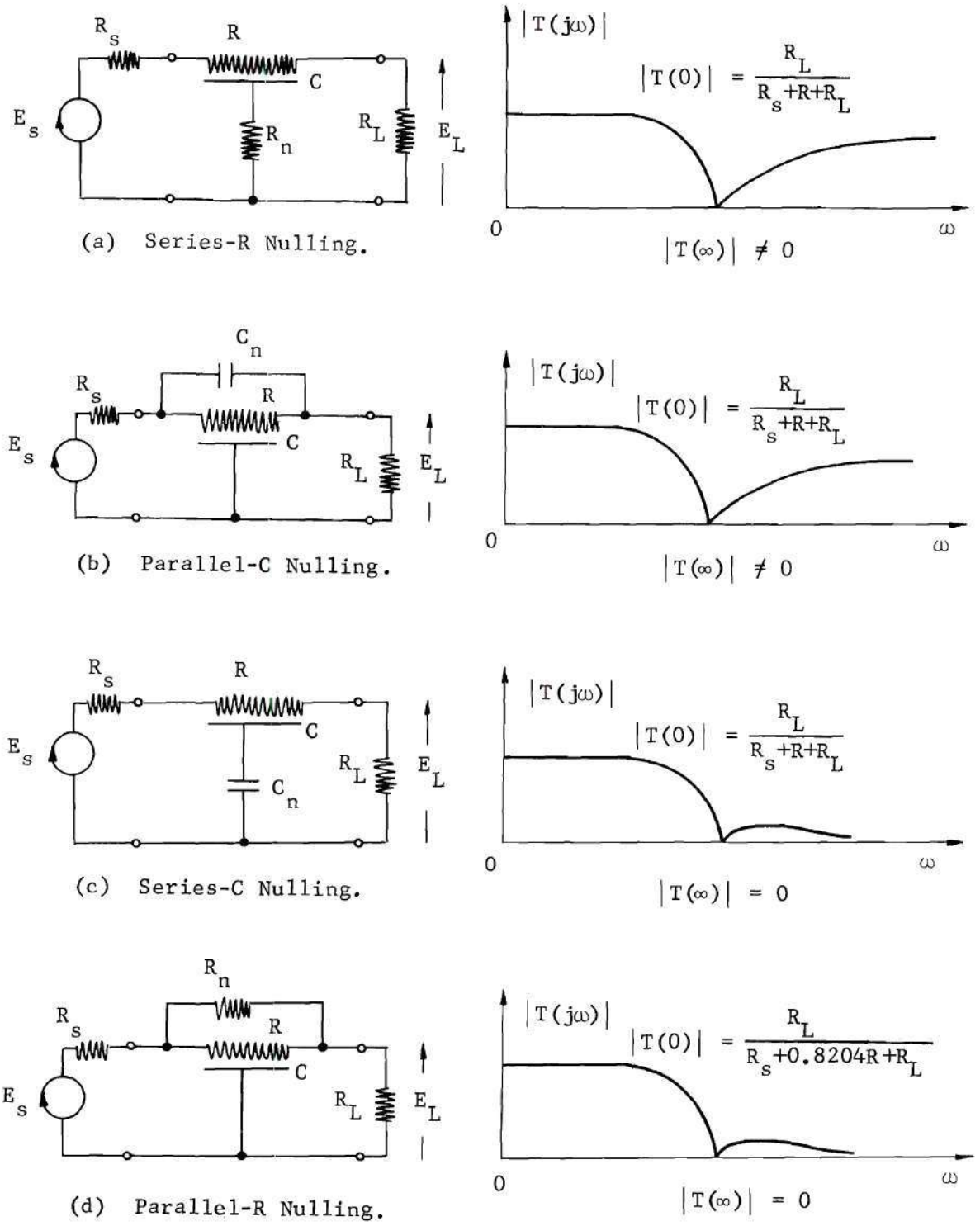

(a) Series-R Nulling.

(b) Parallel-C Nulling.

(c) Series-C Nulling.

(d) Parallel-R Nulling.

Figure 2.7 Doubly-Terminated Coupling Networks and Typical Overall Voltage Transfer Response Curves.

load resistances, the externally connected null-producing element will also affect the overall voltage transfer response. Figure 2.7 shows the four coupling networks in the doubly-terminated case. The overall voltage transfer function is now

$$T(j\omega) \triangleq \left.\frac{E_L}{E_s}\right|_{s=j\omega} . \qquad (2.9)$$

In the first case, that of series-R nulling, the DC value of $|T(j\omega)|$ is no longer unity. As $\omega \to 0$, the capacitance of the line is effectively open-circuited, and the circuit reduces to a simple series connection of the resistors R_s, R, and R_L. The DC value of $|T(j\omega)|$ is then found by simple voltage division to be

$$|T(0)| = \frac{R_L}{R_s+R+R_L} < 1 . \qquad (2.10)$$

In addition to this reduced low-frequency value, the overall response is altered at high frequencies since R_n and R are effectively in parallel, and the response no longer approaches a zero asymptote. Since the main interest of this investigation is in directly-coupled base-band amplifier configurations, the doubly-terminated coupling network with series-R nulling must be eliminated as a possible choice.

The second case, that of parallel-C nulling, has the same low-frequency response value as the first, and because of the capacitive voltage divider effect of C_n and C the response at high frequencies again approaches a non-zero value. The high-frequency response of this circuit also eliminates it from further consideration.

The third and fourth cases, those of series-C and parallel-R nulling respectively, both have capacitive paths shunting the load at high frequencies, and the response approaches zero with increasing frequency. Theoretically at least, both could be used in conjunction with a tunnel diode to form a directly-coupled base-band amplifier. Certain practical considerations, however, rule in favor of one over the other. First of all, the DC response of the circuit with parallel-R nulling will be higher than that utilizing series-C nulling. This is because at DC the resistor R_n appears directly in parallel with the line resistance R, and the equivalent resistance of the parallel combination is

$$R_p = \frac{R_n R}{R_n + R} = \frac{(4.56814R)R}{5.56814R} = 0.8204\ R \qquad (2.11)$$

The low-frequency value of the transfer ratio is then

$$|T(0)| = \frac{R_L}{R_s + 0.8204R + R_L} > \frac{R_L}{R_s + R + R_L}\ , \qquad (2.12)$$

and the response at low frequencies will be the higher of the two. In addition, the physical layout of the circuit using series-C nulling is more cumbersome and more prone to involve parasitic elements than the two-port employing parallel-R nulling. This is recognized from the fact that the model transmission lines used are on the order of one foot square and will therefore require standoff insulators to isolate the conducting layer (a copper sheet) from the chassis so that between the two the nulling element C_n may be connected. If the conducting plate of the transmission line is physically separated from the chassis, then the effective flux linkage areas of the two meshes of the network

are increased, and this physical realization will have more parasitic inductance in both the input and output meshes than the circuit using parallel-R nulling. If parallel-R nulling is used, the conducting plate of the model transmission line is bolted directly to the chassis so that there is a common ground both physically and electrically, the construction is simpler, and the parasitic inductance introduced in the input and output meshes is held to a minimum. For these reasons, the coupling network utilizing parallel-R nulling was chosen for the amplifier configurations investigated in this thesis.

The Amplifier Configurations

Now that a choice has been made for the prototype coupling circuit, we are in a position to consider the specific amplifier configurations which are investigated in the work that follows. In order to negate some of the losses in the doubly-terminated circuit, a tunnel diode is imbedded in the network so that the overall network will have a gain greater than unity and thereby become a useful amplifier. The position in which the tunnel diode is placed defines the type of amplifier.

A Transmission Amplifier is defined as one in which a source and load terminate opposite ports of a reciprocal two-port network with a tunnel diode, suitably biased in the negative-resistance region, placed across one of these ports [5]. This type of amplifier is shown in Figure 2.8 The configuration with the tunnel diode across the input port will be designated as the Transmission I amplifier, and it will be designated as the Transmission II amplifier when the tunnel diode is placed across the output port.

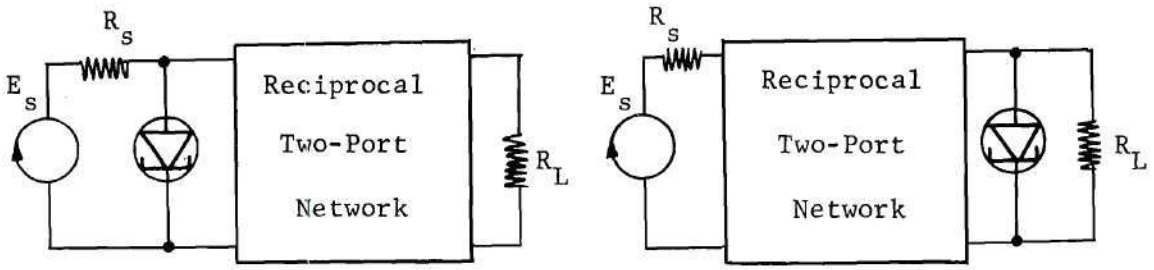

Transmission I Amplifier. Transmission II Amplifier.

Figure 2.8 Transmission Amplifier Configurations.

For the work at hand each reciprocal two-port network indicated in Figure 2.8 is the RC transmission line with a parallel-R nulling element as shown in Figure 2.7(d). The complete amplifiers, including bias supplies, are shown in Figure 2.9.

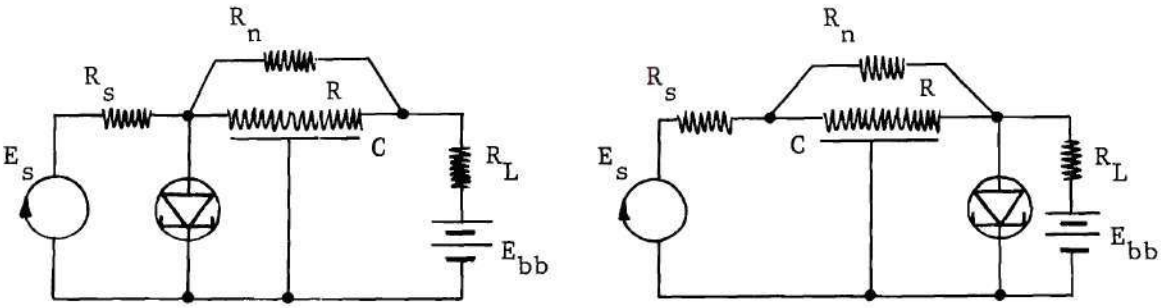

Transmission I Amplifier. Transmission II Amplifier.

Figure 2.9 Transmission Amplifiers Utilizing the Uniform RC Line and Parallel-R Nulling Element.

A Series Amplifier is defined here as one in which a source and load terminate opposite ports of a reciprocal two-port network but with the tunnel diode inserted in series with the top lead of the two-port either between the source and the two-port or between the two-port and

the load. This type of amplifier is shown in Figure 2.10. The configuration with the diode between source and two-port will be designated as the Series I amplifier, and it will be designated as the Series II amplifier when the tunnel diode is placed between the two-port and the load. The complete amplifiers, including bias supplies, are then as shown in Figure 2.11.

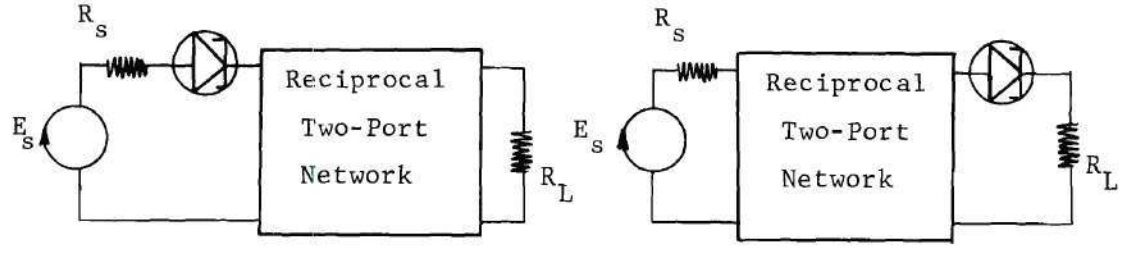

Series I Amplifier. Series II Amplifier.

Figure 2.10 Series Amplifier Configurations.

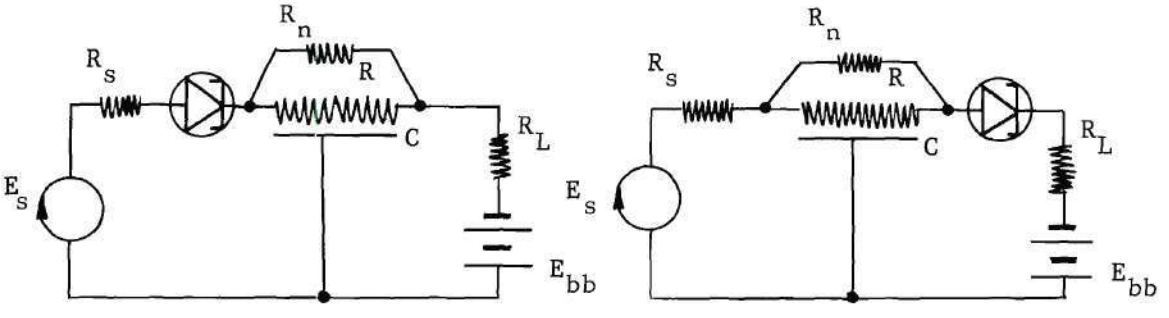

Series I Amplifier. Series II Amplifier.

Figure 2.11 Series Amplifiers Utilizing the Uniform RC Line and Parallel-R Nulling Element.

A Reflection Amplifier is defined here as one in which a source and load terminate the same port of a reciprocal two-port network and a tunnel diode, suitably biased in the negative-resistance region, terminates the other port. This type of amplifier is shown in Figure 2.12. The complete amplifier, including the bias supply, is shown in Figure 2.13.*

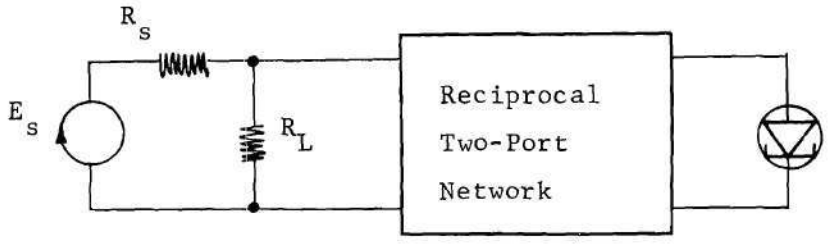

Figure 2.12 The Reflection Amplifier Configuration.

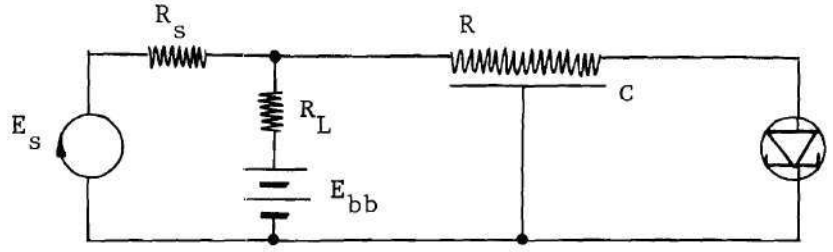

Figure 2.13 The Reflection Amplifier Utilizing the Uniform RC Transmission Line.

---

* The geometry of the Reflection amplifier prevents the production of real-frequency transmission zeros through the use of a single external element, hence the absence of R_n in Figure 2.13.

The gain function employed in this study is the insertion power gain (IPG) which is defined in Figure 2.14.

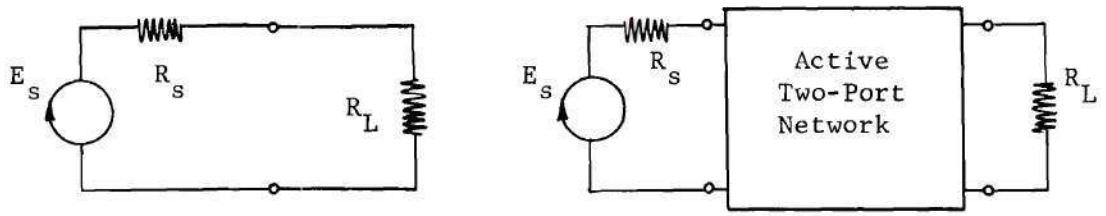

(a) Source connected directly to load. (Power to load = P_{LO}.)

(b) Active two-port inserted between source and load. (Power to load = P_{LA}.)

$$\text{IPG} = \begin{pmatrix}\text{Insertion}\\ \text{Power}\\ \text{Gain}\end{pmatrix} \triangleq \frac{\begin{pmatrix}\text{Power delivered to the load}\\ \text{with active two-port in place.}\end{pmatrix}}{\begin{pmatrix}\text{Power delivered to the load when}\\ \text{connected directly to source.}\end{pmatrix}} = \frac{P_{LA}}{P_{LO}}$$

Figure 2.14 Definition of the Insertion Power Gain (IPG).

There are other definitions of power gain which are in common use. They usually depend on some degree of impedance matching between source and load. In practice, however, it is more common to be faced with the problem of providing gain between a source and load of fixed impedances, and the definition given above is the most useful in this case since it provides a measure of the effectiveness of the active two-port that is inserted between the source and load.

The IPG for the general amplifier shown in Figure 2.14(b) is

$$\text{IPG} = (R_s+R_L)^2 \left| \frac{-y_{12N}}{R_s R_L |y|_N + R_s y_{11N} + R_L y_{22N} + 1} \right|^2_{s=j\omega}, \qquad (2.13)$$

where y_{11N}, y_{12N}, y_{22N}, and $|y|_N$ are the overall y-parameters and system determinant of the active coupling network.

Taking the Transmission I amplifier, for example, the y-parameters of the active two-port coupling network are

$$y_{11N} = Y_d + (y_{11}+G_n) \quad , \tag{2.14}$$

$$-y_{12N} = -y_{12} + G_n \quad , \tag{2.15}$$

$$y_{22N} = y_{11} + G_n \quad , \tag{2.16}$$

and

$$|y|_N = y_{11N}y_{22N} - y_{12N}^2$$

$$= [Y_d + (y_{11}+G_n)] \cdot (y_{11}+G_n) - (y_{12}-G_n)^2, \tag{2.17}$$

where y_{11} and y_{12} are y-parameters of the RC line alone, Y_d is the admittance of the tunnel diode, and $G_n = 1/R_n$ is the conductance of the null-producing element.

With proper adjustment of the circuit parameters the IPG-frequency response has the general form shown in Figure 2.15. Adjustment of $-y_{12N}$ through the use of the null-producing conductance G_n produces a null in the response at ω_n near the band edge, and the gain in the pass band is greater than unity.

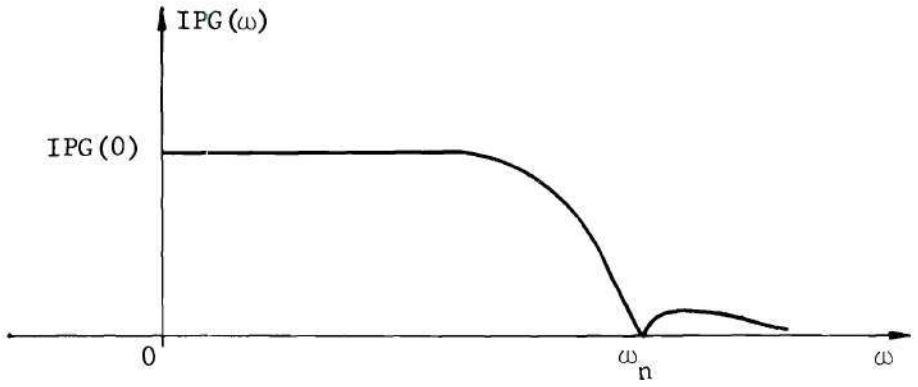

Figure 2.15 General IPG-Frequency Response of the Transmission I Amplifier.

The low-frequency value of the IPG can be found by taking the limit of equation (2.13) as ω approaches zero, or it may be found from a low-frequency equivalent circuit of the Transmission I amplifier. The low-frequency gain is found to be

$$IPG(0) = (R_s+R_L)^2 \left| \frac{1}{R_s R_L(-G_d) + R_s(1-R_p G_d) + R_L + R_p} \right|^2, \qquad (2.18)$$

where $-G_d$ is the negative conductance of the tunnel diode, and R_p is the parallel combination of the line resistance R and the null-producing resistance R_n. Equation (2.18) shows that, theoretically at least, the IPG may be made very large in the pass band.

In order to illustrate more clearly the amplifying mechanism in the frequency range of the pass band, it is useful to resort to the low-frequency equivalent circuit of the amplifier and the technique of load-line analysis. The low-frequency equivalent circuit of the Transmission I amplifier for zero-signal condition is shown in Figure 2.16.

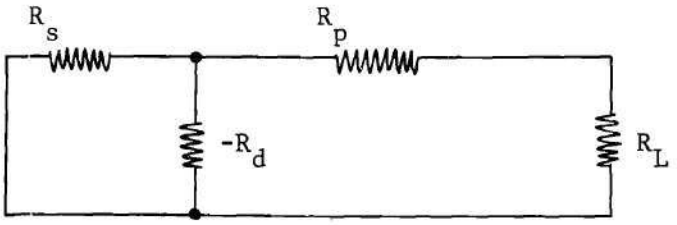

Figure 2.16 Low-Frequency Equivalent Circuit of the Transmission I Amplifier Under No-Signal Condition.

The equivalent resistance of the circuit external to the diode is

$$R_{eq} = \frac{R_s(R_p + R_L)}{R_s + R_p + R_L} . \qquad (2.19)$$

The volt-ampere characteristic of the tunnel diode is shown in Figure 2.17. The slope of the characteristic in the linear region is $-G_d = -1/R_d$. Superimposed on the characteristic is the dynamic load line of slope $-1/R_{eq}$. (It is assumed that the circuit is biased properly so that the load-line intersects the diode characteristic in the negative-resistance region as shown).

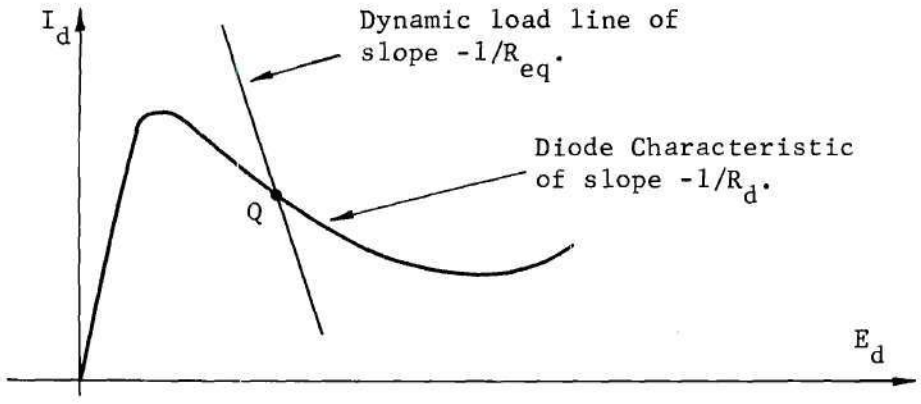

Figure 2.17 Load-Line Analysis of Transmission I Amplifier.

In light of equation (2.19), equation (2.18) may be cast in the form

$$IPG(0) = (R_s+R_L)^2 \left| \frac{R_d}{(R_s+R_p+R_L)(R_d-R_{eq})} \right|^2 . \qquad (2.20)$$

Now, considering the slope of the dynamic load line and the form of equation (2.20), it is apparent that as R_{eq} approaches R_d in value (i.e., as the slope of the dynamic load line approaches that of the diode characteristic) the insertion power gain can assume very large values. This point of view will be useful in the next two chapters where the stability criteria and gain-bandwidth properties are discussed.

It should be noted that all of the practical amplifier configurations shown in Figures 2.9, 2.11, and 2.13 are directly-coupled, and the DC bias circuit is not isolated from the signal circuit in any of these configurations. There are several reasons for this. These reasons are now presented.

One method of isolating the bias and signal circuits employs inductors that act as radio-frequency chokes to the signal components but act as short circuits to the DC bias voltages and currents. It should be noted, however, that the object here is to realize strictly RC amplifier configurations in order to take advantage of the microminiature integrated circuit technology (where inductance is very difficult to achieve). In addition to this is the fact that if the circuits are free of inductance, the stability problem is simplified a great deal, and the resulting stability criteria are very simple and easy to meet. For these reasons inductors as isolating elements are ruled out of consideration.

Another standard technique for isolating the bias and signal circuits lies in the use of capacitance coupling. Here, the signal components are coupled into and out of the circuit through capacitors that act as short circuits to the signal components but act as open circuits to the DC bias currents and voltages. The absence of inductance eliminates the possibility of tuned tank circuits, and in this case it can be shown that the signal gain of a capacitance-coupled circuit will always be less than that of a directly-coupled circuit. In addition, the low-frequency response of the capacitance-coupled circuits is degraded while the directly-coupled circuits possess a response that is flat down to zero frequency. For these reasons capacitance coupling is also ruled out of consideration, and all the amplifiers to be investigated are directly-coupled.

The type of coupling to be used is intimately related to the problem of circuit stability, and the supporting details of the arguments presented above will be given in the next chapter where the stability criteria are developed.

CHAPTER III

THE STABILITY CRITERIA

Basic Assumptions

An important question to be answered regarding any amplifier configuration that utilizes a negative-resistance device is whether or not the circuit can be made stable. The practical and theoretical aspects of this facet of the investigation are dealt with in this chapter.

Incremental signal models of the tunnel diode are shown below in Figure 3.1. The ohmic losses in the leads and semiconductor material are represented by the series resistance R_s, and the parasitic inductance of the leads by the series inductance L_s. The junction capacitance

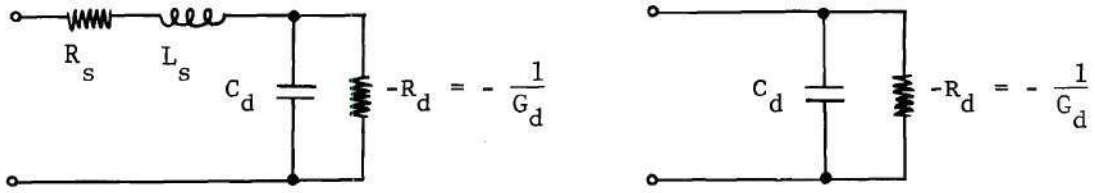

(a) Model containing ohmic losses (R_s) and parasitic lead inductance (L_s).

(b) Model with negligible ohmic losses and parasitic lead inductance.

Figure 3.1 Incremental Signal Models of the Tunnel Diode.

of the diode is represented by the shunt capacitance C_d, and the dynamic negative resistance is represented by the shunt resistance of value $-R_d$. The complete incremental signal model is as shown in Figure 3.1(a).

With the continuing advances being made in the semiconductor technology and packaging techniques, however, the series resistance and inductance can be made very small to the point of becoming negligible for most purposes. This is especially true in the case of the microminature diodes which would be used in the integrated versions of the amplifiers under investigation. A distinct advantage of microminiaturization is that parasitic elements are also reduced in size and effect. In the work that follows, the series resistance and inductance are assumed negligible, and the incremental model of the tunnel diode is taken to be that shown in Figure 3.1(b).

Another assumption of practical importance is that the parasitic inductance of the circuit layout is negligible. This point was raised earlier in Chapter II with the choice of the transmission line coupling network to be used. It should be stressed that any practical layout of the amplifiers considered here must be made with this point in mind. An effort must be made to eliminate, as far as possible, any stray inductance that might be present in the circuits. As stated before, the object here is to make the overall circuits strictly RC. This not only takes advantage of the integrated circuit technology, but it will allow the use of a theorem due to Mitra concerning the pole-zero properties of a strictly RC network containing a single tunnel diode [6]. Mitra's theorem is the heart of the technique used here to investigate the signal stability of the proposed amplifier configurations, and it is very important that the conditions allowing its use be approached as closely as is practically possible. Again, it should be noted that with thin-film microminiature fabrication, the networks <u>will</u> be almost ideally RC,

and the conditions allowing the use of Mitra's theorem will be approached even more closely than is possible with the expanded scale prototypes used in the experimental work of this investigation. At any rate, a stability criterion is only as good as its practical application. If, after taking the needed precautions in the physical layout of a circuit, a proposed stability criterion fails, then it is the task of the investigator to revise the incremental signal model of the circuit in such a way as to arrive at a practical working solution. Since the experimental work of this investigation bears out the validity of the stability criteria established here, the assumption of negligible stray inductance is considered a reasonable one with the comforting thought that it is even more accurate in the case of thin-film microminiature construction.

Bias Point Stability and Coupling Considerations

The first part of the stability criterion concerns the DC operating point, or bias point, of the tunnel diode. This aspect of the stability problem is discussed in terms of the Transmission I amplifier in Figure 3.2. The DC equivalent circuit for the Transmission I amplifier is shown in Figure 3.3.

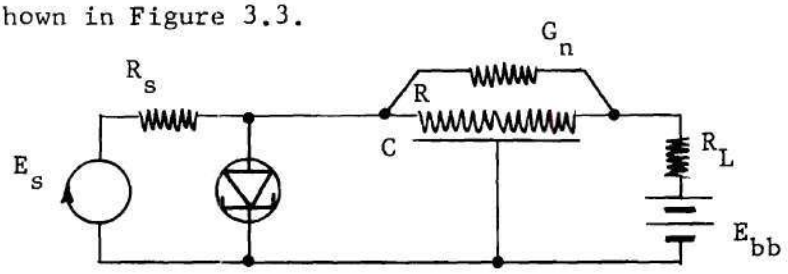

Figure 3.2 Transmission I Amplifier.

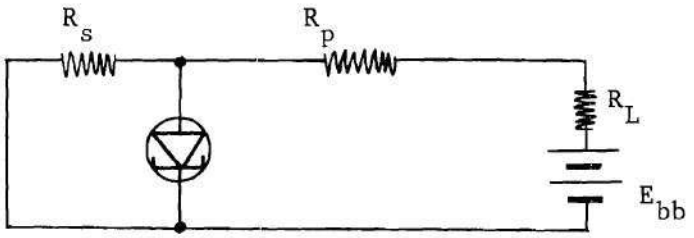

$$R_p \triangleq \frac{R_n R}{R_n + R}$$

Figure 3.3 DC Equivalent Circuit of the Transmission I Amplifier.

The static volt-ampere characteristic of the tunnel diode with a superimposed DC (or static) load line is shown in Figure 3.4.

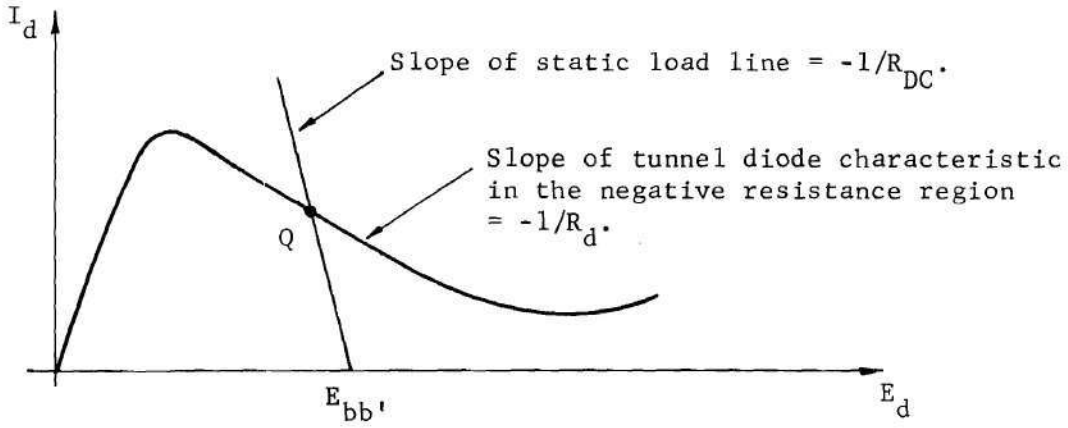

Figure 3.4 Static Load-Line Analysis.

For a stable bias point, the slope of the static load line must be such that it intersects the tunnel diode characteristic at only one point. The static load line is given by the linear volt-ampere relationship at the terminals of a DC Thevenin equivalent circuit taken with respect to the diode. For a single intersection of the static load line with the diode characteristic in the negative-resistance region E_{bb} (and hence the Thevenin voltage E_{bb}') must be adjusted properly, and the magnitude of the diode's negative resistance, R_d, must be greater than the DC Thevenin resistance of the external circuit, i.e.,

$$R_d > R_{DC} \cdot \tag{3.1}$$

From Figure 3.3, the DC stability criterion for the Transmission I amplifier takes the form

$$R_d > R_{DC} = \frac{R_s(R_p+R_L)}{(R_s+R_p+R_L)} \cdot \tag{3.2}$$

A summary of the DC stability criteria for the amplifiers under investigation is as follows:

Reflection: $$R_d > R + \frac{R_s R_L}{R_s+R_L} \quad , \tag{3.3}$$

Transmission I: $$R_d > \frac{R_s(R_p+R_L)}{R_s+R_p+R_L} \quad , \tag{3.4}$$

Transmission II: $$R_d > \frac{R_L(R_p+R_s)}{R_s+R_p+R_L} \quad , \tag{3.5}$$

Series I: $$R_d > R_s+R_p+R_L \quad , \tag{3.6}$$

Series II: $$R_d > R_s+R_p+R_L \quad , \tag{3.7}$$

where

$$R_p \overset{\Delta}{=} R_n R/(R_n+R) = 0.8204\ R \quad . \tag{3.8}$$

In addition to a single intersection of the static load line and the diode characteristic, good bias stability requires that small changes

in the supply voltage E_{bb} (and hence the Thevenin voltage E_{bb}') should have a minimum effect on the location of the bias point, Q. The ideal situation would be to have a static load line that is vertical in slope. Since this corresponds to a DC equivalent circuit of zero resistance, a vertical static load line would be impossible to achieve without the use of a choke inductor to couple the supply voltage directly to the tunnel diode. Since inductors have been ruled out of consideration for reasons previously discussed, this brings to mind the possibility of improving the bias stability by isolating the bias circuit and signal circuit through the use of capacitance coupling. With this approach it might be possible to adjust the DC resistance of the equivalent circuit to a minimum while retaining control of the resistance offered to the signal components. If so, it would be possible, hopefully, to achieve a nearly vertical static load line (resulting in very good bias stability) and at the same time adjust the dynamic load line, as discussed in the previous chapter, so that its slope approaches that of the diode characteristic (resulting in very high gain for the signal components in the pass band).

One possibility of capacitance coupling in the Transmission I amplifier is shown in Figure 3.5. To set the operating point, we must satisfy the bias stability criterion

$$R_d > R_{DC} = R_s \ . \tag{3.9}$$

The incremental signal model of the amplifier in the frequency range of the pass band is shown in Figure 3.6. (Here, it is assumed that we have perfect coupling by the capacitance C_c and that the frequencies are low enough so that the total line capacitance C and the diode shunt

capacitance C_d are essentially open-circuited).

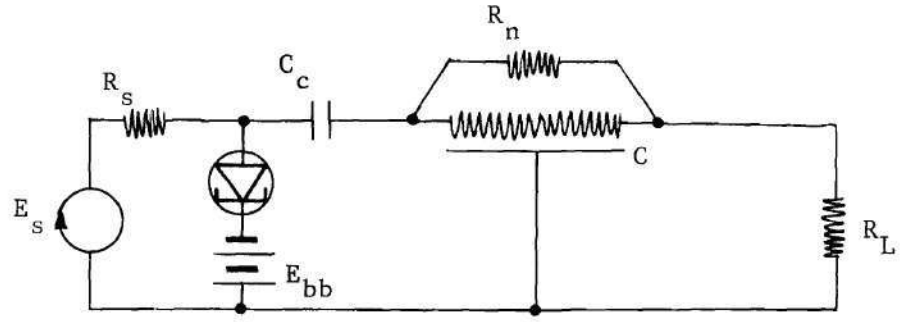

Figure 3.5 Transmission I Amplifier with Capacitance Coupling to Isolate Bias and Signal Circuits.

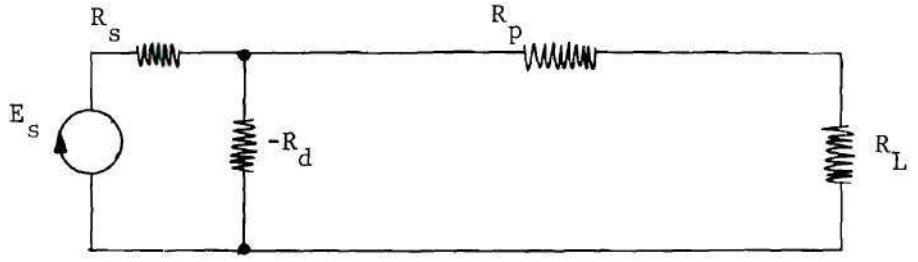

Figure 3.6 Incremental Signal Model of the Transmission I Amplifier in the Pass-Band Frequency Range.

As shown in the previous chapter, the resistance external to the diode in this incremental signal model is

$$R_{eq} = \frac{R_s(R_p+R_L)}{R_s+R_p+R_L} \quad , \tag{3.10}$$

and this resistance value governs the slope of the dynamic (signal) load line. The diode characteristic with both the static and dynamic load lines superimposed in shown in Figure 3.7.

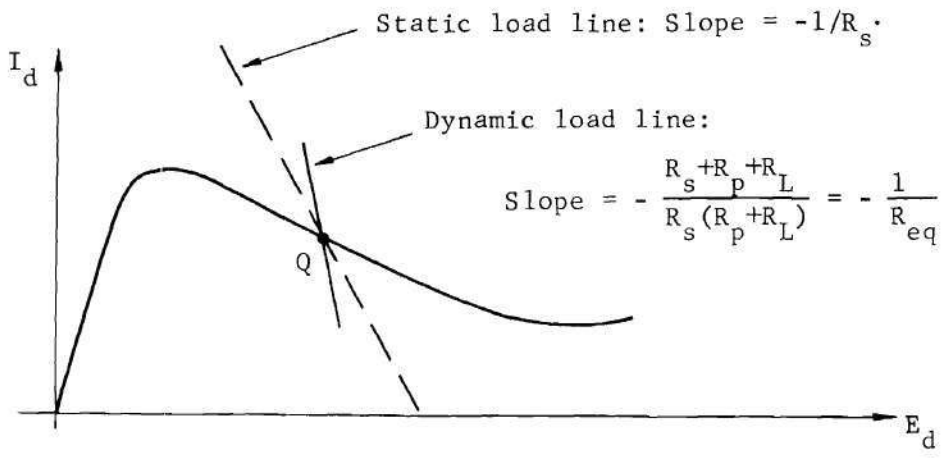

Figure 3.7 The Static and Dynamic Load-Line Analysis of the Transmission I Amplifier with Capacitance Coupling.

It is obvious from Figure 3.7 and the values of R_{DC} and R_{eq} given above that, with capacitance coupling, the slope of the dynamic load line will be steeper than that of the static load line. This will always be true in the amplifier configurations under investigation, since the equivalent resistance of the signal circuit, R_{eq}, will always be less than the resistance of the DC equivalent circuit, R_{DC}. This will be true for any practical orientation of the coupling capacitance(s) and the supply voltage. By the same type of analysis, it is observed that the same state of affairs exists in the other amplifier configurations as well. This result is the opposite of what we hoped for.

In a directly-coupled amplifier, the resistance of the bias circuit, R_{DC}, and the resistance of the signal circuit, R_{eq}, are the same, and the static and dynamic load lines are identical. We can therefore draw the following conclusion: For the same degree of bias stability (static load lines of the same slope) a directly-coupled amplifier will exhibit higher gain for the signal components than a capacitance-coupled

amplifier, and the gain exhibited by the directly-coupled amplifier is the maximum possible for the given degree of bias stability. This result, plus the fact that the response of a capacitance-coupled amplifier is degraded at very low frequencies, is one motivation for considering only directly-coupled amplifier configurations in this investigation. In short, there is nothing to be gained by using capacitance coupling to isolate the bias and signal circuits in any of the amplifiers under consideration.

At this point it should be noted that a fundamental limitation of both practical and theoretical importance is involved in the conclusion stated above. As we have seen, a directly-coupled amplifier possesses a single load line that serves for both the static and dynamic behavior, and once the slope is fixed (thus fixing the degree of bias point stability) the maximum possible gain for this condition is simultaneously achieved. As the slope of this load line is made to approach that of the tunnel diode characteristic (so that high gain results), the stability of the bias point becomes more critical (small changes in E_{bb} will now cause large changes in the bias point voltage). Therefore, a fundamental limitation exists in amplifiers of this type in that there will be a trade-off between the conditions of high bias point stability and high signal gain. This will be discussed further after the signal stability criterion has been developed.

Signal Stability

The second part of the overall stability criterion is concerned with the stability of the amplifiers for the signal components. The

method of establishing the signal stability criterion will now be presented with the Series I amplifier taken as an example.

The incremental signal model of the Series I amplifier is shown in Figure 3.8. The short-circuit admittance parameters for the two-port N are

$$y_{11N} = y_{22N} = y_{11} + G_n \,, \tag{3.11}$$

and

$$y_{12N} = y_{21N} = y_{12} - G_n \,, \tag{3.12}$$

where y_{11} and y_{12} are the parameters of the line alone.

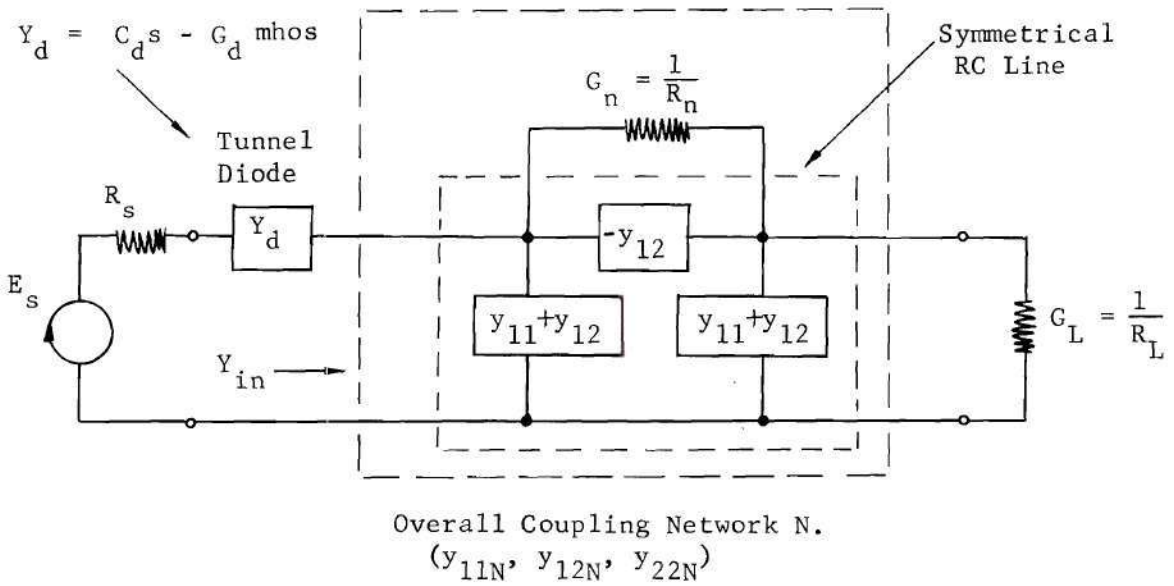

Figure 3.8 Incremental Signal Model of Series I Amplifier.

The y-parameter determinant for the two-port N is then

$$|y|_N = y_{11N}y_{22N} - y_{12N}y_{21N}$$

$$= (y_{11}+G_n)^2 - (y_{12}-G_n)^2$$

$$= 2G_n(y_{11}+y_{12}) + (y_{11}^2-y_{12}^2)$$

$$= 2G_n(y_{11}+y_{12}) + |y| \quad , \tag{3.13}$$

where $|y|$ is the determinant for the line parameters only. The loaded input admittance to the network N is

$$Y_{in} = \frac{y_{11N}G_L + |y|_N}{(y_{22N}+G_L)} \quad , \tag{3.14}$$

and the total series impedance seen by the voltage source E_s is

$$Z = R_s + \frac{1}{Y_d} + \frac{(y_{22N}+G_L)}{y_{11N}G_L + |y|_N}$$

$$= \frac{Y_d(R_s y_{11N}+R_s R_L|y|_N) + y_{11N}+R_L|y|_N + Y_d(R_L y_{22N}+1)}{Y_d(y_{11N}+R_L|y|_N)} \quad . \tag{3.15}$$

Substituting equations (3.11) and (3.13) and grouping terms yields

$$Z = \frac{\left[\begin{array}{l} [Y_d(R_s+R_L+2G_nR_sR_L) + 2G_nR_L + 1] \cdot y_{11} \\ \quad + [2G_nR_L(Y_dR_s+1)] \cdot y_{12} \\ \quad + \{Y_d[R_sG_n+R_sR_L|y| + R_LG_n+1] + R_L|y| + G_n\} \end{array}\right]}{[Y_d(2R_LG_n + 1)]\, y_{11} + 2Y_dR_LG_ny_{12} + Y_d(R_L|y|+G_n)}. \qquad (3.16)$$

For the symmetrical uniform RC transmission line the short-circuit admittance parameters are

$$y_{11} = \frac{(a\sqrt{s})}{R} \cdot \frac{\cosh(a\sqrt{s})}{\sinh(a\sqrt{s})} \quad , \qquad (3.17)$$

$$y_{12} = -\frac{(a\sqrt{s})}{R} \cdot \frac{1}{\sinh(a\sqrt{s})} \quad , \qquad (3.18)$$

and

$$|y| = \frac{(a\sqrt{s})^2}{R^2} \quad , \qquad (3.19)$$

where

$$a = \sqrt{RC} \quad . \qquad (3.20)$$

Now, substituting these expressions into equation (3.16) and multiplying the numerator and denominator by $R^2 \sinh(a\sqrt{s})$ to clear fractions, we get

$$Z = \frac{\left[\begin{array}{l} R[Y_d(R_s+R_L+2G_nR_sR_L) + 2G_nR_L + 1]\ (a\sqrt{s})\ \cosh(a\sqrt{s}) \\ - R[2G_nR_L(Y_dR_s+1)]\ (a\sqrt{s}) \\ + \left\{\begin{array}{l} Y_d[R_sR_L(a\sqrt{s})^2 + G_nR^2(R_s+R_L) + R^2] \\ + R_L(a\sqrt{s})^2 + G_nR^2 \end{array}\right\} \sinh(a\sqrt{s}) \end{array}\right]}{(\text{Denominator})} \quad . \qquad (3.21)$$

The driving-point impedance of the circuit is then

$$Z(a\sqrt{s}) = \frac{N(a\sqrt{s})}{D(a\sqrt{s})} \ , \qquad (3.22)$$

where $N(a\sqrt{s})$ and $D(a\sqrt{s})$ are the numerator and denominator of the expression considered as functions of $a\sqrt{s}$, and the short-circuit natural frequencies of the network are the zeros of $N(a\sqrt{s})$.

Considering equation (3.21), the numerator function may be written in the form

$$N(a\sqrt{s}) = P(a\sqrt{s}) \cdot \sinh(a\sqrt{s}) + Q(a\sqrt{s}) \cdot \cosh(a\sqrt{s}) - W(a\sqrt{s}) \ , \qquad (3.23)$$

where

$$P(a\sqrt{s}) = Y_d[R_sR_L(a\sqrt{s})^2 + G_nR^2(R_s+R_L)+R^2] + R_L(a\sqrt{s})^2 + G_nR^2, \qquad (3.24)$$

$$Q(a\sqrt{s}) = [Y_d(R_s+R_L + 2G_nR_sR_L) + 2G_nR_L+1] \cdot R \cdot (a\sqrt{s}) \ , \qquad (3.25)$$

and

$$W(a\sqrt{s}) = 2G_nR\ R_L(Y_dR_s+1)(a\sqrt{s}) \ . \qquad (3.26)$$

The question of stability then reduces to finding the values of s for which $N(a\sqrt{s})$ is zero, or for which

$$P(a\sqrt{s}) \cdot \sinh(a\sqrt{s}) - W(a\sqrt{s}) + Q(a\sqrt{s}) \cdot \cosh(a\sqrt{s}) = 0 \ . \qquad (3.27)$$

Now, substituting

$$Y_d = C_d s - G_d = \frac{C_d}{a^2} (a\sqrt{s})^2 - G_d \ , \qquad (3.28)$$

into equations (3.24), (3.25), and (3.26) and making use of the DC stability criterion, $R_d > R_s+R_p+R_L$, the functions $P(a\sqrt{s})$, $W(a\sqrt{s})$, and $Q(a\sqrt{s})$ may be cast in the following forms:

$$P(a\sqrt{s}) = D \cdot (a\sqrt{s})^4 + E \cdot (a\sqrt{s})^2 + F \ , \qquad (3.29)$$

where

$$D = \frac{C_d}{a^2} R_s R_L > 0 \ , \qquad (3.30)$$

$$E = \frac{C_d}{a^2} [G_n R^2 (R_s+R_L) + R^2] + G_d R_L (R_d-R_s) > 0 \ , \qquad (3.31)$$

and

$$F = G_d G_n R^2 \{R_d - (R_s+R_L+R_n)\} \begin{matrix} > \\ = \\ < \end{matrix} 0. \qquad (3.32)$$

$$W(a\sqrt{s}) = (a\sqrt{s})[G \cdot (a\sqrt{s})^2 + H] \ , \qquad (3.33)$$

where

$$G = 2G_n R R_s R_L \frac{C_d}{a^2} > 0 \ , \qquad (3.34)$$

and

$$H = 2G_dG_nRR_L(R_d-R_s) > 0 \ . \tag{3.35}$$

Likewise

$$Q(a\sqrt{s}) = (a\sqrt{s})\ [J \cdot (a\sqrt{s})^2 + K] \ , \tag{3.36}$$

where

$$J = 2G_nRR_sR_L \frac{C_d}{a^2} + \frac{C_dR}{a^2}(R_s+R_L) > 0$$

$$= G + M \ , \tag{3.37}$$

and

$$K = 2G_dG_nRR_L(R_d-R_s) + G_dR[R_d-(R_s+R_L)] > 0$$

$$= H + N \ , \tag{3.38}$$

where H and N are both positive constants.

The governing equation (3.27) may now be written in the form

$$[D \cdot (a\sqrt{s})^4 + E \cdot (a\sqrt{s})^2 + F] \sinh(a\sqrt{s})$$

$$- (a\sqrt{s})[G \cdot (a\sqrt{s})^2 + H - \{J \cdot (a\sqrt{s})^2 + K\} \cosh(a\sqrt{s})] = 0. \tag{3.39}$$

Employing equations (3.37) and (3.38) this may be rewritten as

/

$$[D \cdot (a\sqrt{s})^4 + E \cdot (a\sqrt{s})^2 + F] \sinh(a\sqrt{s})$$

$$-(a\sqrt{s}) \begin{bmatrix} [G \cdot (a\sqrt{s})^2 + H][1 - \cosh(a\sqrt{s})] \\ -[M \cdot (a\sqrt{s})^2 + N] \cosh(a\sqrt{s}) \end{bmatrix} = 0 . \qquad (3.40)$$

At this point it is necessary to make use of Mitra's theorem which states that the driving-point impedance of a strictly RC network containing a single tunnel diode can have at most one zero on the positive real axis in the s-plane [7]. Since the network is strictly RC, the zeros of the driving-point impedance must fall on the σ-axis (i.e., they must be purely real), and using the result of Mitra's theorem it is known that, at most, there can be only one zero on the positive σ-axis in the s-plane. Hence, there can be at most one natural frequency that falls in the right-half s-plane causing instability. The question is then posed: Is there a positive real value of s for which equation (3.40) is satisfied? Taking s to be purely real and positive, the following change of variables is made:

$$(a\sqrt{s}) = x, \ (\pm \text{ real}) . \qquad (3.41)$$

Equation (3.40) may now be written as

$$(D \cdot x^4 + E \cdot x^2 + F) \sinh x$$

$$- x\{(G \cdot x^2 + H)(1 - \cosh x) - (M \cdot x^2 + N) \cosh x\} = 0, \qquad (3.42)$$

where the constants D, E, G, H, M, N, and a, are all real and positive, and the variable x is a purely real variable.

Equation (3.42) is very difficult to solve in closed form. If part of it is transposed, however, so that it takes the form

$$(D \cdot x^4 + E \cdot x^2 + F) \sinh x$$

$$= x\{(G \cdot x^2 + H)(1 - \cosh x) - (M \cdot x^2 + N) \cosh x\} , \qquad (3.43)$$

then the left and right members of equation (3.43) may be plotted graphically to determine if there are any intersections other than at $x = 0$. [The point $x = 0$ is a degenerate point since it will always be a root of equation (3.43). This is the result of clearing fractions of the form $\cosh(a\sqrt{s})/\sinh(a\sqrt{s})$ or $1/\sinh(a\sqrt{s})$ in the numerator and denominator of the expression for the driving-point impedance thereby placing the factor sinhx in the left member of equation (3.43).]

The signal stability criterion is then established by finding the relation between the constants of equation (3.43) for which there are no intersection points corresponding to values of x other than $x = 0$. This is arrived at by the following sequence of steps:

1.) The left member of equation (3.43),

$$L(x) = (D \cdot x^4 + E \cdot x^2 + F) \cdot \sinh x , \qquad (3.44)$$

is sketched as shown in Figure 3.9.

2.) The right member of equation (3.43) ,

$$R(x) = x[(G \cdot x^2 + H)(1 - \cosh x) - (M \cdot x^2 + N) \cosh x] , \qquad (3.45)$$

is sketched as shown in Figure 3.10.

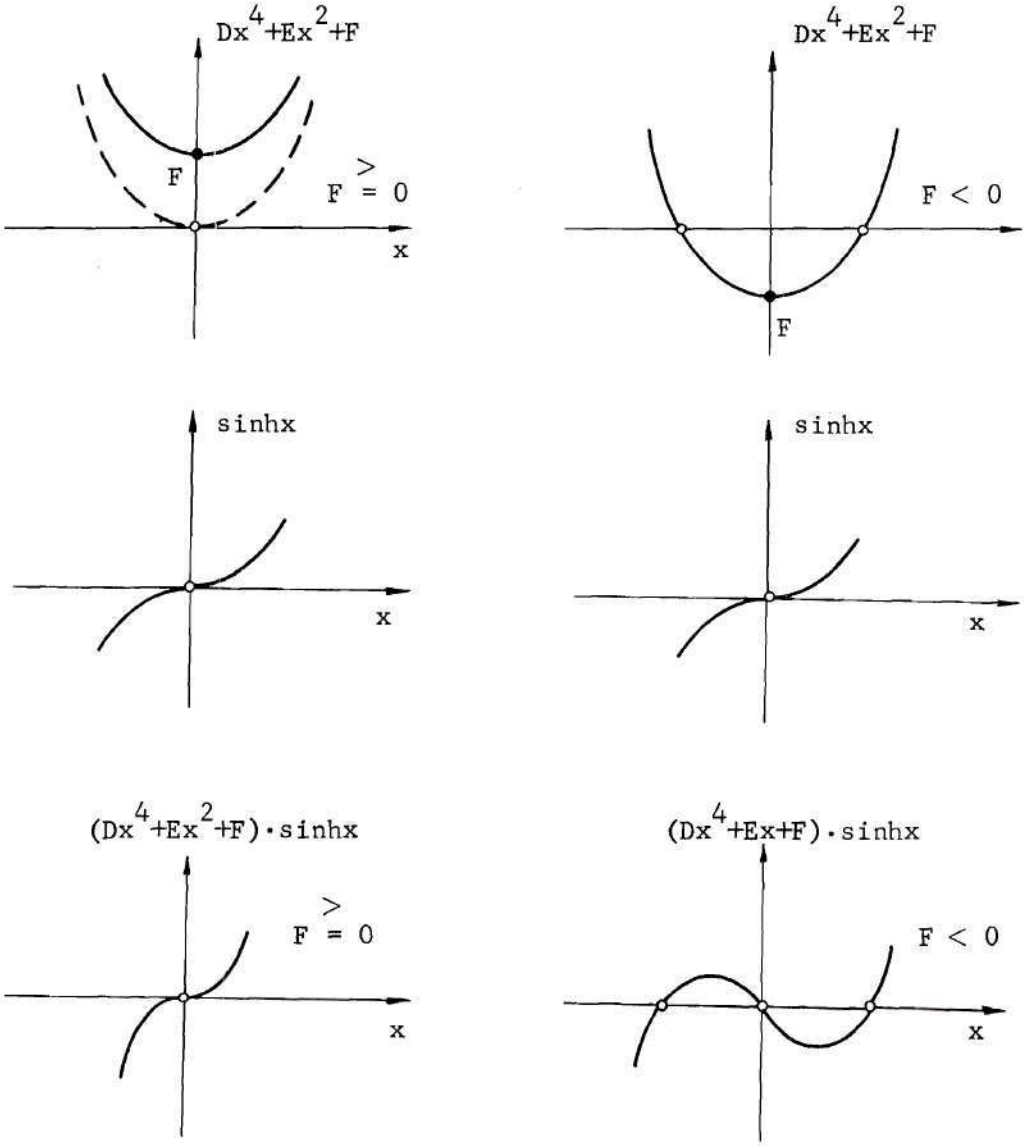

(a) Sketch of left member of equation (3.43) for case where $F \geq 0$.

(b) Sketch of left member of equation (3.43) for case where $F < 0$.

Figure 3.9 Sketches of the Left Member of Equation (3.43), $L(x) = (Dx^4+Ex^2+F) \cdot \sinh x$.

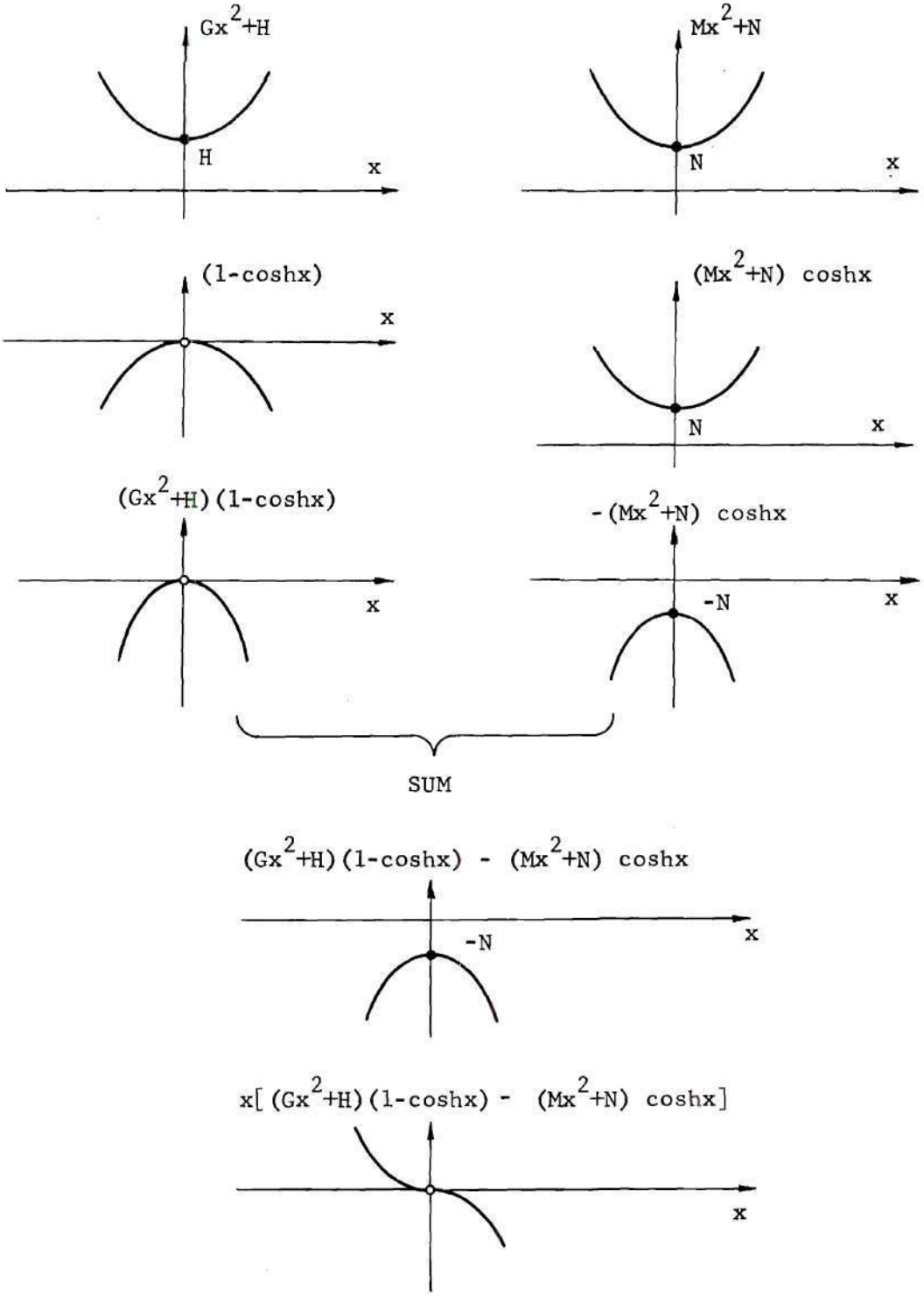

Figure 3.10 Sketch of the Right Member of Equation (3.43), $R(x) = x[(Gx^2+H)(1-coshx) - (Mx^2+N)\ coshx]$.

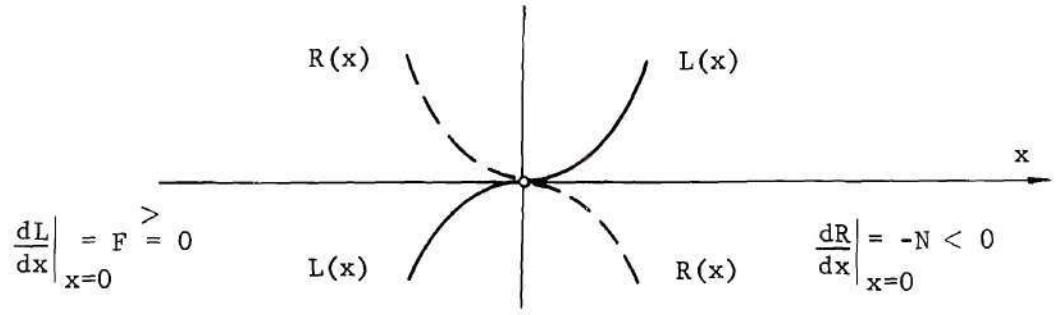

(a) No intersection other than at x=0 for $F \geq 0$.

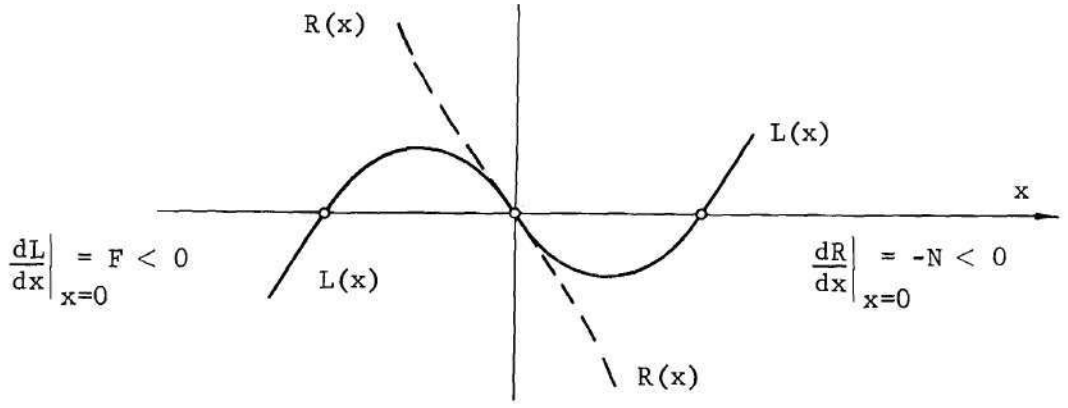

(b) No intersection except at x=0 for $F < 0$ if, at x=0, the slope of R(x) is less than the slope of L(x).

Figure 3.11 Superposition of R(x) and L(x) to Inspect for Intersection Points Other than at x=0.

3.) The sketches of L(x) and R(x) are then superimposed, as in Figure 3.11, and inspected for intersections other than the one at x = 0.

4.) From Figure 3.11, it is concluded that there are no other intersections of R(x) and L(x), and hence no positive-real zeros of the driving-point impedance, if

$$\left.\frac{dL}{dx}\right|_{x=0} > \left.\frac{dR}{dx}\right|_{x=0} , \tag{3.46}$$

or

$$F > -N . \tag{3.47}$$

The interpretation of expression (3.47) in terms of equations (3.32) and (3.38) yields the incremental signal stability criterion for the Series I amplifier as

$$R_d > R_s + \frac{RR_n}{R+R_n} + R_L . \tag{3.48}$$

It should be noted that the signal stability criterion given by expression (3.48) and the DC stability criterion given by expression (3.6) are identical. This means that for the Series I configuration, if the bias point is stabilized, then the circuit is automatically stable for the signal components as well. Applying this procedure to the other amplifiers to be studied yielded the same general result: Stabilizing the DC bias point completely stabilizes the circuit.

A summary of the overall stability criteria is given below:

Reflection: $$R_d > R + \frac{R_s R_L}{R_s + R_L} \quad . \tag{3.49}$$

Transmission I: $$R_d > \frac{R_s (R_p + R_L)}{R_s + R_p + R_L} \quad , \tag{3.50}$$

Transmission II: $$R_d > \frac{R_L (R_p + R_s)}{R_s + R_p + R_L} \quad , \tag{3.51}$$

Series I: $$R_d > R_s + R_p + R_L \tag{3.52}$$

and

Series II: $$R_d > R_s + R_p + R_L \quad , \tag{3.53}$$

where

$$R_p = \frac{R R_n}{R_n + R} = 0.8204 \; R \quad . \tag{3.54}$$

The simplicity of this general result is another motivation for the use of direct coupling. For directly-coupled amplifiers the question of stability is answered by one simple criterion. It must be noted, however, that the gain-stability limitation mentioned previously is now extended to the signal case as well. Since the problems of static and signal stability are identical and governed by a single load line, it must be reiterated that there is a trade-off between the conditions of high signal gain and high stability margin, where stability is now taken to mean total (both static and signal) stability.

CHAPTER IV

GAIN-BANDWIDTH PROPERTIES AND DESIGN PROCEDURES

Fundamental Gain-Bandwidth Considerations

The gain-bandwidth properties of any amplifier are always of prime importance, and this aspect of the investigation is dealt with in this chapter.

In connection with a general base-band amplifier and its gain-frequency response, we have three definitions of fundamental importance:

Gain-Area:
$$GA_{\omega} \triangleq \int_0^{\infty} IPG(\omega)\, d\omega \,, \tag{4.1}$$

Pass-Band Gain-Area:
$$PBGA_{\omega} \triangleq \int_0^{\omega_{hp}} IPG(\omega)\, d\omega \,, \tag{4.2}$$

Gain-Bandwidth Product:
$$GBP_{\omega} \triangleq IPG(0) \cdot \omega_{hp} \,. \tag{4.3}$$

Likewise, the same definitions may be made in terms of the Hertzian frequency f instead of the angular frequency ω, i.e.,

$$GA_f \triangleq \int_0^{\infty} IPG(2\pi f)\, df \,, \tag{4.4}$$

$$PBGA_f \triangleq \int_0^{f_{hp}} IPG(2\pi f)\, df \,, \tag{4.5}$$

and

$$GBP_f \overset{\Delta}{=} IPG(0) \cdot f_{hp} \ . \tag{4.6}$$

Since $\omega = 2\pi f$ it is clear that

$$GA_\omega = 2\pi(GA_f) \ , \tag{4.7}$$

$$PBGA_\omega = 2\pi(PBGA_f) \ , \tag{4.8}$$

and

$$GBP_\omega = 2\pi(GBP_f) \ . \tag{4.9}$$

In the work to follow, both forms of these definitions will be used with the choice based on convenience. Hereafter, the subscripts ω and f will be dropped except in those cases where confusion might arise. It is understood that any result arrived at with one form is equally valid with the other provided the factor 2π (or $1/2\pi$) is properly taken into account.

The gain-area (GA) is the total area bounded by the gain-frequency response curve. It is this fund of gain-area with which the network designer has to work in order to meet the usual specifications of DC gain, half-power frequency, shape of the gain-frequency response curve, and so forth. As far as the synthesis or design of base-band amplifiers is concerned, the most general problem concerns itself with approaching the near-ideal condition where most of the gain-area is devoted to the pass-band gain-area (PBGA) with as little area as possible employed above the cutoff frequency. The gain-bandwidth product (GBP) is a useful measure

of the ideal situation that is desired. The GBP represents the area under an ideal low-pass gain function of flat gain IPG(0) and pass-band ω_{hp} (or f_{hp}). While no actual amplifier can ever achieve this type of idealized low-pass response, the GBP is useful in that it is a convenient figure of merit, assuming the design is a good one and the gain in the pass-band is reasonably flat with little roll-off until the frequency nears the band edge.

A knowledge of the GA is sometimes useful in predicting an upper bound on the maximum ideal flat gain achievable over a band of frequencies. More specifically, an upper bound can be placed on the achievable GBP. The method is as follows [8]: The GA is found as

$$GA \triangleq \int_0^\infty IPG(\omega)\ d\omega = \Gamma\ . \tag{4.10}$$

We then have an upper bound on the PBGA since

$$PBGA = \int_0^{\omega_{hp}} IPG(\omega)\ d\omega' \leq GA = \Gamma\ . \tag{4.11}$$

Now, suppose that it is possible to shape IPG(ω) so that in the pass-band ($0 \leq \omega \leq \omega_{hp}$) it is equal to a constant, G_0. Then, irrespective of the behavior of IPG(ω) outside this frequency band, it is true that

$$PBGA = \int_0^{\omega_{hp}} G_0\ d\omega = \omega_{hp} \cdot G_0 \leq \Gamma\ . \tag{4.12}$$

Clearly for a given bandwidth ω_{hp}, the maximum flat gain cannot exceed

$$G_{0_{max}} = \frac{\Gamma}{\omega_{hp}} = \frac{GA}{\omega_{hp}} . \tag{4.13}$$

The result is that if the maximum flat gain $G_{0_{max}}$ were realized over the frequency band $0 \leq \omega \leq \omega_{hp}$, then

$$PBGA = \omega_{hp} \cdot G_{0_{max}} = \Gamma = GA , \tag{4.14}$$

and all of the GA would be utilized in an ideal low-pass characteristic as shown in Figure 4.1.

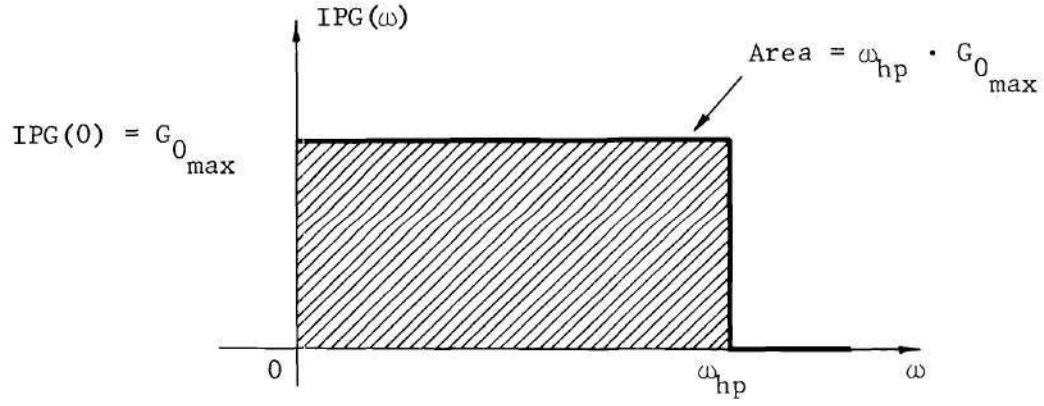

Figure 4.1 An Ideal Low-Pass Gain Function.

For this idealized case the GBP is maximum, and

$$GBP\Big|_{max} = G_{0_{max}} \cdot \omega_{hp} . \tag{4.15}$$

Using equation (4.13) we can write (4.15) as

$$GBP\Big|_{max} = \frac{GA}{\omega_{hp}} \cdot \omega_{hp} = GA \ . \qquad (4.16)$$

We then have the result that the GA is an upper bound on the GBP, and knowing the GA (or an upper bound on the GA) gives us a bound on the achievable GBP or on the maximum flat gain attainable over a band of frequencies. Likewise, from equations (4.2) and (4.3), we see that

$$PBGA \leq GBP \ , \qquad (4.17)$$

and the GBP is an upper bound on the PBGA.

An Elementary Amplifier

In order to extend the ideas above to the case where a negative resistance is involved, it is convenient to consider the elementary amplifier shown in Figure 4.2.

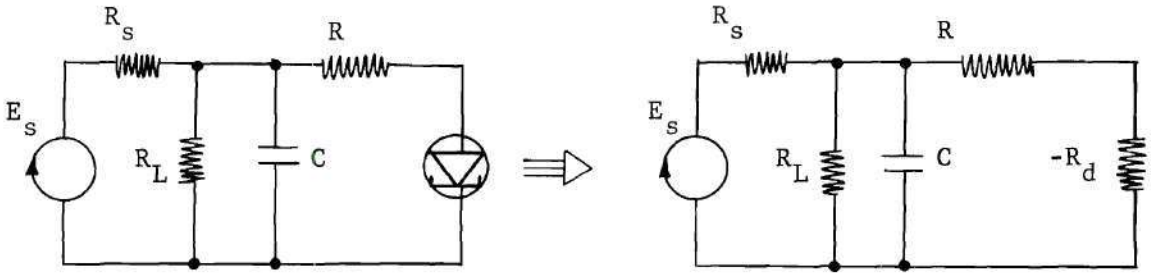

Figure 4.2 An Elementary Negative-Resistance Amplifier.

This circuit may be considered a very simple lumped-element approximation of the Reflection amplifier where the total line

capacitance is lumped across the load, and the capacitance of the tunnel diode is assumed to be negligibly small. As might be expected, the gain-frequency response of this amplifier is not close enough on a point-by-point basis to that of the Reflection amplifier to warrant using it as an approximation. This elementary amplifier does, however, exhibit a similar base-band frequency response, an identical DC gain, and its gain-bandwidth properties provide further insight and motivation for the study of the more complicated lumped/distributed-parameter configurations of this investigation.

For this elementary amplifier, the IPG is

$$IPG(\omega) = \left(\frac{R_d - R}{R_d - R_{eq}}\right)^2 \frac{1}{1 + \left(\frac{\omega}{\omega_{hp}}\right)^2} , \tag{4.18}$$

where

$$\omega_{hp} = \left(\frac{R_d - R_{eq}}{R_d - R}\right) \frac{1}{R_x C} , \tag{4.19}$$

$$R_{eq} = R + R_x , \tag{4.20}$$

and

$$R_x = \frac{R_s R_L}{R_s + R_L} . \tag{4.21}$$

The PBGA associated with the IPG of (4.18) is

$$PBGA_{\omega} = \frac{(R_d - R)}{(R_d - R_{eq})} \cdot \frac{1}{R_x C} \cdot \frac{\pi}{4} , \tag{4.22}$$

the GBP is

$$GBP_{\omega} = \left[\frac{R_d - R}{R_d - R_{eq}}\right] \frac{1}{R_x C} \quad , \tag{4.23}$$

and the GA is

$$GA_{\omega} = \left[\frac{R_d - R}{R_d - R_{eq}}\right] \cdot \frac{1}{R_x C} \cdot \frac{\pi}{2} \quad . \tag{4.24}$$

From equations (4.22), (4.23), and (4.24), we see that the properties stated in the preceding section are exhibited by this elementary amplifier, i.e.

$$PBGA < GBP < GA \quad . \tag{4.25}$$

The salient point here is that through control of the factor $(R_d - R_{eq})$, all three of these quantities may be made <u>arbitrarily large</u> despite the fact that the source resistance, load resistance, and capacitance across the load are all <u>fixed</u>. The mechanism through which this phenomenon occurs can readily be seen with the aid of equations (4.18), (4.19), (4.22), (4.23), and (4.24). If we make the definition

$$K \overset{\Delta}{=} \frac{(R_d - R)}{(R_d - R_{eq})} = \frac{(R_d - R)}{(R_d - R) - R_x} \quad , \tag{4.26}$$

then

$$IPG(\omega) = K^2 \cdot \frac{1}{1 + \left(\frac{\omega}{\omega_{hp}}\right)^2} \quad , \tag{4.27}$$

$$\omega_{hp} = \frac{1}{K\, R_x C} \quad , \tag{4.28}$$

$$PBGA_{\omega} = K \cdot \frac{1}{R_x C} \cdot \frac{\pi}{4} \quad , \tag{4.29}$$

$$GBP_{\omega} = K \cdot \frac{1}{R_x C} \quad , \tag{4.30}$$

and

$$GA_{\omega} = K \cdot \frac{1}{R_x C} \cdot \frac{\pi}{2} \quad . \tag{4.31}$$

Now , as the DC value of the gain is increased, the half-power frequency ω_{hp} does decrease as one would expect, but from equations (4.26) and (4.27) we see that IPG(0) increases as K^2, and ω_{hp} decreases as 1/K. The DC gain simply increases faster than the half-power frequency decreases, and from equations (4.29), (4.30), and (4.31) it is clear that

$$PBGA < GBP < GA \quad , \tag{4.32}$$

and each can be made arbitrarily large while still satisfying this inequality.

Obviously, there are practical problems connected with achieving this state of affairs. First of all, the factor

$$(R_d - R_{eq}) = R_d - R - R_x \quad , \tag{4.33}$$

is intimately connected with the overall stability of the amplifier. By

inspection, the stability criterion for the circuit is

$$(R_d - R_{eq}) = R_d - R - R_x > 0 \ . \qquad (4.34)$$

To achieve arbitrarily large gain values, however, it is precisely this factor that must be made arbitrarily small. Theoretically, it is possible to do this while satisfying (4.34), but practically it is very difficult to accomplish. The situation calls for a tunnel diode characteristic and load line that are arbitrarily close in slope. Small perturbations in the supply voltage and/or the resistance values would then have a drastic effect on the overall stability of the circuit. Hence, any practical attempt to achieve an arbitrarily large GBP will encounter the gain-stability limitation discussed in the previous chapter. Another problem of a practical nature is that the GBP for this amplifier can be made arbitrarily large only for the conditions of very high gain and very small bandwidth. Practically speaking, this is far too restrictive. It would be much more desirable to have more flexibility in shaping the IPG(ω) function so that any arbitrarily large value selected for the GA could be distributed in a manner to achieve a large GBP at some fixed value of DC gain. Thus we see that, even though this simple negative-resistance amplifier can theoretically achieve an unbounded GBP, the property is of very limited practical value.

At this point one might wonder about the practical gain-bandwidth limitations and the direction a feasible design procedure might follow. The basic question to be answered can be put in two forms:

1.) For a specified value of DC gain, IPG(0), what are $(f_{hp})_{max}$ and $(GBP_f)_{max}$?

or

2.) For a specified value of f_{hp}, what are $[IPG(0)]_{max}$ and $(GBP_f)_{max}$?

Before answering these questions it should be noted that there are two basic assumptions made in all of the work that follows: The source and load resistances are fixed, and there is a practical minimum value of the capacitance C beyond which it cannot (or should not) be reduced. In the case of the elementary amplifier, the minimum value of C corresponds to the parasitic shunt capacitance across the load. In the case of the distributed RC lines to be used in the work that follows, the minimum value of C corresponds to the practical minimum value attainable for the line capacitance. There is a limit on the minimum value of this capacitance because, as the thickness of the dielectric layer is increased, fringing effects eventually change the electrical properties of the line to the point that the two-port parameters given by equations (2.3) and (2.4) no longer apply [9]. With these points in mind, we may now answer the question(s) above.

From equation (4.28) we may write

$$f_{hp} = \frac{1}{2\pi R_x CK} , \tag{4.35}$$

where

$$K = \sqrt{IPG(0)} . \tag{4.36}$$

Since the source and load resistances are fixed, it is convenient to consider their ratio, a, defined by

$$R_s = a\, R_L \,. \tag{4.37}$$

Using (4.21), (4.36), and (4.37), equation (4.35) may be cast in the form

$$f_{hp} = \frac{(a+1)}{2\pi R_L C \cdot a\sqrt{IPG(0)}} \,. \tag{4.38}$$

If we define the normalized half-power frequency as

$$(f_{hp})_N \overset{\triangle}{=} 2\pi R_L C \cdot (f_{hp}) \,, \tag{4.39}$$

then we have

$$(f_{hp})_N = \frac{a+1}{a\sqrt{IPG(0)}} \,. \tag{4.40}$$

The graph of (4.40) for some typical values of the ratio a is shown in Figure 4.3. Likewise, we can define the normalized gain-bandwidth product as

$$\begin{aligned}(GBP)_N &\overset{\triangle}{=} 2\pi R_L C \cdot (GBP) \\ &= 2\pi R_L C \cdot [IPG(0) \cdot f_{hp}] \\ &= IPG(0) \cdot (f_{hp})_N \\ &= \left(\frac{a+1}{a}\right)\sqrt{IPG(0)} \,. \end{aligned} \tag{4.41}$$

The graph of (4.41) for some typical values of the ratio a is shown in Figure 4.4 With the aid of Figures 4.3 and 4.4, the basic questions

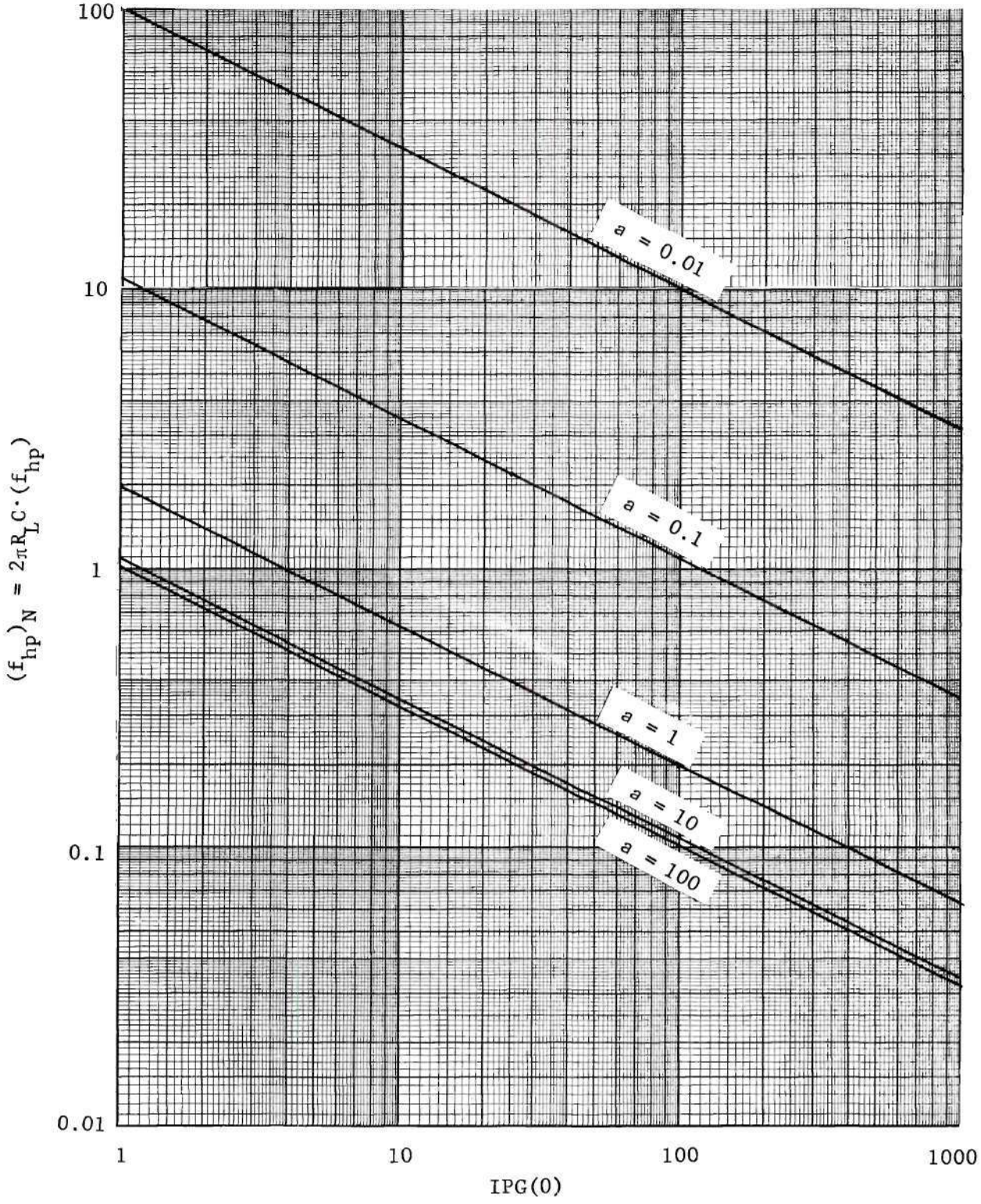

Figure 4.3 Normalized Half-Power Frequency vs. IPG(0) for the Elementary Amplifier.

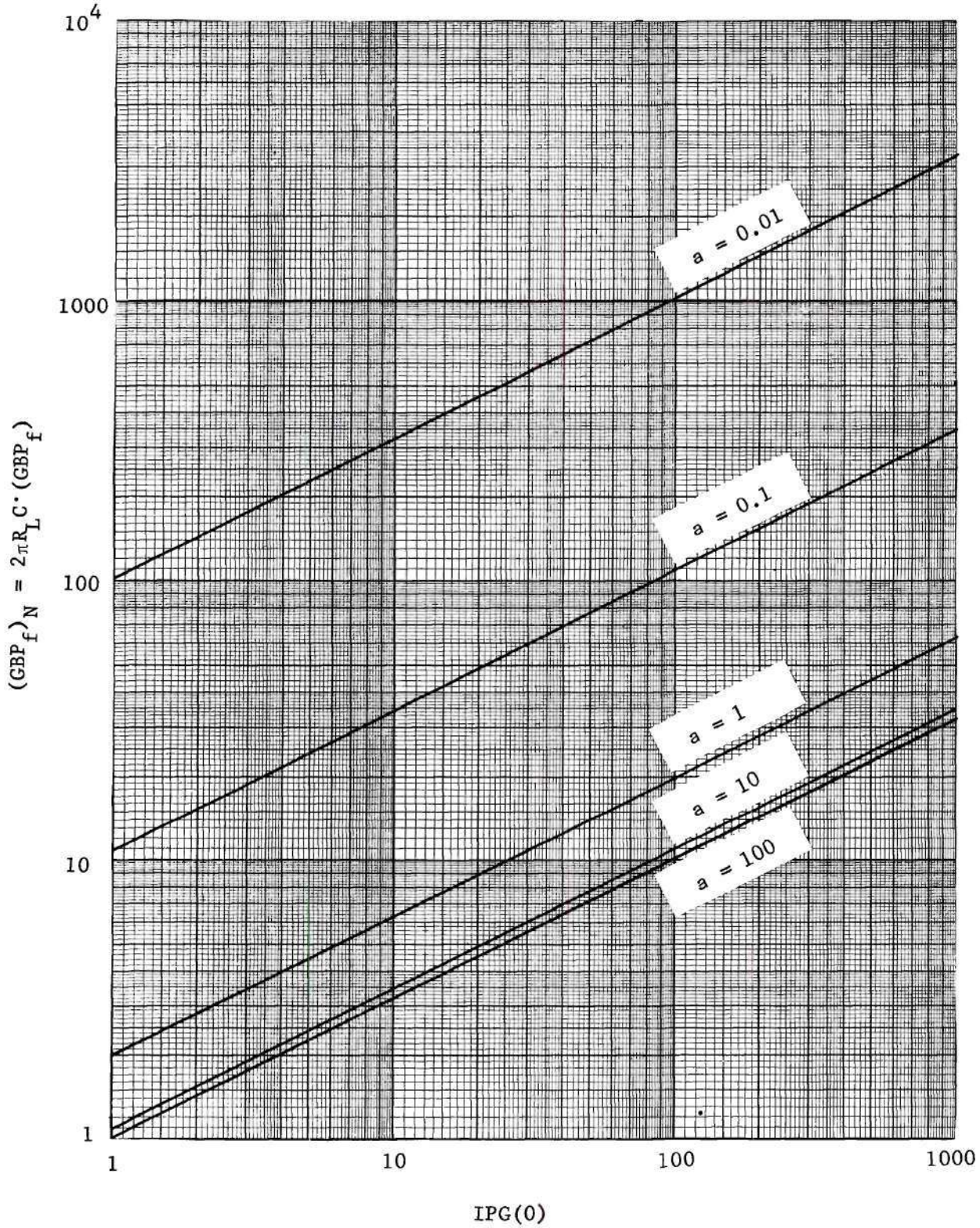

Figure 4.4 Normalized Gain-Bandwidth Product vs. IPG(0) for the Elementary Amplifier.

posed above can now be answered.

For specified values of IPG(0) and source and load resistances, the corresponding value of $(f_{hp})_N$ is read directly from Figure 4.3. Then, at that value of IPG(0), we compute

$$(f_{hp})_{max} = \frac{(f_{hp})_N}{2\pi R_L C_{min}} , \tag{4.42}$$

where R_L is the specified load resistance and C_{min} is the minimum possible value of the capacitance C. Likewise, for the specified values of IPG(0) and resistances, $(GBP)_N$ is taken directly from Figure 4.4. At that value of IPG(0) we compute

$$GBP_{max} = \frac{(GBP)_N}{2\pi R_L C_{min}} . \tag{4.43}$$

On the other hand, if f_{hp} is specified, we compute

$$(f_{hp})_{N_{min}} = 2\pi R_L C_{min} \cdot (f_{hp}) , \tag{4.44}$$

and since IPG(0) is a decreasing function of $(f_{hp})_N$, we can take $IPG(0)]_{max}$ directly from Figure 4.3. At that value of IPG(0), we can take $(GBP)_N]_{max}$ directly from Figure 4.4 and compute

$$GBP_{max} = \frac{(GBP)_N]_{max}}{2\pi R_L C_{min}} . \tag{4.45}$$

As stated previously, this elementary amplifier is not intended as a good approximation for any of the amplifiers to be considered, but

as we shall see it does possess some similar properties, and the results given here point the way for the analysis to follow.

The Reflection Amplifier

Gain-Bandwidth Properties

The Reflection amplifier, shown in Figure 4.5, is the simplest of the five amplifiers investigated in this thesis. The expression for its IPG is given in Appendix A, and some typical frequency response curves are shown in Figures 4.6 and 4.7.

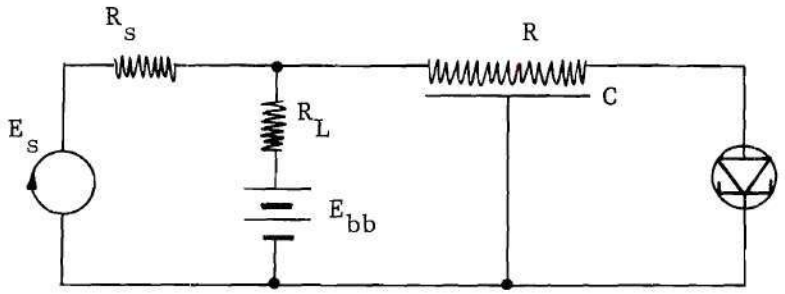

Figure 4.5 The Reflection Amplifier.

The response curves shown in Figure 4.6 indicate that, as the magnitude of the negative resistance approaches the value of the external circuit resistance, the following occur: The DC gain increases, the half-power frequency decreases, and the GBP increases. This behavior is very similar to that observed in the elementary amplifier of the preceding section, and leads one to wonder if the GBP of the Reflection amplifier might also be made arbitrarily large.

The answer to this question is, in this case, more difficult to attain. An exact closed-form expression for f_{hp} is very difficult to find for the Reflection amplifier utilizing the distributed-parameter RC

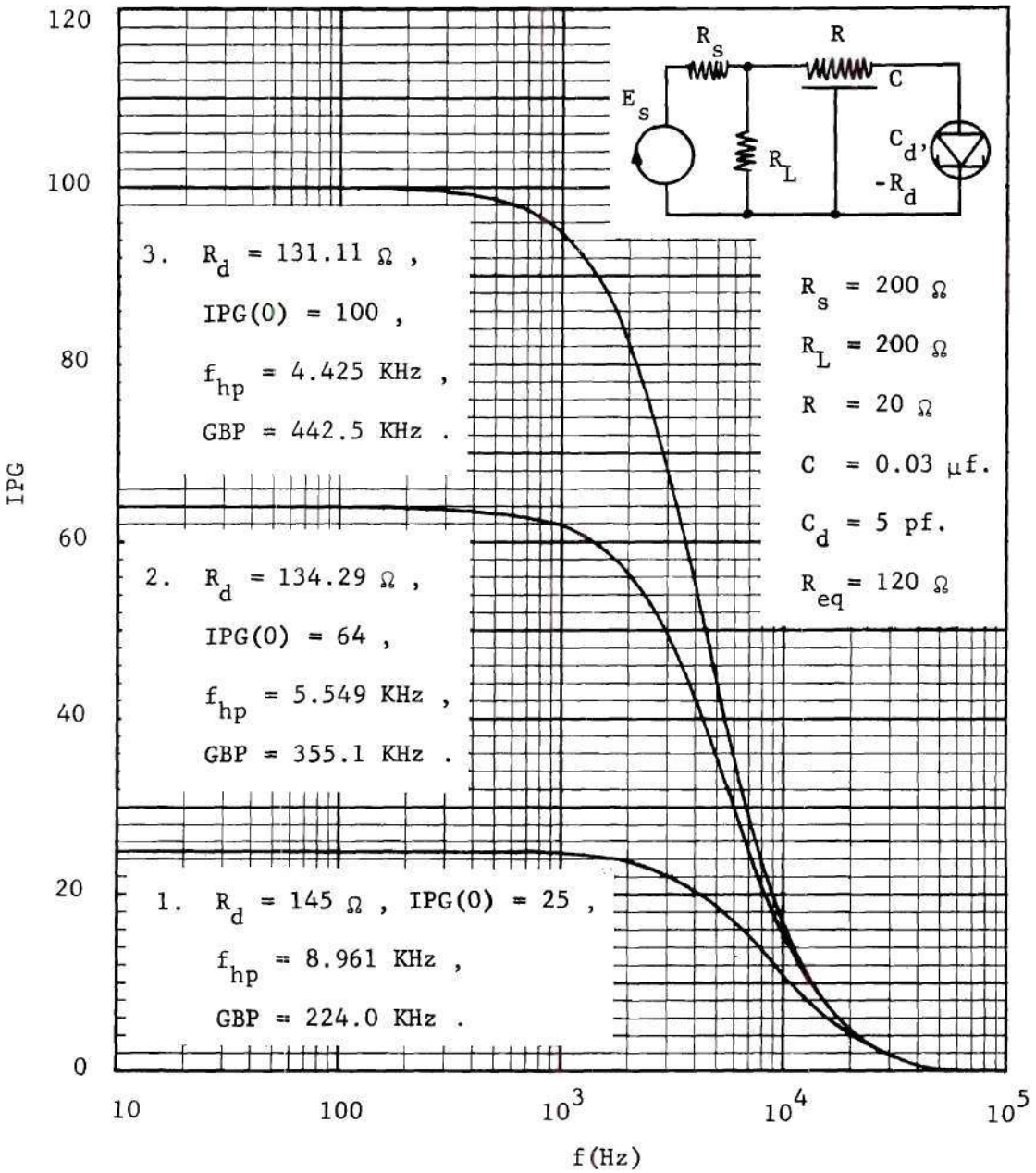

Figure 4.6 Typical IPG-Frequency Response Curves for the Reflection Amplifier.

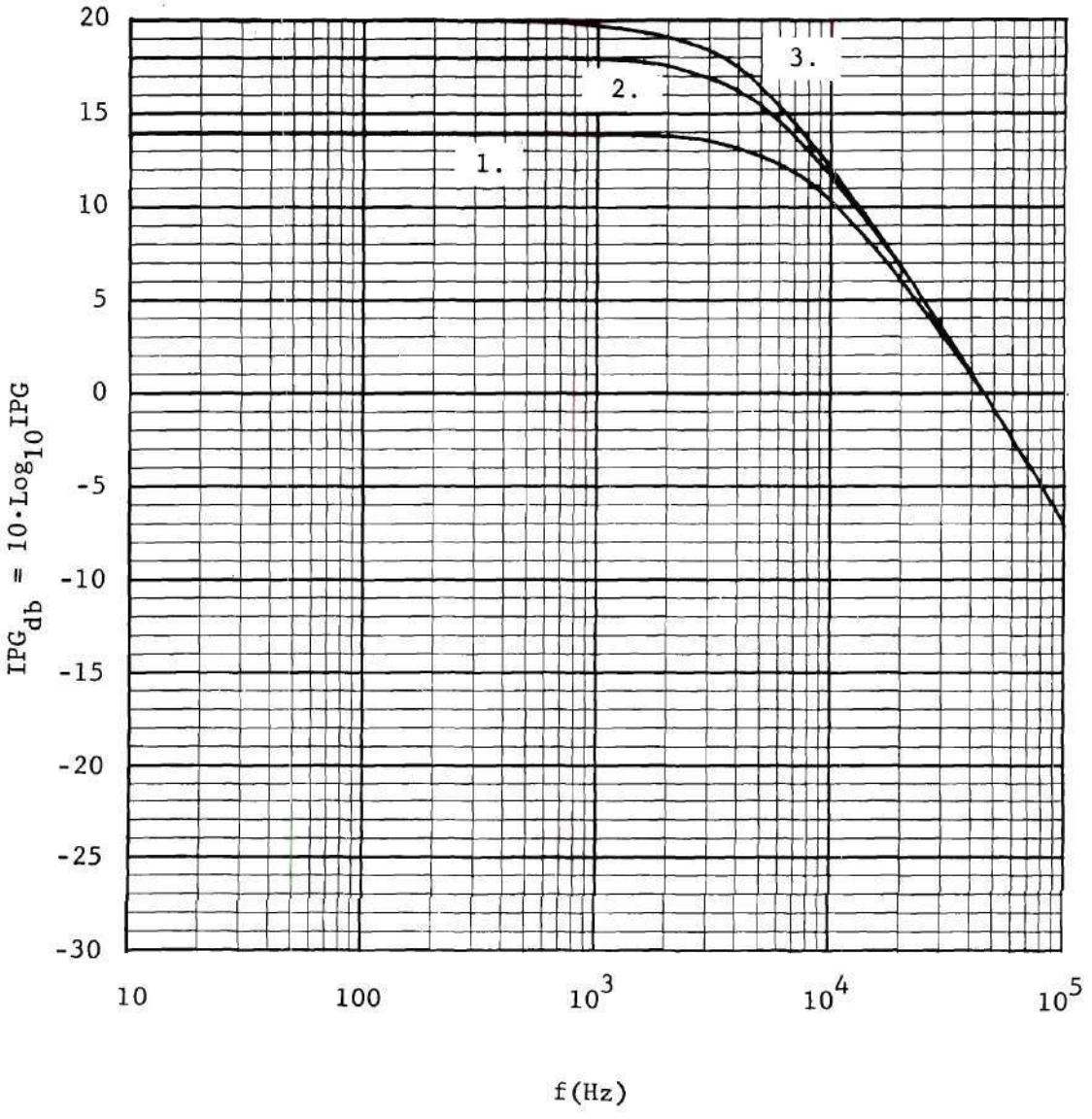

Figure 4.7 The IPG-Frequency Response Curves of Figure 4.6 in Decibels.

transmission line. An alternate approach, however, can be made via the fundamental definitions given at the beginning of this chapter. The basic inequality

$$\text{PBGA} < \text{GBP} \tag{4.46}$$

and its graphical interpretation, shown in Figure 4.8, can be used to advantage here. In Appendix B it has been shown that the PBGA of the

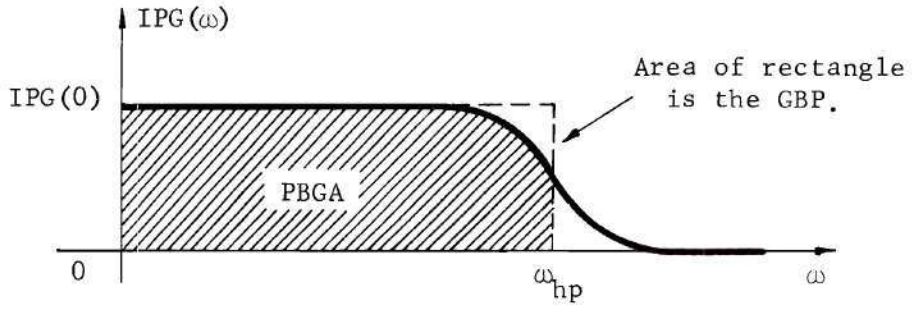

Figure 4.8 Graphical Interpretation of (4.46).

Reflection amplifier may be made arbitrarily large, and in light of (4.46) it is then obvious that there is no upper bound on the GBP of the Reflection amplifier. This statement is based, of course, on strictly theoretical considerations. As in the case of the elementary amplifier of the preceding section, the property of unlimited GBP in the Reflection amplifier is of very limited practical value. This is true precisely for the same reasons as with the elementary amplifier: An arbitrarily large GBP can be achieved only in the high-gain narrow-band mode, and any attempt to achieve this in practice will invariably meet with the gain-stability limitations discussed previously. With these points in mind, a practical consideration of the gain-bandwidth properties and a

feasible design procedure will be patterned after the techniques developed for the elementary amplifier of the preceding section.

The first step to be taken is that of establishing a useful analytical approximation for the half-power frequency of the Reflection amplifier. An incremental model of the Reflection amplifier with a Norton equivalent circuit taken at the input is shown in Figure 4.9.

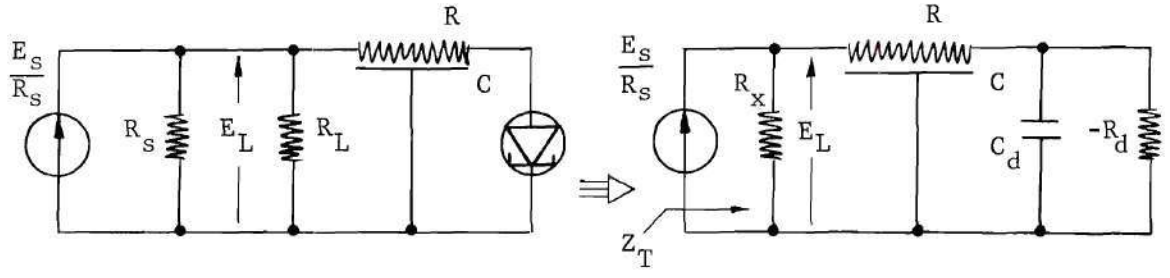

Figure 4.9 Incremental Model of the Reflection Amplifier.

The IPG can be cast in the form

$$IPG(\omega) = \left(\frac{R_s + R_L}{R_s R_L}\right)^2 \left|Z_T(j\omega)\right|^2$$

$$= \left(\frac{1}{R_x}\right)^2 \left|Z_T(j\omega)\right|^2 \quad , \tag{4.47}$$

where Z_T is the impedance indicated in Figure 4.9. The IPG thus reaches half its DC value when the magnitude of the impedance Z_T goes to $1/\sqrt{2}$ of its DC value. The input impedance Z_T is found to be

$$Z_T = \frac{R_x R_d R\Theta \cosh\Theta + (R_d C_d s - 1) R_x R^2 \sinh\Theta}{\left[\begin{array}{l} R_d R\Theta \cosh\Theta + (R_d C_d s - 1) R^2 \sinh\Theta \\ +(R_d C_d s - 1)\, R_x R\Theta \cosh\Theta + R_x R_d \Theta^2 \sinh\Theta \end{array}\right]} \quad , \tag{4.48}$$

where

$$\Theta = \sqrt{RCs} \ . \tag{4.49}$$

It has been found that, in the frequency range of interest here, a reasonable approximation for the hyperbolic functions in (4.48) is made by truncating their series expansions after the first three terms. Thus we take

$$\cosh\Theta \cong 1 + \frac{\Theta^2}{2!} + \frac{\Theta^4}{4!} = (1 + \frac{\Theta^2}{2} + \frac{\Theta^4}{24}) \ , \tag{4.50}$$

and

$$\sinh\Theta \cong \Theta + \frac{\Theta^3}{3!} + \frac{\Theta^5}{5!} = \Theta(1 + \frac{\Theta^2}{6} + \frac{\Theta^4}{120}) \ . \tag{4.51}$$

Substitution of (4.49), (4.50), and (4.51) in (4.48) yields an expression which is a rational function of the complex frequency variable, s. Numerical experience has shown that, in the frequency range of interest, the terms involving constants and the first power of s are predominant, and the impedance Z_T is approximated by

$$Z_T \cong \frac{\left[[(60R_xR_dR - 20R_xR^2)C + 120R_xRR_dC_d]s + 120R_x(R_d-R) \right]}{\left[[\{120R_xR_d + 60R(R_d-R_x) - 20R^2\}C + 120(R+R_x)R_dC_d]s + 120(R_d-R-R_x) \right]} \ . \tag{4.52}$$

Equation (4.52) is of the form

$$Z_T(s) \cong \frac{ks + m}{ds + e} \ . \tag{4.53}$$

This approximate expression for Z_T has the DC value

$$Z_T(0) = \frac{m}{e} = \frac{(R_d-R)}{(R_d-R-R_x)} = \frac{(R_d-R)}{(R_d-R_{eq})} , \tag{4.54}$$

which is an <u>exact</u> expression, and the angular frequency at which the magnitude of Z_T goes to $1/\sqrt{2}$ of this value is closely approximated by

$$\omega_{hp} \cong \frac{e}{d} . \tag{4.55}$$

Thus, we have

$$f_{hp} \cong \frac{6(R_d-R_{eq})}{2\pi[\{6R_xR_d + 3R(R_d-R_x) - R^2\} C + 6(R+R_x)R_dC_d]} . \tag{4.56}$$

Numerical experience also indicates that the denominator term of (4.56) involving the diode capacitance C_d will always be several orders of magnitude smaller than the other denominator term involving the line capacitance C. This is a consequence of the fact that the diode capacitance is always a very small parasitic quantity, and the line capacitance is a quantity that will be fixed by design and possesses a practical minimum value beyond which it should not be reduced if the distributed RC line is to retain the two-port properties that were assumed at the outset of the investigation. The expression of (4.56) does indeed show the general effect of each circuit parameter on the half-power frequency. Since C_d will always be much smaller than the line capacitance C, we can use the simpler expression

$$f_{hp}]_{\substack{\text{Reflection}\\ \text{amplifier}}} \cong \frac{6(R_d-R_{eq})}{2\pi[\,6R_xR_d + 3R(R_d-R_x) - R^2]C} , \tag{4.57}$$

where

$$R_{eq} = R + R_x \quad , \tag{4.58}$$

and

$$R_x = \frac{R_sR_L}{R_s+R_L} . \tag{4.59}$$

As in the previous section dealing with the elementary amplifier, the half-power frequency must now be expressed as a function of the DC gain value. The DC gain is of the form

$$IPG(0) \overset{\triangle}{=} K^2 , \tag{4.60}$$

and, from Appendix A, we find that

$$K = \frac{R_d-R}{R_d-R_{eq}} = \frac{R_d-R}{R_d-R-R_x} . \tag{4.61}$$

From (4.61) we see that, for a specified DC gain of value K^2, we must have

$$R_d = \left(\frac{K}{K-1}\right) R_x + R , \tag{4.62}$$

and this expression will be useful later in the design of the Reflection amplifier. Using (4.62) we can write

$$(R_d-R_{eq}) = (R_d-R) - R_x = \frac{R_x}{(K-1)} . \tag{4.63}$$

Substituting (4.63) into (4.57) and eliminating R_d with (4.62) yields

$$f_{hp} \cong \frac{1}{2\pi C} \frac{6R_x}{K[6R_x^2 + 6RR_x + 2R^2] - (3RR_x + 2R^2)} . \tag{4.64}$$

In the design problem, we will be given the desired value of IPG(0) and f_{hp} (with specified values of source and load resistances), and it will be our task to select the parameter values of the active insertion two-port so as to meet the design specifications. It is convenient at this point to define two design parameters in the form of resistance ratios in order to generalize, as far as possible, the results of this section as well as the design procedure that follows. Specifically, these design parameters (a and b) are defined by the relations

$$R_s = aR_L , \tag{4.65}$$

and

$$R = bR_s = abR_L . \tag{4.66}$$

Using (4.65) and (4.66), (4.64) may be cast in the form

$$f_{hp} \cong \frac{1}{2\pi R_L C} \frac{6(a+1)}{\left[K[6a + 6a(a+1)b + 2a(a+1)^2b^2] - [3a(a+1)b + 2a(a+1)^2b^2]\right]} . \tag{4.67}$$

It is convenient to again define the normalized half-power frequency as

$$(f_{hp}) \triangleq 2\pi R_L C \cdot (f_{hp}) . \tag{4.68}$$

Thus, for the Reflection amplifier we have

$$(f_{hp})_N \underset{\text{Reflection}}{\cong} \frac{6(a+1)}{\left[K[6a + 6a(a+1)b + 2a(a+1)^2b^2] \right] \atop \left[-[3a(a+1)b + 2a(a+1)^2b^2] \right]} \quad . \tag{4.69}$$

Likewise, it is again convenient to define the normalized gain-bandwidth product as

$$\begin{aligned} (GBP)_N &\overset{\Delta}{=} 2\pi R_L C \cdot (GBP) \\ &= 2\pi R_L C \cdot [IPG(0) \cdot f_{hp}] \\ &= IPG(0) \cdot (f_{hp})_N \quad . \end{aligned} \tag{4.70}$$

Therefore, for the Reflection amplifier we have

$$(GBP)_N \underset{\text{Reflection}}{\cong} \frac{IPG(0) \cdot 6(a+1)}{\left[K[6a + 6a(a+1)b + 2a(a+1)^2b^2] \right] \atop \left[-[3a(a+1)b + 2a(a+1)^2b^2] \right]} \quad . \tag{4.71}$$

Expressions (4.69) and (4.71) may be used to construct families of curves that give the normalized half-power frequency and gain-bandwidth product as a function of the DC gain, IPG(0). Examples of this construction for typical values of the parameters a and b are shown in Figures 4.10 and 4.11.

These curves are used in precisely the same manner as those for the elementary amplifier. For specified values of IPG(0), source and load resistances, and a selected value of line resistance, the corresponding value of $(f_{hp})_N$ is taken directly from Figure 4.10. For that value of

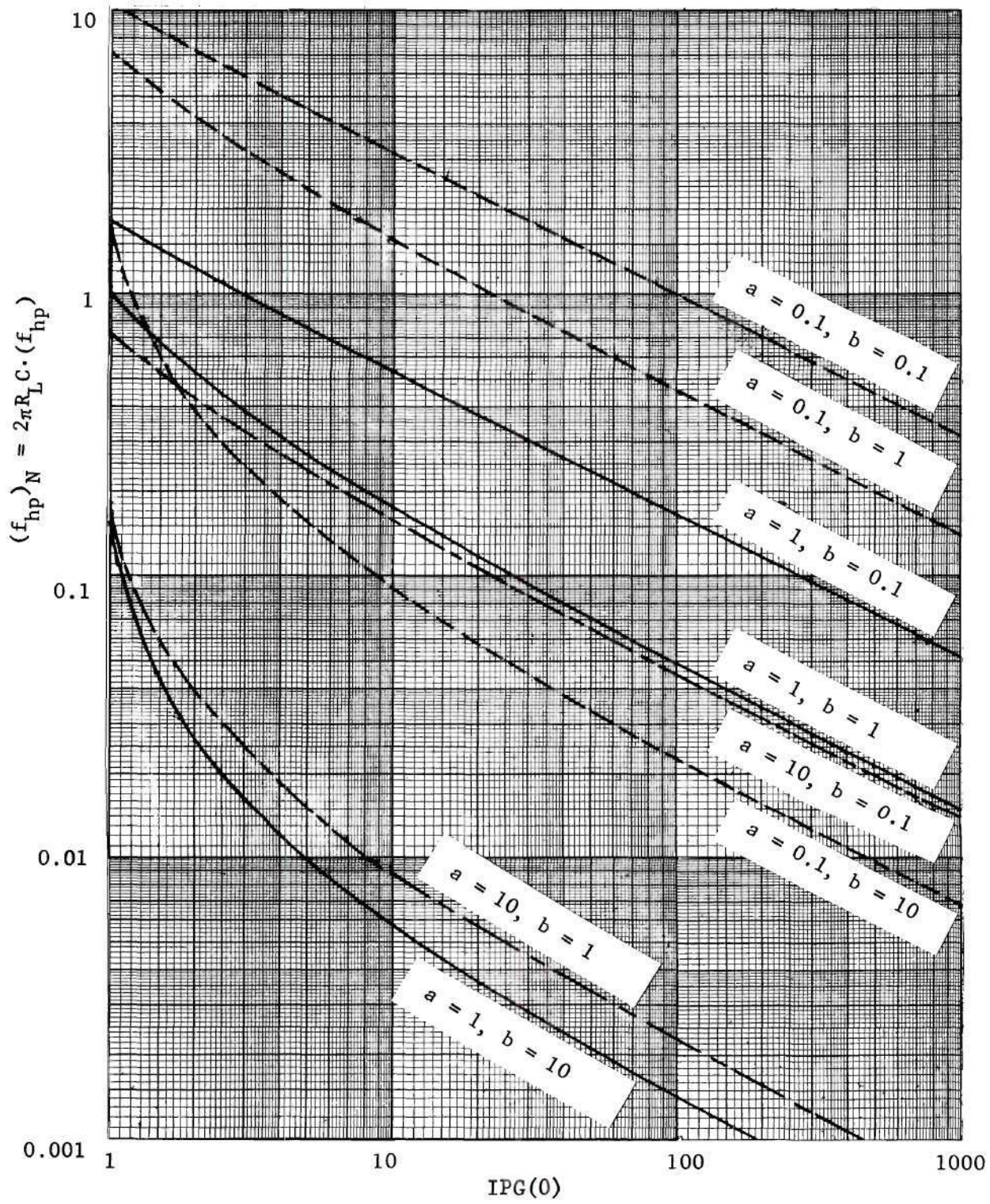

Figure 4.10 Normalized Half-Power Frequency vs. IPG(0) for the Reflection Amplifier.

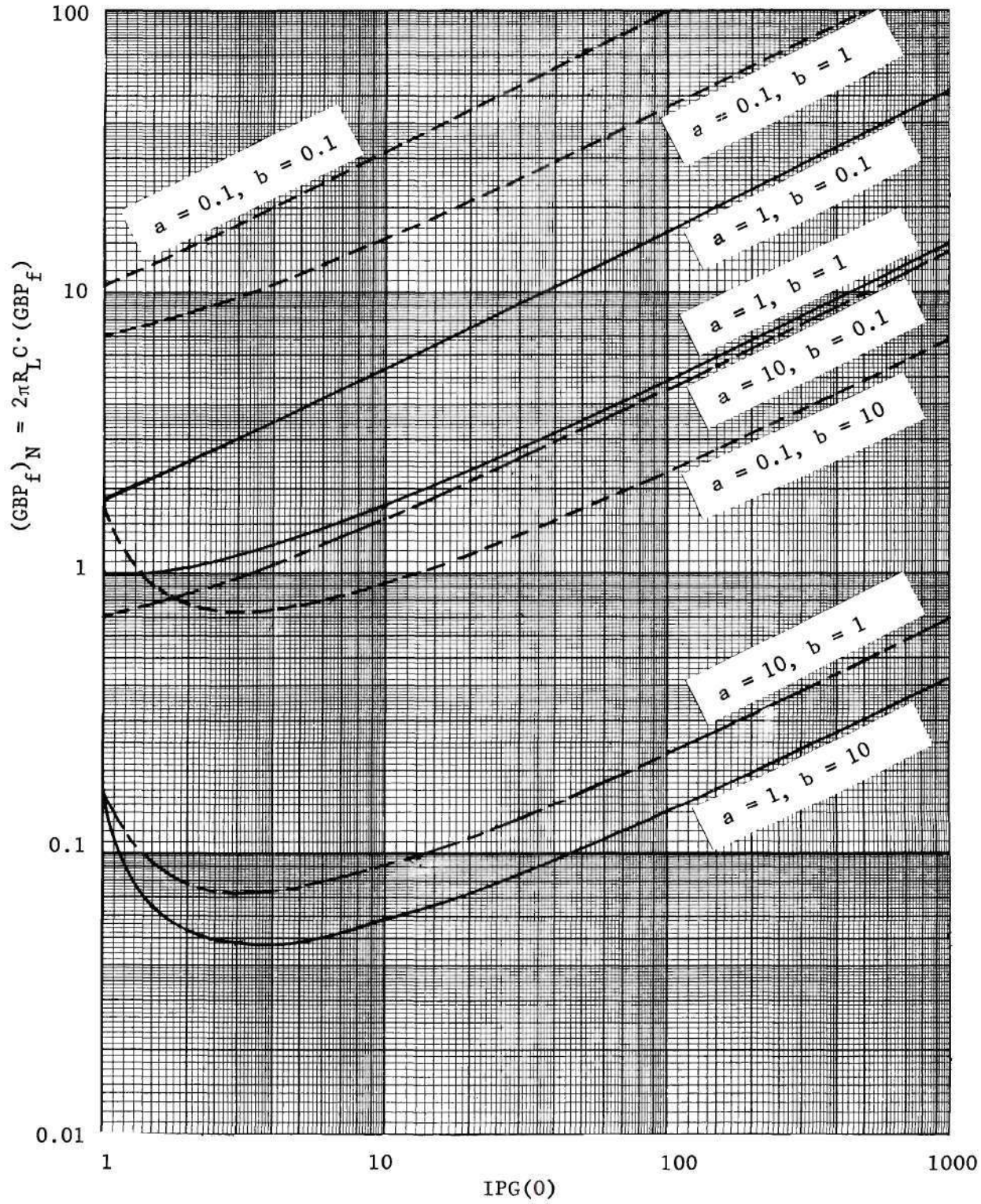

Figure 4.11 Normalized Gain-Bandwidth Product vs. IPG(0) for the Reflection Amplifier.

IPG(0) we compute

$$(f_{hp})_{max} = \frac{(f_{hp})_N}{2\pi R_L C_{min}} \quad , \tag{4.72}$$

where R_L is the specified load resistance, and C_{min} is the minimum allowable value of the line capacitance. Likewise for the specified values of IPG(0) and the resistance ratios (a and b), the $(GBP)_N$ is taken directly from Figure 4.11. We then compute

$$(GBP)_{max} = \frac{(GBP)_N}{2\pi R_L C_{min}} \quad . \tag{4.73}$$

If, however, f_{hp} is specified (along with the appropriate resistance values), we compute

$$(f_{hp})_{N_{min}} = 2\pi R_L C_{min} \cdot (f_{np}) \quad , \tag{4.74}$$

and since IPG(0) is a decreasing function of $(f_{hp})_N$, we take $IPG(0)]_{max}$ directly from Figure 4.10. At this value of IPG(0) we take $(GBP)_N]_{max}$ directly from Figure 4.11, and compute

$$(GBP)_{max} = \frac{(GBP)_N]_{max}}{2\pi R_L C_{min}} \quad . \tag{4.75}$$

As an example of the accuracy attainable with the curves of Figures 4.10 and 4.11 let us consider the response curves shown in Figure 4.6. For the circuit parameters designated, a=1, b=0.1, and $2\pi R_L C = 37.69908 \times 10^{-6}$. From Figures 4.10 and 4.11 we read and compute

the following:

1. At IPG(0) = 25, $(f_{hp})_N \cong 0.334 \rightarrow f_{hp} \cong 8.86$ KHz ,

$(GBP)_N \cong 8.4 \rightarrow GBP \cong 222.8$ KHz ,

2. At IPG(0) = 64, $(f_{hp})_N \cong 0.210 \rightarrow f_{hp} \cong 5.570$ KHz ,

$(GBP)_N \cong 13.2 \rightarrow GBP \cong 350.14$ KHz ,

and

3. At IPG(0) = 100, $(f_{hp})_N \cong 0.164 \rightarrow f_{hp} \cong 4.350$ KHz ,

$(GBP)_N \cong 16.4 \rightarrow GBP \cong 435.0$ KHz .

These "predicted" values are all within two per cent of the exact values calculated via the transfer function and shown in Figure 4.6.

Another functional relationship that is very useful to the network designer is found by considering the approximation for $(f_{hp})_N$ as a function of the resistance ratio b with the ratio a and IPG(0) taken as parameters. Rewriting equation (4.69), we have

$$(f_{hp})_N \underset{\text{Reflection}}{\cong} \frac{6(a+1)}{[2a(a+1)^2(K-1)]b^2 + [3a(a+1)(2K-1)]b + [6aK]} . \qquad (4.76)$$

This is of the form

$$(f_{hp})_N \cong \frac{N}{D\,b^2 + Eb + F} , \qquad (4.77)$$

where the coefficients N, D, E, and F indicated in (4.76) are all positive if $K = \sqrt{IPG(0)} > 1$. For all positive coefficients, the general

shape of the graph of (4.76) is shown in Figure 4.12.

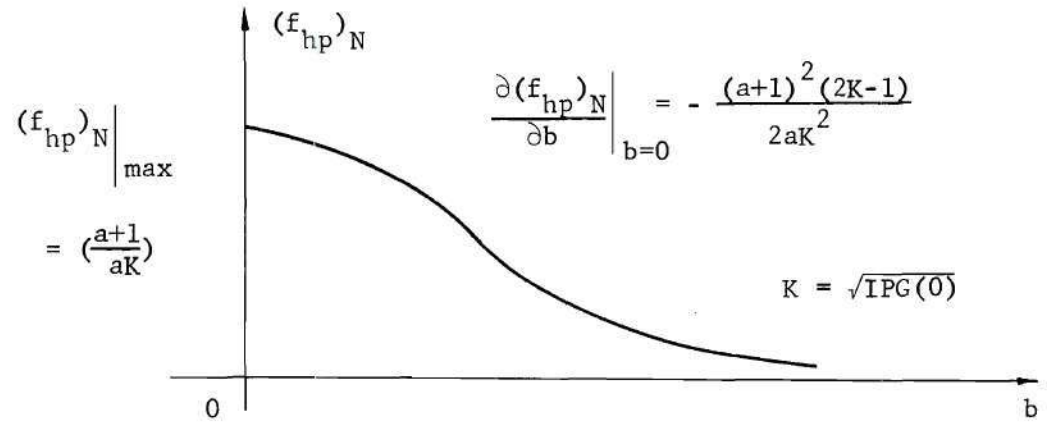

Figure 4.12 Normalized Half-Power Frequency vs. b for the Reflection Amplifier.

Examples of this graph for selected values of IPG(0) and the parameter a are shown plotted to logarithmic scales in Figures E.1, E.2, and E.3 of Appendix E.

To illustrate the usefulness of these graphs, let us consider one step in the design of the three amplifiers presented in Figure 4.6. The details of the complete design procedure will be covered in the following section, and for the present we will be concerned only with choosing the values of the line parameters R and C. The specifications for the three amplifiers are:

1. IPG(0) = 25, f_{hp} = 8.961 KHz with $R_s = R_L$ = 200Ω, (a=1),
2. IPG(0) = 64, f_{hp} = 5.549 KHz with $R_s = R_L$ = 200Ω, (a=1),

and

3. IPG(0) = 100, f_{hp} = 4.425 KHz with $R_s = R_L$ = 200Ω, (a=1).

At this point it should be noted that there is a certain degree of

flexibility characteristic of the design problem. The network designer has the freedom to choose the value of R (and hence the ratio parameter b) and then compute the value of C required to achieve the specified half-power frequency, or he could choose the value of C and compute the value of R needed. As we shall see, there are definite considerations to be made when making this choice such as the role of the line resistance in the stability criterion and the resulting magnitudes required of the remaining circuit parameters, but these are details to be covered in the next section. For the sake of illustration here, let us choose $R = 20\Omega$ so that $b = 0.1$ for all three amplifiers. From Figures E.1, E.2, and E.3 we find:

$$1. \quad (f_{hp})_N \cong 0.328,$$

$$2. \quad (f_{hp})_N \cong 0.205,$$

and

$$3. \quad (f_{hp})_N \cong 0.164.$$

Since

$$(f_{hp})_N \overset{\Delta}{=} 2\pi R_L C \cdot (f_{hp}) , \tag{4.78}$$

we compute the required value of the line capacitance as

$$C = \frac{(f_{hp})_N}{2\pi R_L \cdot (f_{hp})} . \tag{4.79}$$

For the three cases at hand, we find:

$$1. \quad C \cong \frac{(0.328)}{2\pi(200)(8.91 \times 10^3)} = 0.02912 \ \mu f ,$$

$$2.\quad C \cong \frac{(0.205)}{2\pi(200)(5.549 \times 10^{3})} = 0.02939\ \mu f\ ,$$

and

$$3.\quad C \cong \frac{(0.164)}{2\pi(200)(4.425 \times 10^{3})} = 0.02949\ \mu f\ .$$

Each of these values is within three percent of the exact value used in the calculations for the frequency responses of Figure 4.6, and this is within the tolerance that can be expected of the physical circuit components.

Design Considerations

Generally speaking, the question of utmost importance in the initial stage of the design problem is that of overall circuit stability and the consequences of the inherent gain-stability limitation. For the Reflection amplifier, the stability criterion is

$$R_d > R_{eq} = R + \frac{R_s R_L}{R_s + R_L}\ . \tag{4.80}$$

In terms of the resistance ratio parameters, this expression may be written as

$$R_d > R_{eq} = \left[ab + \frac{a}{(a+1)}\right] R_L\ . \tag{4.81}$$

For a specified value of IPG(0) = K^2, the value of the required diode resistance is given in (4.61) as

$$R_d = \left(\frac{K}{K-1}\right) \frac{R_s R_L}{R_s + R_L} + R\ , \tag{4.82}$$

and, in terms of the resistance ratios, this may be written as

$$R_d = \left[\left(\frac{K}{K-1}\right) \frac{a}{a+1} + ab \right] R_L \ . \tag{4.83}$$

Inspection of (4.81) in terms of (4.83) shows that the stability criterion is always met if the diode resistance is selected via (4.83). In a practical design, however, the margin by which R_d is greater than R_{eq} should not be fixed arbitrarily. In general, the design procedure should be one in which this degree of "stability margin" is taken into account and related to the other performance specifications of gain and half-power frequency. In this light, it is convenient to assign the diode resistance with the relation

$$R_d = \left(1 + \frac{\Lambda}{100}\right) R_{eq}, \tag{4.84}$$

where Λ is defined as the <u>percent stability margin</u>. Substituting (4.83) and the equality of (4.81), we can write

$$(\Lambda)_{\text{Refl.}} = \frac{100}{(K-1)[(a+1)b+1]} \ . \tag{4.85}$$

From (4.85), it is apparent that

$$\Lambda_{\text{Refl.}} \leq \frac{100}{(K-1)} \ , \tag{4.86}$$

with the equality satisfied only when b=0. From the above expression we deduce that

$$\text{IPG}(0)_{\text{Refl.}} \overset{\Delta}{=} K^2 \leq \left(\frac{100}{\Lambda} + 1\right)^2 \ . \tag{4.87}$$

This is an interesting expression in that it is another manifestation of the previously discussed gain-stability limitation. If, for example, practical considerations dictate a stability margin of ten per cent (Λ=10), then we know at the outset that the DC gain cannot exceed 121, and it will be less than this value for all values of b greater than zero.

Graphs of (4.85), considering Λ as a function of the parameter b, are also useful to the network designer. From (4.85) we find

$$\frac{\partial \Lambda}{\partial b} = - \frac{100}{(K-1)} \quad \frac{(a+1)}{[(a+1)b+1]^2} \quad , \tag{4.88}$$

and the general shape of the graph of (4.85) is shown in Figure 4.13.

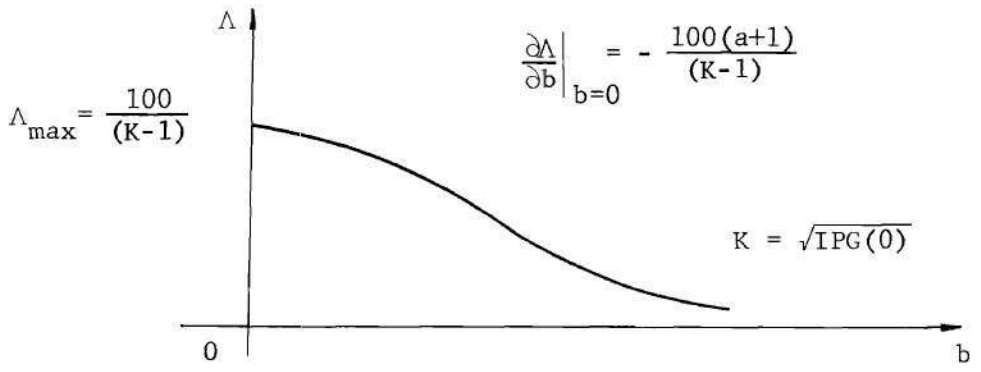

Figure 4.13 Percent Stability Margin vs. b for the Reflection Amplifier.

Families of this graph, for selected values of IPG(0) and the parameter a, are shown plotted to logarithmic in Figures E.4, E.5, and E.6 of Appendix E.

As stated previously, the design problem of interest here is one

in which the desired values of IPG(0) and f_{hp} are specified along with the source and load resistances that terminate the insertion two-port. The task of the network designer is to select the parameter values of the insertion two-port so that the design specifications are met while, at the same time, taking into account any practical limitations that might have an effect on the performance of the amplifier.

In addition to the practical considerations presented in Chapters II and III regarding the physical layout of these amplifiers and its effect on the circuit stability, there are other salient points that should be kept in mind. An upper limit on the design parameter b can arise from several causes. Let us assume first that the source and load resistances are fixed (hence a is fixed), and we are given a transmission line of fixed area and geometry. There is an upper limit on the resistance per square that can be achieved reliably with the present state-of-the-art thin-film technology.* Hence, the total line resistance for the given geometry will have some upper limit, R_{max}. Since

$$R = abR_L, \tag{4.89}$$

we have

$$b_{max} = \frac{R_{max}}{aR_L} . \tag{4.90}$$

Another factor that can limit the parameter b to some maximum value is its relationship to the half-power frequency and the line capacitance, C. From Figure 4.12 we are reminded that $(f_{hp})_N$ is a

---

* Holland cites this upper limit in the order of 4000 ohms per square [10].

decreasing function of b. For a specified value of half-power frequency, f_0, we compute the required line capacitance from (4.79) as

$$C = \frac{(f_{hp})_N}{2\pi R_L \cdot f_0} \quad . \tag{4.91}$$

Hence, the required line capacitance is a decreasing function of b. The present thin-film technology is also limited in the minimum value of the capacitance per unit area that can be attained with reliability.* It is this limit beyond which the capacitance per unit area must be decreased by increasing the thickness of the dielectric film. If this is carried too far, however, the transmission line is no longer described by the two-port parameters assumed at the outset of this study. Thus, increasing b eventually leads to a point where the line capacitance attainable with the given line geometry is reduced to

$$C_{min} = \frac{(f_{hp})_{N\ min}}{2\pi R_L \cdot f_0} \quad , \tag{4.92}$$

and a further increase in the parameter b is not possible. Another point that dictates against high values of b is that the required diode resistance given in (4.83) increases linearly with b, and large values of b can require large values of R_d in the design. This is impractical since the tunnel diode is inherently a low impedance device, and values of R_d nominally greater than 600 ohms are uncommon. The most stringent limitation on the maximum value of b, however, is the fact that the

---

* Holland cites this value in the order of 0.001 μf per cm^2 [11].

percent stability margin, Λ, is a decreasing function of b. In every case, there is some minimum value of the stability margin, Λ_{min}, beyond which any design would be impractical. Thus, design parameter b has an upper limit placed on it by a decreasing stability margin. The specific value of Λ_{min} (and hence b_{max}) depends on the power supply used, its internal resistance, the regulation of its supply voltage, the tolerances of the resistors in the circuit, and any other practical considerations that may affect the location and stability of the operating point and the associated load line. In any particular application, a decision will have to be made on an acceptable Λ_{min} consistent with sound engineering judgement. It appears, then, that we should attempt to make the parameter b as small as possible. This seems reasonable since the stability margin increases with decreasing b, and the required value of diode resistance decreases with decreasing b. On the other hand, decreasing b beyond a certain point leads to other problems of a practical nature. The present thin-film technology also has limitations on the minimum resistance per square and the maximum capacitance per unit area that can be reliably achieved.* Hence, for a given line geometry, the line resistance will have some lower limit, R_{min}, and b is limited to

$$b_{min} = \frac{R_{min}}{aR_L} . \tag{4.93}$$

In addition, since $(f_{hp})_N$ increases with decreasing b, we see from (4.91) that for a specified half-power frequency, f_0, the required line

---

* Holland cites these values in the order of 0.36 ohms per square and 0.3 μf per cm^2, respectively [12].

capacitance increases with decreasing b. Thus, decreasing b will eventually lead to a point where the required line capacitance increases to

$$C_{max} = \frac{(f_{hp})_{N\ max}}{2\pi R_L \cdot f_0} , \qquad (4.94)$$

beyond which it cannot be increased with the given line geometry. Hence, the design parameter b also has a lower limit on its range because of the limitation on the maximum capacitance that is attainable.

There is an additional point that should be considered. The magnitude of the diode resistance must be greater than the sum of the resistors R and the parallel combination of R_s and R_L. Since tunnel diodes with a negative resistance of 600 ohms or more are relatively uncommon, R_{eq} given by (4.81) should be in a range falling below 600 ohms. From the curves of Appendix E we also see that, for $a \leqq 1$, we get large values of $(f_{hp})_N$ and very large values of Λ, particularly for $b \leqq 0.1$. Thus we see that the Reflection amplifier is best suited for those cases where R_s is equal to or less than R_L and the overall impedance level is low.

Design Example and Experimental Results

As an example of a typical design procedure, let us consider the following problem: A Reflection amplifier is desired that will operate between equal source and load terminations of 790 ohms while providing an IPG of 25(13.98 db) in the pass band with a half-power bandwidth of 6.5 KHz. For equal values of R_s and R_L (a=1) and IPG(0) = 25, the curves of Figures E.1 and E.4 serve as the basis of the design. Simultaneous consideration of both curves points out the freedom allowed the

designer in the choice of the parameter b. For the case at hand, it was decided to choose b = 0.057, thus attaining the relatively high stability margin that may be achieved for this relatively low value of IPG(0). At the same time, this value of b results in a near-maximum value of $(f_{hp})_N$ and a physically realizable value of the required diode resistance, R_d, consistent with the specified values of the parameter a and IPG(0).

For IPG(0) = 25(K=5), a = 1, and b = 0.057, the curves of Figures E.1, and E.4 yield respectively

$$(f_{hp})_N \cong 0.350 \ ,$$

and

$$\Lambda \cong 22.5 \ .$$

For the specified value f_{hp} = 6.5 KHz = f_0, (4.91) is used to compute the required value of line capacitance as

$$C = \frac{(f_{hp})_N}{2\pi R_L \cdot f_0}$$

$$= \frac{0.350}{(6.28318)(790)(6.5\times10^3)}$$

$$= 10.848 \text{ nf} \ . \qquad (4.95)$$

The required line resistance is

$$R = bR_s$$

$$= (0.057)(790)$$

$$= 45.03 \ \Omega \ , \qquad (4.96)$$

and the required value of diode resistance is computed from (4.83) as

$$R_d = \left[\left(\frac{K}{K-1}\right)\left(\frac{a}{a+1}\right) + ab \right] R_L$$

$$= \left[\left(\frac{5}{4}\right)\left(\frac{1}{2}\right) + 0.057 \right] (790)$$

$$= 538.78\ \Omega\ . \qquad (4.97)$$

In the experimental verification of these results, a model of the uniform line was fabricated using radio-frequency shielding paint and Mylar film, as described in Chapter II. It is appropriate at this point to describe the technique used in measuring its parameters. The total line resistance, R, may be accurately determined by a simple DC measurement with an impedance bridge connected to the terminals 1-2 indicated in Figure 4.14. The measurement of the effective line capacitance C

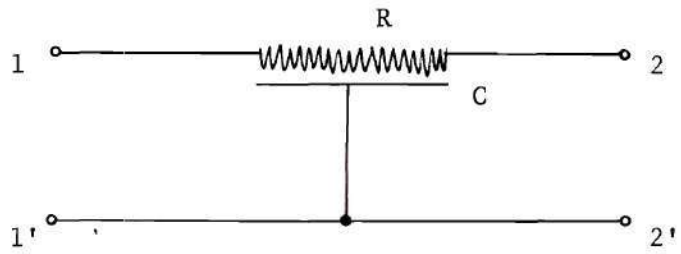

Figure 4.14 The Uniform RC Transmission Line.

is not as simple, however. Most impedance bridges measure capacitive reactance at a nominal frequency of 1.0 KHz, and a capacitance measurement made between terminals 1-1' or 2-2' will be in error since the impedance measured there will possess a resistive component at frequencies above DC. Depending on the relative magnitudes of R and C and the

frequency of measurement, the error may or may not be significant. Because of this ambiguity, the above technique of measuring C is not recommended. A more accurate method makes use of the null properties of the uniform line summarized in Figure 2.6 of Chapter II. As indicated by Figure 2.6(a), a transmission zero can be achieved by connecting a resistance in two-port series with the line. This situation is indicated in Figure 4.15 and is the basis of the capacitance measurement. The line resistance, R, as well as the null-producing resistance, R_n, can be

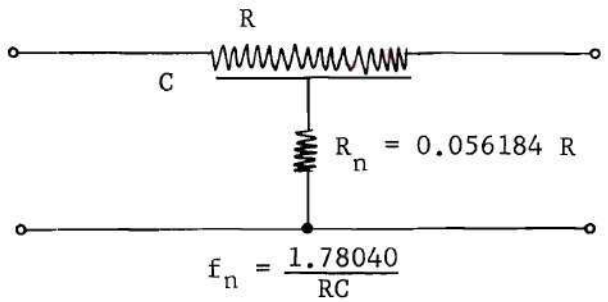

Figure 4.15 RC Transmission Line with Series Null-Producing Resistance.

measured accurately with a bridge, and the null frequency can be measured accurately with an electronic counter. The effective line capacitance is then computed from the null frequency expression as

$$C = \frac{1.78040}{R \cdot f_n} \quad . \tag{4.98}$$

The parameters of the model transmission line fabricated for this design example were measured using the above technique and found to be

$$R = 45.0\ \Omega\ ,$$

and

$$C = 10.9 \text{ nf} .$$

A Hoffman 1N2928 tunnel diode (having a nominal shunt capacitance, C_d, of 50 pf) biased at 160 mv was used to achieve the required negative resistance. The bias adjustment of the tunnel diode as well as the actual measurement of IPG vs. frequency is facilitated by the relationship between the IPG and voltage amplification of the general amplifier shown in Figure 4.16.

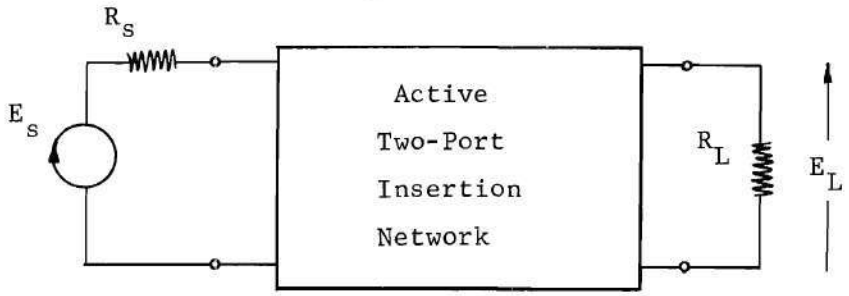

Figure 4.16 The General Amplifier Configuration.

The definition of insertion power gain is

$$IPG \triangleq \frac{\left(\begin{array}{c}\text{Power delivered to the load with} \\ \text{the active two-port inserted.}\end{array}\right)}{\left(\begin{array}{c}\text{Power delivered to the load when} \\ \text{connected directly to the source.}\end{array}\right)} = \frac{P_{LA}}{P_{LO}} \tag{4.99}$$

From Figure 4.16 we see that

$$P_{LO} = \left[\frac{|E_s(j\omega)|R_L}{(R_s + R_L)}\right]^2 \cdot \frac{1}{R_L}$$

$$= \frac{|E_s(j\omega)|^2 R_L}{(R_s + R_L)^2} , \tag{4.100}$$

and

$$P_{LA} = \frac{|E_L(j\omega)|^2}{R_L} \quad . \tag{4.101}$$

Thus

$$IPG(\omega) = \frac{|E_L(j\omega)|^2}{R_L} \cdot \frac{(R_s+R_L)^2}{|E_s(j\omega)|^2 \cdot R_L}$$

$$= \frac{(R_s+R_L)^2}{R_L^2} \cdot \left|\frac{E_L(j\omega)}{E_s(j\omega)}\right|^2$$

$$= \left(\frac{R_s+R_L}{R_L}\right)^2 \cdot |A_v(j\omega)|^2 \quad , \tag{4.102}$$

where

$$A_v(j\omega) \triangleq \frac{E_L(j\omega)}{E_s(j\omega)} \tag{4.103}$$

is, by definition, the complex voltage amplification of the overall amplifier configuration. Thus, we see that the IPG may be measured by simply measuring the magnitude of the voltage amplification. At DC, we have

$$IPG(0) = \left(\frac{R_s+R_L}{R_L}\right)^2 \cdot |A_v(0)|^2 \quad . \tag{4.104}$$

Using previous definitions, we may write this as

$$K^2 = (a+1)^2 \cdot |A_v(0)|^2 \quad , \tag{4.105}$$

and we have the simple relationship

$$K = (a+1) \cdot |A_v(0)| \ . \qquad (4.106)$$

Therefore, for a specified value of $IPG(0) = K^2$ and resistance ratio a, the input voltage is fixed at a very low frequency, the bias is adjusted so that

$$|A_v(0)| = \frac{K}{(a+1)} \ , \qquad (4.107)$$

and that value of bias is maintained throughout the measurement of $|A_v(j\omega)|$ over the frequency range of interest. For the example under discussion, K = 5, and a = 1, thus the bias was adjusted to achieve a low-frequency voltage amplification of $|A_v(0)| = 5/2 = 2.5$.

The resulting frequency response is shown in Figure 4.17. The solid curve depicts the theoretically predicted response calculated via the exact gain expression given in Appendix A. Superimposed are points representing the measurements made on the prototype amplifier. The experimental results were in close agreement with the calculated response as well as the results predicted from the design curves of Figures E.1 and E.4. The exact value of f_{hp} for the chosen set of parameters was calculated to be 6.674 KHz which was 2.7 per cent higher than the design goal of 6.5 KHz. The value of f_{hp} achieved experimentally was 6.810 KHz which was 4.8 per cent higher than the design goal. These results are well within the tolerances normally accepted in practice. If greater accuracy is desired, the most efficient and rapid method of achieving it is by making a few incremental changes in the value of the line capacitance used in the computer calculation of the exact response. The value

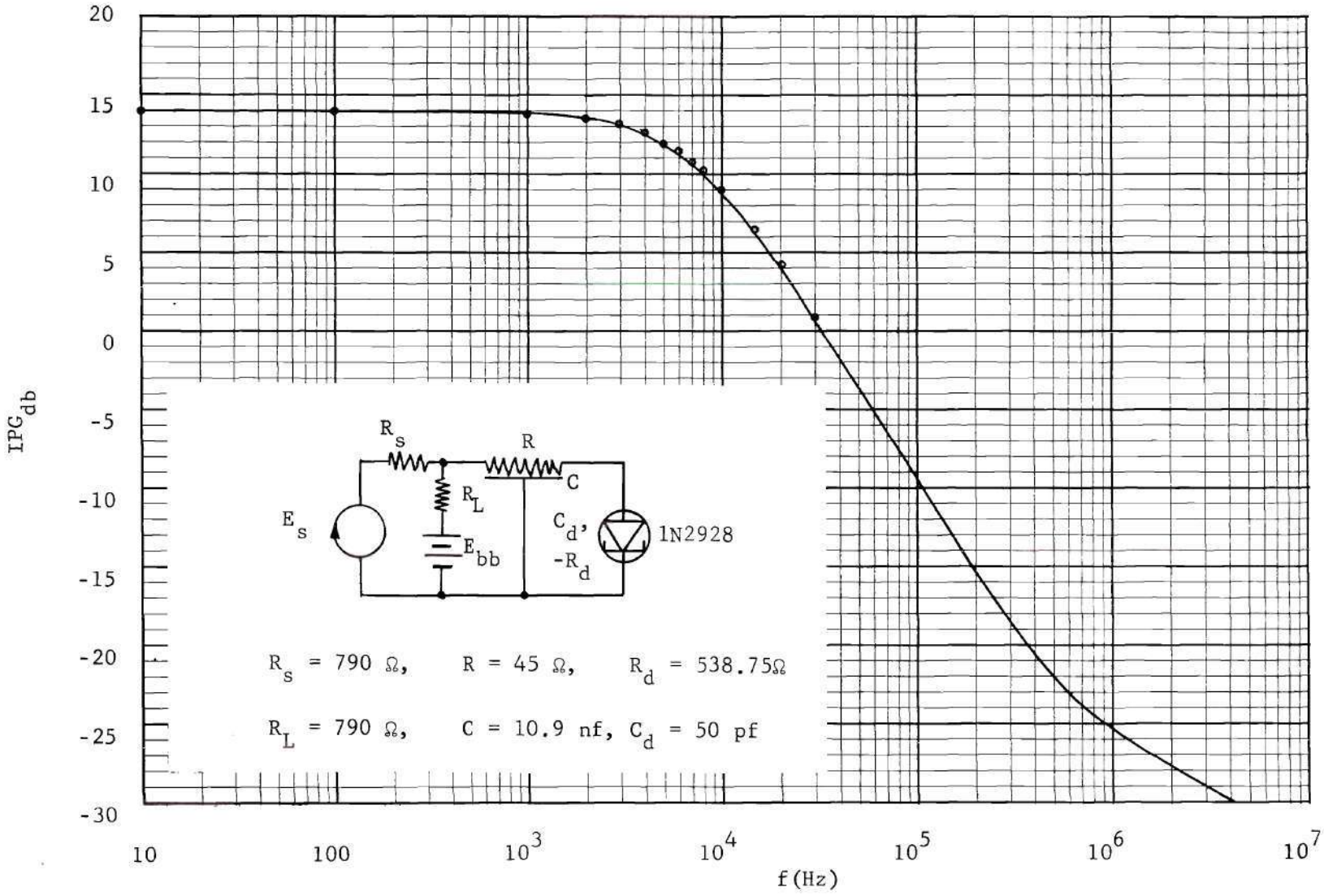

Figure 4.17 IPG-Frequency Response of Prototype Reflection Amplifier.

of line capacitance required for a specified half-power frequency can then be found to any desired degree of accuracy by making a few reiterative calculations.

The Series Amplifiers

Gain-Bandwidth Properties

The next amplifiers to be discussed are of the Series type. The Series I and Series II configurations are shown in Figure 4.18, and expressions for their IPG are given in Appendix C.

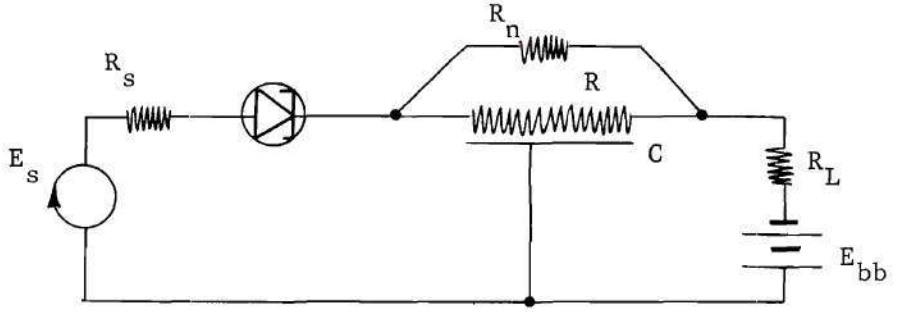

(a) The Series I Amplifier.

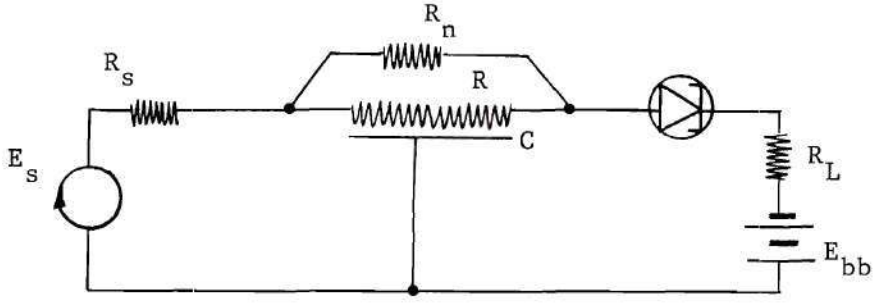

(b) The Series II Amplifier.

Figure 4.18 The Series Amplifier Configurations.

At this point, it should be noted that there is a symmetry of form in all of the analytical work describing the Series amplifiers. Since

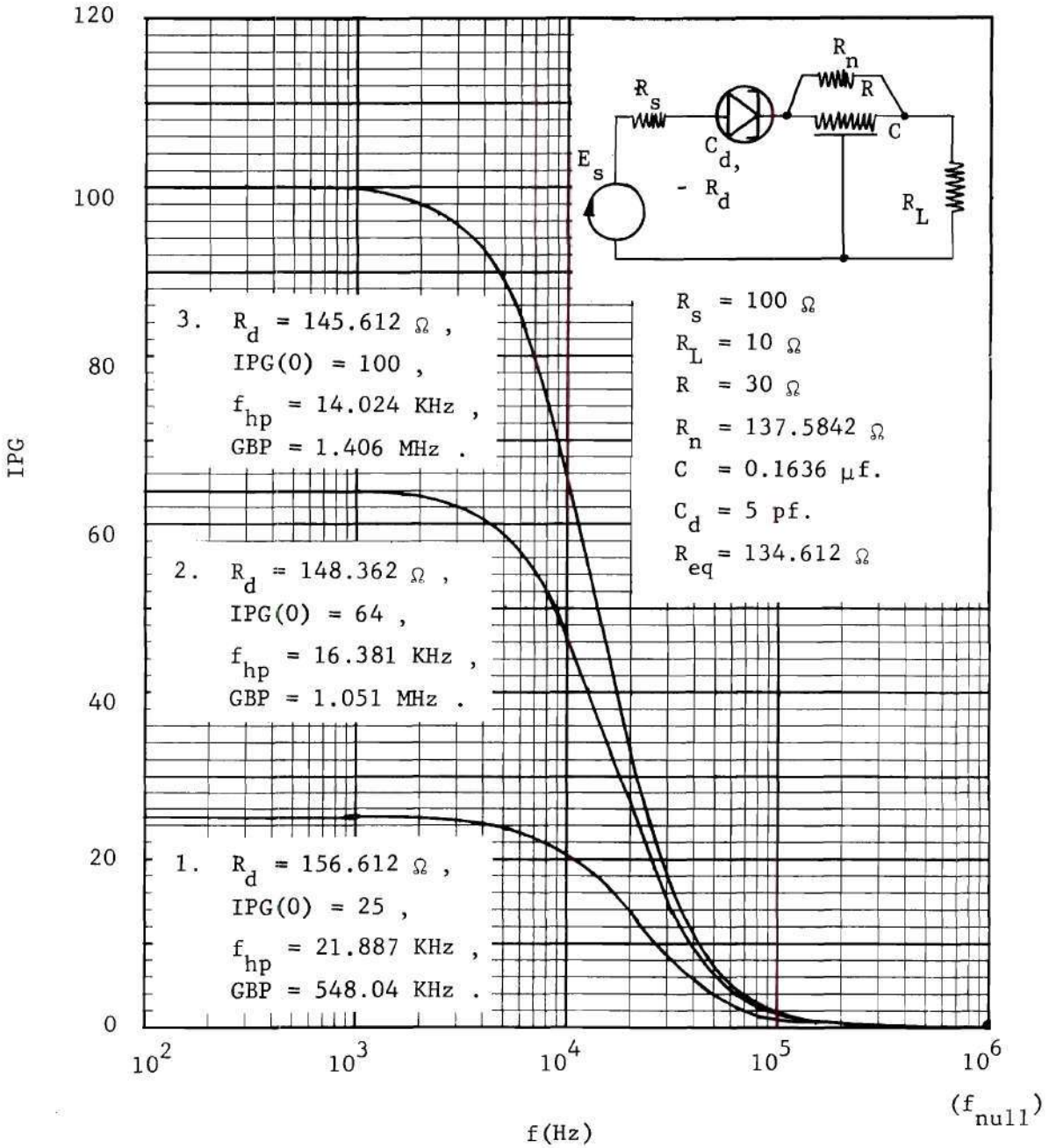

Figure 4.19 Typical IPG-Frequency Response Curves for the Series I Amplifier.

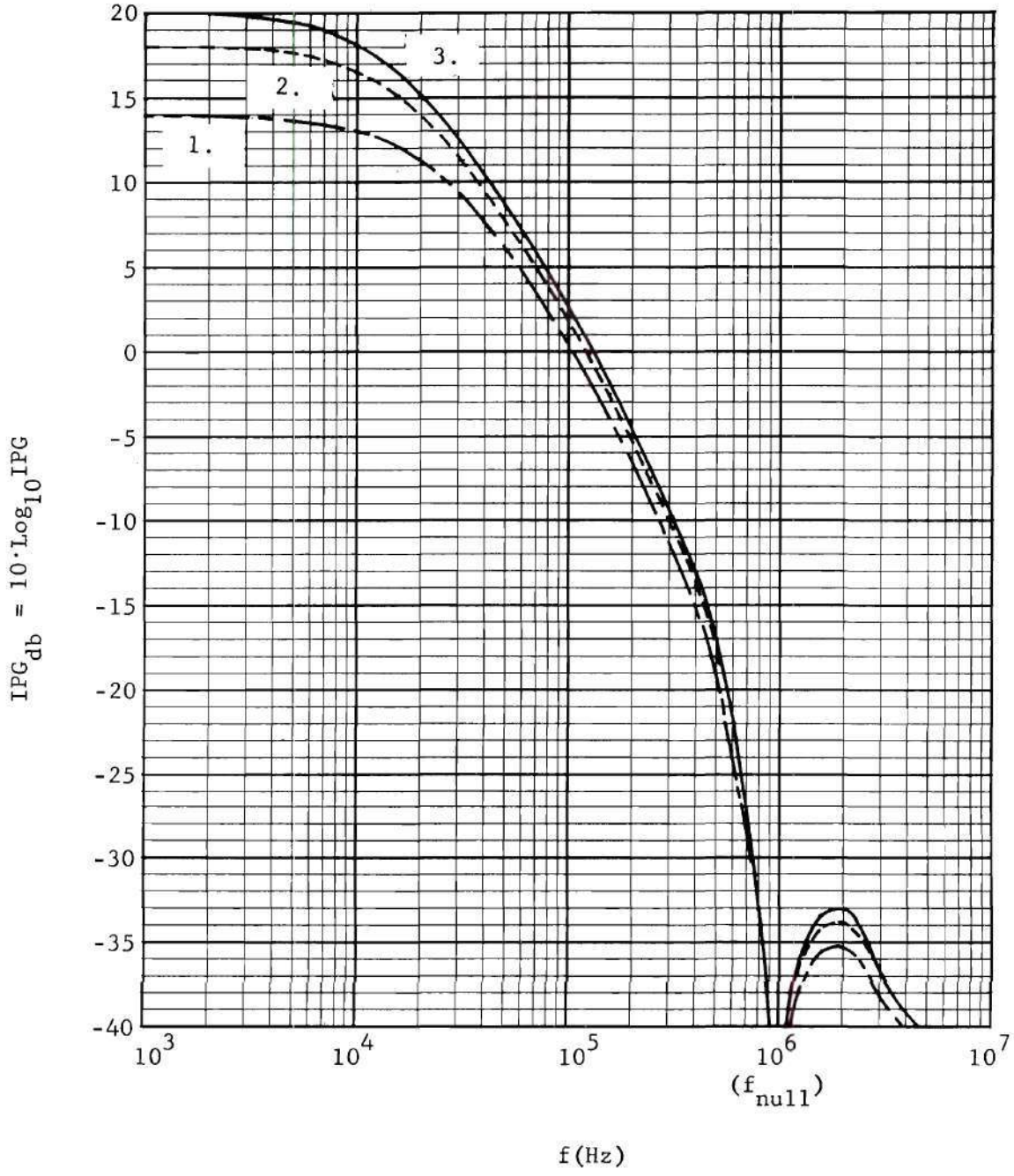

Figure 4.20 The IPG-Frequency Response Curves of Figure 4.19 in Decibels.

the networks are reciprocal, any result derived for the Series I configuration is equally valid for the Series II configuration provided an interchange is made between R_s and R_L everywhere in the analysis. With this point in mind, the Series I configuration occupies the majority of the following presentation, but the behavior of the Series II amplifier is simultaneously discussed, if the proper interpretation is made.

Some typical response curves for the Series I amplifier are shown in Figures 4.19 and 4.20. Again, we see that as the magnitude of the negative resistance approaches the resistance of the external circuit, the gain increases, the half-power frequency decreases, and the gain-bandwidth product increases. By exactly the same type of reasoning and analysis made for the Reflection amplifier, it has been found that the PBGA of the Series I amplifier may be made arbitrarily large, and there is no upper bound on the GBP of the Series I amplifier. Likewise, this property is of the same limited use as in the Reflection amplifier (for exactly the same reasons discussed there), and a practical consideration of the gain-bandwidth properties of the Series I amplifier will follow a pattern similar to that developed in the preceding sections.

A useful analytical approximation for the half-power frequency may be found from the expression for the IPG given in Appendix C. From the expression in Appendix C, the IPG may be expressed as

$$\text{IPG} = (R_s + R_L)^2 \, |\text{Ratio}|^2, \tag{4.108}$$

where

$$\text{Ratio} = \frac{Y_d[\Theta + G_n R \sinh \Theta]}{\left[\begin{array}{l} R_L(R_s Y_d+1)(sC) \sinh\Theta + [JY_d+K]\Theta \cosh\Theta \\ - [L(R_s Y_d+1)]\Theta + R(MY_d+G_n) \sinh\Theta \end{array}\right]} , \quad (4.109)$$

$$\Theta = \sqrt{RCs} , \quad (4.110)$$

and the remaining terms and constants in (4.109) are defined in Appendix C. Again, taking the approximate expressions

$$\cosh \Theta \cong (1 + \frac{\Theta^2}{2} + \frac{\Theta^4}{24}) , \quad (4.111)$$

and

$$\sinh \Theta \cong \Theta(1 + \frac{\Theta^2}{6} + \frac{\Theta^4}{120}) , \quad (4.112)$$

and retaining only those terms involving constants and the first power of s, we can approximate the indicated ratio by

$$\text{Ratio} \cong \frac{[-20G_dG_nR\Theta^2 - G_d(120+120G_nR) + 120(1+G_nR)C_ds]}{\left[\begin{array}{l} 120(R_L-R_LR_sG_d)Cs + 60(K-JG_d)\Theta^2 + 20(RG_n-RMG_d)\Theta^2 \\ + 120(J-LR_s+RM)C_ds + 120[(K-JG_d)-L(1-R_sG_d) \\ + (RG_n-RMG_d)] \end{array}\right]} . \quad (4.113)$$

If we substitute $\Theta^2 = sRC$, and (as before) neglect the terms involving the diode capacitance, C_d, the approximation becomes

$$\text{Ratio} \cong \frac{-20G_dG_nR^2Cs - 120G_d(1+G_nR)}{\left[\begin{array}{l}[120(R_L-R_LR_sG_d)C + 60(K-JG_d)RC + 20(RG_n-RMG_d)RC]s \\ + 120[(K-JG_d) - L(1-R_sG_d) + (RG_n-RMG_d)]\end{array}\right]} . \quad (4.114)$$

This is of the form

$$\text{Ratio} = \frac{ks + m}{ds + e} , \quad (4.115)$$

and the angular frequency at which the magnitude of this ratio goes to $1/\sqrt{2}$ of its DC value (and the IPG goes to half its DC value) is closely approximated by

$$\omega_{hp} \cong \frac{e}{d} . \quad (4.116)$$

Substituting the expressions for the constants J, K, L, and M from Appendix C, and the expression

$$R_{eq} = R_s + R_L + \frac{RR_n}{R+R_n} , \quad (4.117)$$

where

$$\frac{RR_n}{R+R_n} = R_p = 0.8204\ R , \quad (4.118)$$

enables us to write the approximation for the half-power frequency as

$$f_{hp} \underset{\text{Series I}}{\cong} \frac{1}{2\pi C} \frac{6(R_d - R_{eq})}{\left[\begin{array}{l}[6R_L + 2.64079R]R_d - [6R_sR_L \\ + (2.64079R)(R_s+R_L) + 0.8204R^2]\end{array}\right]} . \quad (4.119)$$

Again, it is convenient to express f_{hp} as a function of the DC gain value. From Appendix C, the DC gain is

$$IPG(0) = \left(\frac{R_s+R_L}{R_s-R_{eq}} \right)^2 \triangleq K^2 , \tag{4.120}$$

where

$$K \triangleq \frac{R_s+R_L}{R_d-R_{eq}} = \frac{R_s+R_L}{R_d - (R_s+R_L) - (0.8204R)} . \tag{4.121}$$

From (4.121) we see that for a specified DC gain of value K^2, we must have

$$R_d = (\frac{K+1}{K})(R_s+R_L) + (0.8204R) , \tag{4.122}$$

and this expression will be useful later in the design of the Series amplifiers. Using (4.121) we can write

$$(R_d-R_{eq}) = \frac{(R_s+R_L)}{K} . \tag{4.123}$$

Substituting (4.123) into (4.119) and eliminating R_d with (4.122) yields

$$f_{hp}\ \text{Series I} \cong \frac{1}{2\pi C} \frac{6(R_s+R_L)}{\left[K[6R_L(0.8204R+R_L) + (1.34610)R^2] + (R_s+R_L)[6R_L + (2.64079)R] \right]} . \tag{4.124}$$

It is convenient at this point to insert the design parameters, a and b, defined by (4.65) and (4.66) as

$$R_s = aR_L \ , \tag{4.125}$$

and

$$R = bR_s = abR_L \ , \tag{4.126}$$

so that the expression for the half-power frequency becomes

$$f_{hp}\Big|_{\text{Series I}} \cong \frac{1}{2\pi R_L C} \cdot \frac{(a+1)}{\left[\begin{array}{l} K[1 + (0.8204)ab + (0.22435)a^2b^2] \\ \quad + (a+1)[1 + (0.44013)ab] \end{array}\right]} \ . \tag{4.127}$$

Again, it is convenient to define the <u>normalized half-power frequency</u> and <u>normalized gain-bandwidth product</u> as in (4.68) and (4.70), so that, for the Series I amplifier, the final results are

$$(f_{hp})_N\Big|_{\text{Series I}} \cong \frac{(a+1)}{\left[\begin{array}{l} K[1 + (0.8204)ab + (0.22435)a^2b^2] \\ \quad + (a+1)[1 + (0.44013)ab] \end{array}\right]} \ . \tag{4.128}$$

and

$$(GBP)_N\Big|_{\text{Series I}} \cong K^2 \cdot (f_{hp})_N = IPG(0) \cdot (f_{hp})_N \ , \tag{4.129}$$

where

$$K \overset{\Delta}{=} \sqrt{IPG(0)} \ . \tag{4.130}$$

Families of curves constructed from (4.128) and (4.129) are shown in Figures 4.21 and 4.22 for selected values of the parameters a and b. These curves are used to describe the gain-bandwidth limitations of the

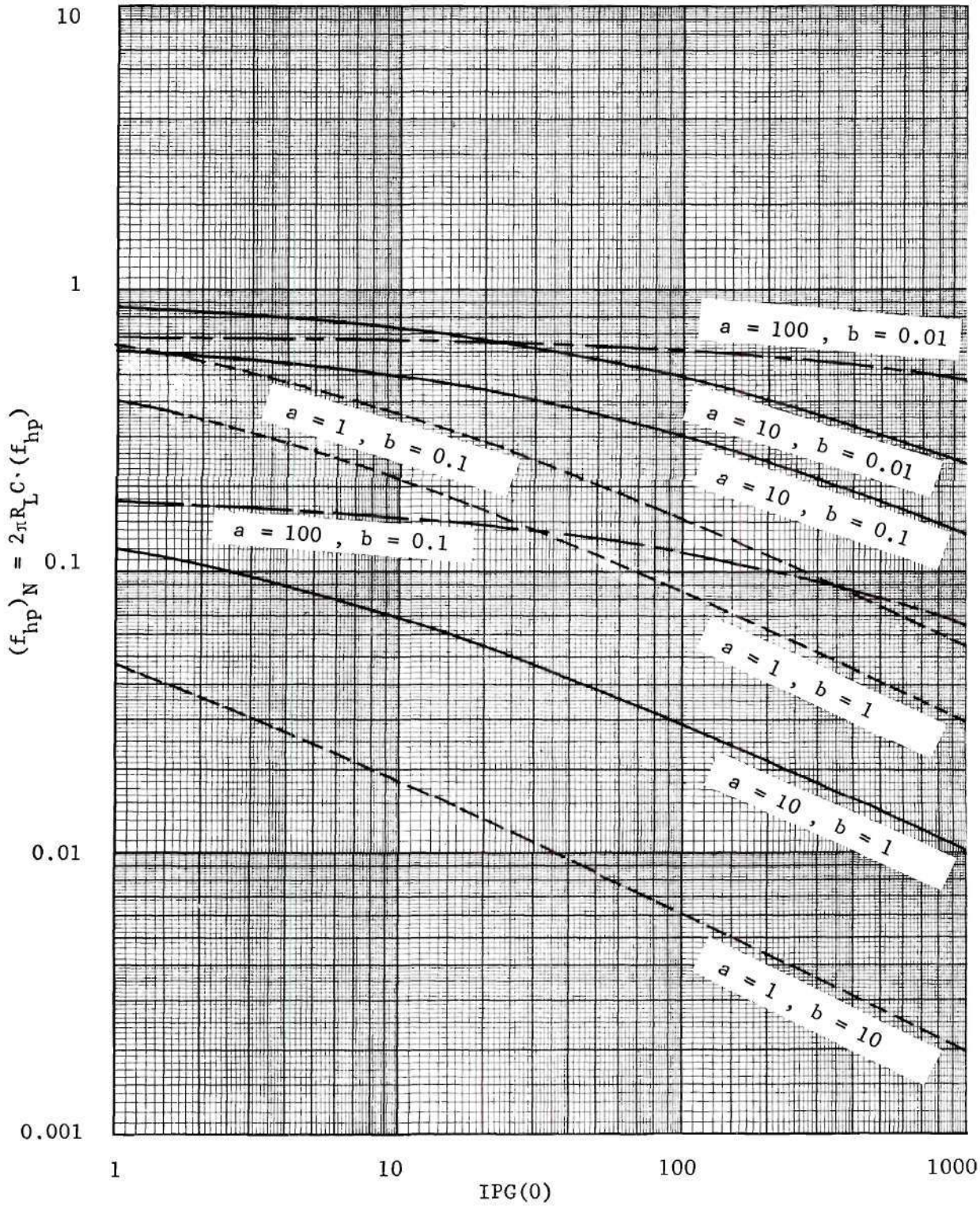

Figure 4.21 Normalized Half-Power Frequency vs. IPG(0) for the Series Amplifier(s).

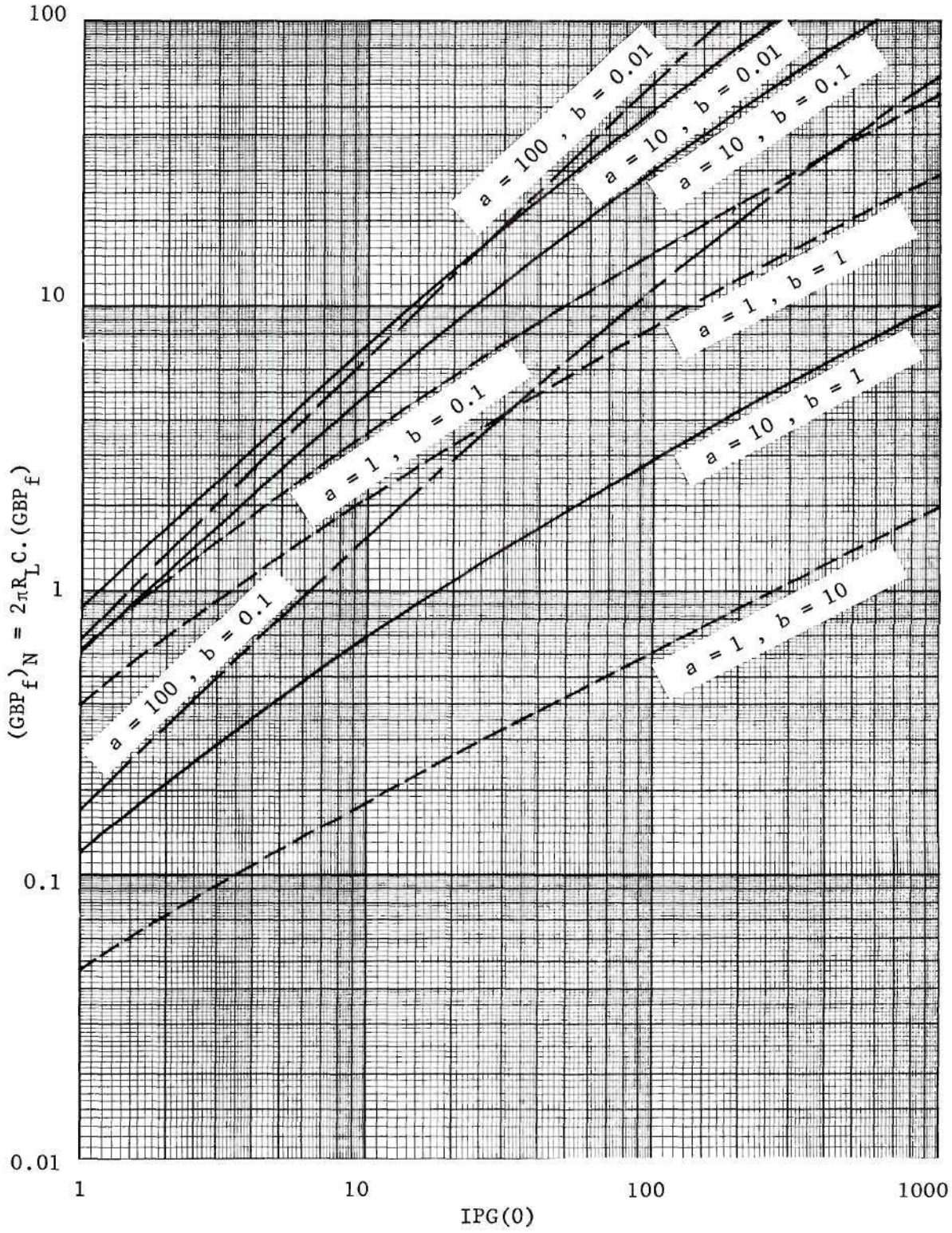

Figure 4.22 Normalized Gain-Bandwidth Product vs. IPG(0) for the Series Amplifier(s).

Series I amplifier in precisely the same manner as those in Figures 4.10 and 4.11 are used to describe the Reflection amplifier, and further discussion of them is unnecessary.

Further paralleling the development of the Reflection amplifier, the description of the Series I amplifier is also facilitated by considering the expression of $(f_{hp})_N$ as a function of the resistance ratio b with the ratio a and IPG(0) taken as parameters. Rewriting (4.128), we have

$$(f_{hp})_N \underset{\text{Series I}}{\cong} \frac{(a+1)}{\left[\begin{array}{l}[(0.22435)a^2K]b^2 + [K+a+1] \\ + [(0.8204)aK + (0.44013)a(a+1)]b\end{array}\right]}, \qquad (4.131)$$

where $K = \sqrt{IPG(0)}$. This is of the form

$$(f_{hp})_N = \frac{M}{Ab^2 + Bb + C}, \qquad (4.132)$$

where the coefficients M, A, B, and C indicated in (4.132) are all positive. The general shape of the graph of (4.132) is shown in Figure 4.23.

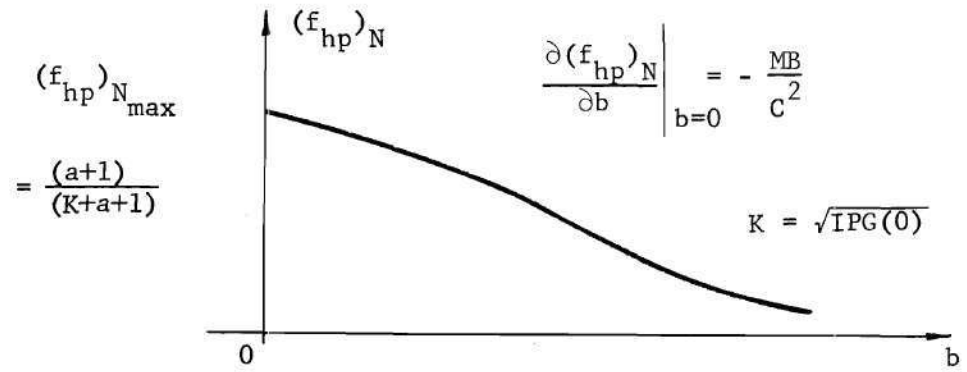

Figure 4.23 Normalized Half-Power Frequency vs. b for the Series I Amplifier.

Families of this graph for selected values of IPG(0) and the parameter a are shown plotted to logarithmic scales in Figures F.1, F.2, and F.3 of Appendix F. These curves play the same role in the description of the Series I amplifier as those of Figures E.1, E.2, and E.3 play in the description of the Reflection amplifier, and further discussion of them is unnecessary.

The presence of the nulling resistor, R_n, in the Series amplifiers offers the network designer additional control in shaping the IPG-frequency response. A hypothetical frequency response is shown in Figure 4.24.

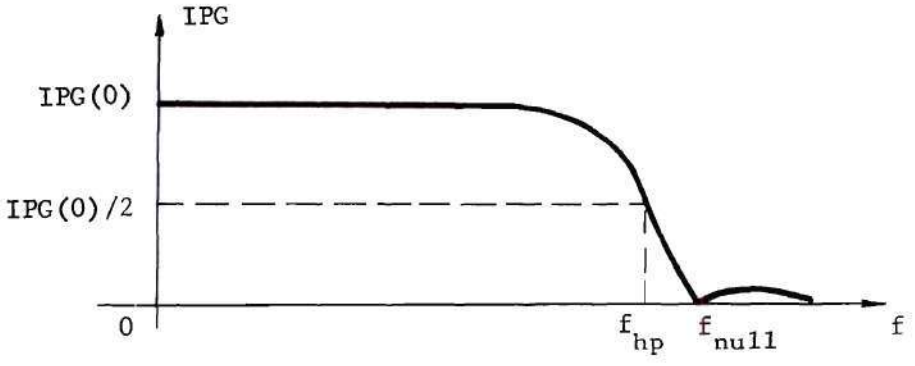

Figure 4.24 Hypothetical Frequency Response of the Series I Amplifier.

From Figure 2.6(d), we know that the null frequency is given by

$$f_{null} = \frac{4.90775}{RC} = \frac{30.8364}{2\pi RC} \quad . \tag{4.133}$$

In terms of the design parameters, a and b, we can write

$$f_{null} = \frac{30.8364}{2\pi R_L C \cdot ab} \quad , \tag{4.134}$$

and we can define the normalized null frequency as

$$(f_{null})_N \triangleq 2\pi R_L C \cdot (f_{null}) \tag{4.135}$$

so that

$$(f_{null})_N = \frac{30.8364}{ab} \quad . \tag{4.136}$$

Considering the hypothetical response depicted in Figure 4.24, it is convenient to define a frequency ratio, δ, as

$$\delta \triangleq \frac{f_{hp}}{f_{null}} = \frac{(f_{hp})_N}{(f_{null})_N} \quad . \tag{4.137}$$

This frequency ratio is a useful measure of the rapidity of cutoff near the edge of the passband. A value of unity for this ratio corresponds to the ideal case where the half-power and null frequencies coincide. A natural question at this point is: For a specified value of IPG(0) and the parameter a, what value of the parameter b results in a maximum value for this frequency ratio, and what is this maximum value? Using (4.136) and (4.137) we can write

$$\delta = \frac{(f_{hp})_N \cdot ab}{(30.8364)} \quad . \tag{4.138}$$

Thus, using (4.131), we have

$$\underset{\text{Series I}}{\delta} \cong \frac{[a(a+1)]b}{\left[\begin{array}{l}[(6.91814)a^2K]b^2 + [30.8364(K+a+1)] \\ \quad + [(25.29818)aK + (13.57202)a(a+1)]b\end{array}\right]} \quad . \tag{4.139}$$

This is of the form

$$\delta = \frac{Nb}{Db^2 + Eb + F} \quad , \tag{4.140}$$

where the coefficients N, D, E, and F indicated in (4.139) are all positive. The general shape of the graph of (4.140) is shown in Figure 4.25.

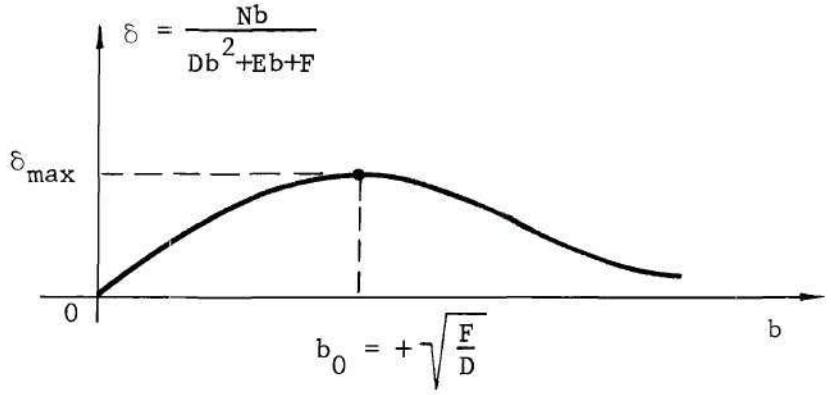

Figure 4.25 Frequency Ratio vs. b for the Series I Amplifier.

The maximum value of the frequency ratio occurs when

$$b = b_0 = +\sqrt{\frac{F}{D}} = \frac{(2.11124)}{a}\sqrt{\frac{K+a+1}{K}} \quad , \tag{4.141}$$

where $K = \sqrt{IPG(0)}$, and the value of δ at this value of b is

$$\delta_{\substack{max \\ Series\ I}} = \frac{(a+1)}{\left[\begin{array}{l}(29.21162)\sqrt{K^2+K(a+1)} \\ \quad + [(25.29818)K + (13.57202)(a+1)]\end{array}\right]} \quad . \tag{4.142}$$

Thus, for any specified values of IPG(0) and the resistance ratio a, the frequency ratio δ has a least upper bound of

$$\text{l.u.b.}\underset{\text{Series I}}{(\ \delta\ )} = \frac{1}{13.57202} = 0.07368\ . \qquad (4.143)$$

Families of curves constructed from (4.139), for selected values of IPG(0) and the parameter a, are shown plotted to logarithmic scales in Figures F.4, F.5, and F.6, of Appendix F. These curves will be useful in the design of the Series amplifiers, which is the next topic of discussion.

Design Considerations

The design considerations to be made for the Series amplifier are very similar to those made for the Reflection amplifier. Except for the inclusion of the frequency ratio δ, and certain salient features characteristic of the Series I amplifier, the pattern of this section follows that set in the discussion of the Reflection amplifier design.

For the Series I amplifier, the stability criterion is

$$R_d > R_{eq} = R_s + \frac{RR_n}{R+R_n} + R_L$$

$$= R_s + 0.8204R + R_L\ . \qquad (4.144)$$

In terms of the design parameters, we have

$$R_d > R_{eq} = [a + (0.8204)ab + 1]\ R_L\ . \qquad (4.145)$$

For a specified value of IPG(0) = K^2, the required diode resistance is given by (4.122) as

$$R_d = (\frac{K+1}{K})(R_s+R_L) + 0.8204\ R, \qquad (4.146)$$

and, in terms of the design parameters, this may be written as

$$R_{d_{\text{Series I}}} = \left[\left(\frac{K+1}{K}\right)(a+1) + (0.8204)ab\right] R_L \ . \tag{4.147}$$

Inspection of (4.145) in terms of (4.147) shows that the stability criterion is always satisfied if the diode resistance is selected via (4.147). Again it is convenient to define the <u>percent stability margin</u>, Λ, by assigning the diode resistance as

$$R_d = \left(1 + \frac{\Lambda}{100}\right) R_{eq} \ . \tag{4.148}$$

Thus, via (4.145) and (4.147), we can express the percent stability margin as

$$(\Lambda)_{\text{Series I}} = \frac{100(a+1)}{K[(a+1) + (0.8204)ab]} \ . \tag{4.149}$$

From (4.149), it is apparent that

$$(\Lambda)_{\text{Series I}} \leq \left(\frac{100}{K}\right) \ , \tag{4.150}$$

with the equality satisfied only when $b = 0$. From (4.150), we deduce that

$$IPG(0)_{\text{Series I}} \overset{\Delta}{=} K^2 \leq \left(\frac{100}{\Lambda}\right)^2 \ . \tag{4.151}$$

Again, we see a manifestation of the inherent gain-stability limitation of these negative-resistance amplifiers. If practicality should dictate

a stability margin of ten per cent ($\Lambda = 10$), then we know at the outset that the DC gain cannot exceed 100, and it will be less than this for all values of b greater than zero. It is of practical value to note that, for identical values of stability margin, the Series I amplifier cannot achieve the gain attainable with the Reflection amplifier. Conversely, for identically specified values of gain, the operation of the Series I amplifier is more critical than the Reflection amplifier since a smaller stability margin is required. These properties can be seen by comparing (4.151) with (4.87) and/or (4.150) with (4.86).

Considering Λ as a function of the design parameter b, we get from (4.149)

$$\frac{\partial \Lambda}{\partial b} = - \frac{100(a+1)}{K} \cdot \frac{(0.8204)a}{[(a+1) + (0.8204)ab]^2} , \qquad (4.152)$$

and the general shape of the graph of (4.149) is shown in Figure 4.26. Families of this curve, for selected values of IPG(0) and the parameter a,

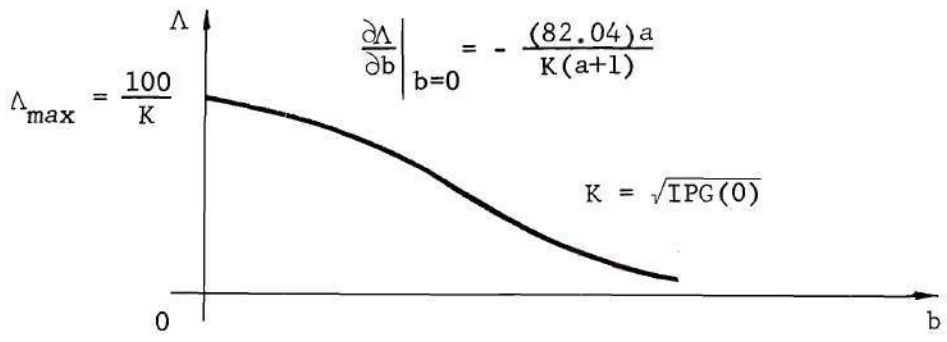

Figure 4.26 Percent Stability Margin vs. b for the Series I Amplifier.

are shown plotted to logarithmic scales in Figures F.7, F.8, and F.9 of Appendix F.

All of the practical limitations discussed in the design of the Reflection amplifier are inherent to the Series amplifiers. The reasons for the limits on the design range of the parameter b are exactly those given in the previous discussion of the Reflection amplifier. One additional point to be considered, however, is that in the configuration of the Series I amplifier the magnitude of the diode resistance must be greater than the sum of the series-connected resistors R_s, R_L, and $R_p = RR_n/(R+R_n)$. Thus, as indicated in (4.145), large values of a or b (or both) must be accompanied, in general, by small values of R_L. Since tunnel diodes with a negative resistance of 600 ohms or more are relatively uncommon, it is observed that the Series I amplifier will be most useful in those cases where the overall impedance level is low. This is more readily seen when it is recognized that the parameter b will, in general, be set at the value b_0 in order to achieve maximum frequency ratio, δ_{max}. If this is the case, we can substitute (4.141) into (4.147) to get the required value of R_d as

$$\underset{(b=b_0)}{R_d} = \left[\left(\frac{K+1}{K}\right)(a+1) + (1.73206)\sqrt{\frac{K+a+1}{K}} \right] R_L \,. \qquad (4.153)$$

From (4.142) and Figures F.4, F.5, and F.6 of Appendix F it is also observed that, for a specified gain, the maximum frequency ratio, δ_{max}, increases with increasing a. With this in mind, we see from (4.153) that the Series I amplifier is best suited for those situations where the overall impedance level is low and R_s is much greater than R_L.

Design Example and Experimental Results

As an example of the design procedure for the Series I amplifier let us consider the following problem: A Series amplifier is desired that will operate between source and load terminations of 300 ohms and 30 ohms respectively, while providing an IPG of 64 (18.06 db) in the pass band with a half-power bandwidth of 120 KHz. At the same time, the maximum possible value of the frequency ratio, δ, is desired.

As pointed out in the preceding section, the Series I configuration is best suited for those cases where the overall impedance level is low and R_s is much greater than R_L. For the case at hand, $R_s = 10R_L$, and the Series I configuration is the logical choice for the design.* Since the specified value for the parameter a is 10, and IPG(0) is specified as 64 (K=8), the curves of Figures F.2, F.5, and F.8 serve as the basis for the design. From Figure F.5, for a = 10, the value of b yielding maximum frequency ratio is taken as $b = b_0 = 0.3$. From Figure F.2 and F.8 (for a = 10, b = 0.3) we read the values

$$(f_{hp})_N \cong 0.16 ,$$

and

$$\Lambda \cong 10 .$$

For the specified value of $f_{hp} = 120$ KHz $= f_0$, the required line capacitance is computed as

---

* From the symmetry-of-form property it follows that the Series II configuration is best suited for those situations where the overall impedance level is low and R_L is much greater than R_s. In a later example dealing with the Transmission amplifiers, the results of making an incorrect choice of configuration will be covered in detail as well as the details of making use of the aforementioned symmetry-of-form property.

$$C = \frac{(f_{hp})_N}{2\pi R_L f_0}$$

$$= \frac{0.16}{(6.28318)(30)(120 \times 10^3)}$$

$$= 7.074 \text{ nf.} \qquad (4.154)$$

The required line resistance is

$$R = b R_s = b_0 R_s$$

$$= (0.3)(300)$$

$$= 90 \ \Omega , \qquad (4.155)$$

and the required value of null resistance shown in Figure 2.6(d) is

$$R_n = 4.56814 R$$

$$= 4.56814 (90)$$

$$= 411.132 \ \Omega . \qquad (4.156)$$

The required value of diode resistance is computed from (4.147) as

$$R_d = [(\frac{K+1}{K})(a+1) + (0.8204)ab] R_L$$

$$= [(\frac{9}{8})(11) + (0.8204)(10)(0.3)] (30)$$

$$= 445.086 \ \Omega . \qquad (4.157)$$

The parameters of the model line fabricated for this example were measured to be

$$R = 90\ \Omega\ ,$$

and

$$C = 7.07\ \text{nf}\ .$$

The null resistance used was measured to be 411 ohms, and a Hoffman 1N2928 tunnel diode (having a nominal shunt capacitance, C_d, of 50 pf) was biased at approximately 120 mv to achieve the appropriate negative resistance. A fine bias adjustment was made via (4.107) so that the low-frequency voltage amplification was

$$\begin{aligned} |A_v(0)| &= \frac{K}{(a+1)} \\ &= \frac{8}{11} \\ &= 0.727\ , \end{aligned} \tag{4.158}$$

and that value of bias was maintained throughout the measurement of the frequency response.

The resulting frequency response is shown in Figure 4.27. The solid curve depicts the theoretically predicted response calculated via the exact gain expression given in Appendix C. The superimposed points represent the measured response and exhibit close agreement with the calculated response. The exact value of f_{hp} for the chosen set of parameters was calculated as 111.553 KHz and was 7.0 per cent lower than the design goal of 120 KHz. The measured value of f_{hp} was 117 KHz and was

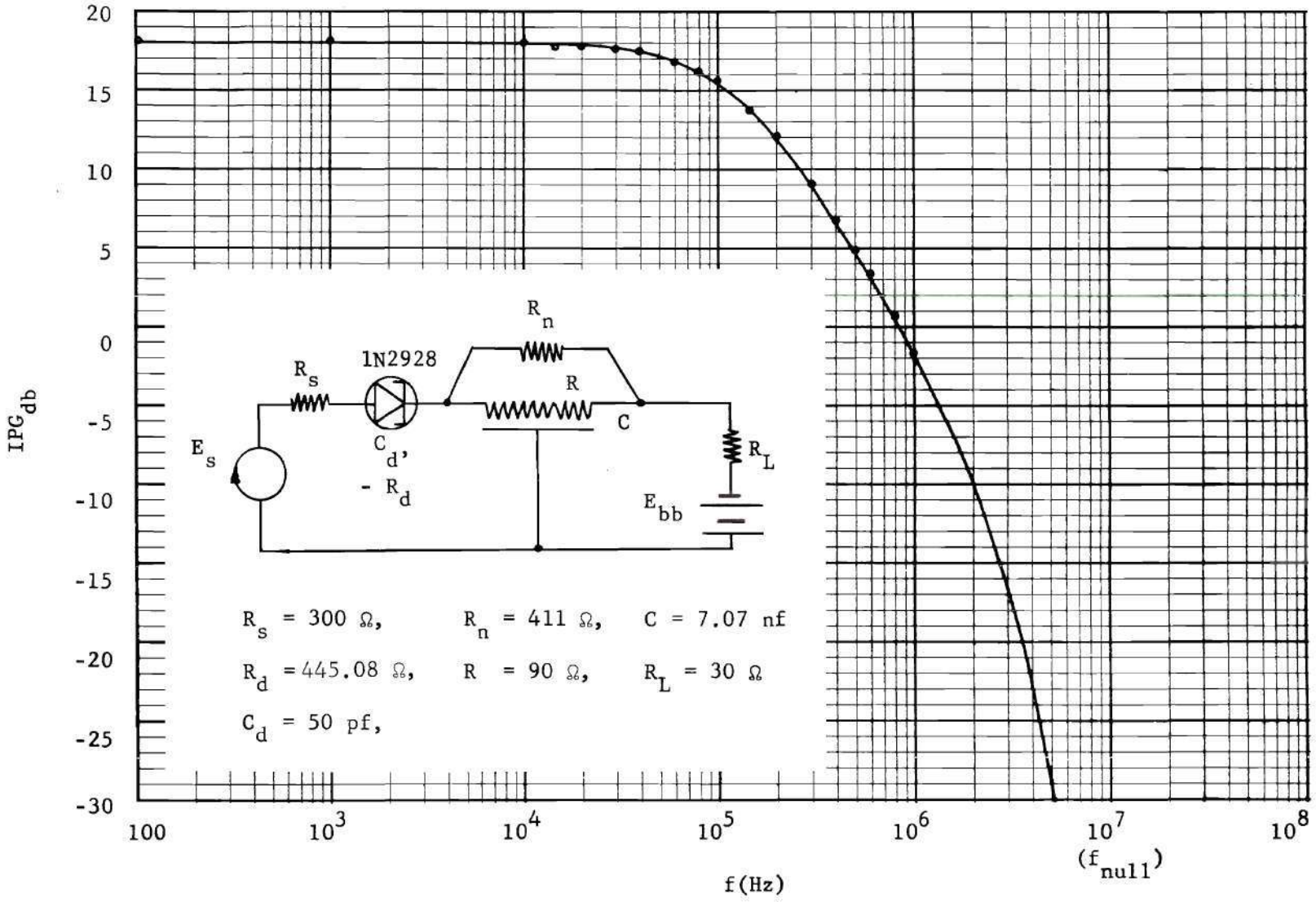

Figure 4.27 IPG-Frequency Response of Prototype Series I Amplifier.

2.5 per cent lower than the design goal. The value of the frequency ratio achieved experimentally was 0.01516 based on the measured values of f_{hp} and the line parameters. This was 2.2 per cent lower than the value 0.0155 predicted by the design curve of Figure F.5.

In general, the experimental results were in close agreement with those calculated from the exact gain expression and even closer to those predicted from the design curves. The largest source of discrepancy was most likely in the measurement of the line capacitance. The technique used in determining the line capacitance depends on the measurement of a null frequency and is quite sensitive to small discrepancies in the value of the nulling resistor used. The overall results of the design procedure were very favorable, however, and fell within the usual tolerances accepted in practice. As stated previously, when greater accuracy is desired, this can be achieved most rapidly and efficiently by making incremental changes in the value of line capacitance used in the computer program for calculating the exact response, and making a few reiterative calculations.

The Transmission Amplifiers

Gain-Bandwidth Properties

The final amplifiers to be discussed are the Transmission type. The Transmission I and II configurations are shown in Figure 4.28, and expressions for their IPG are given in Appendix D.

For the sake of brevity, it is noted at the outset that the methods of analysis developed in the preceding discussion of the Reflection and Series amplifiers apply throughout the analysis of the

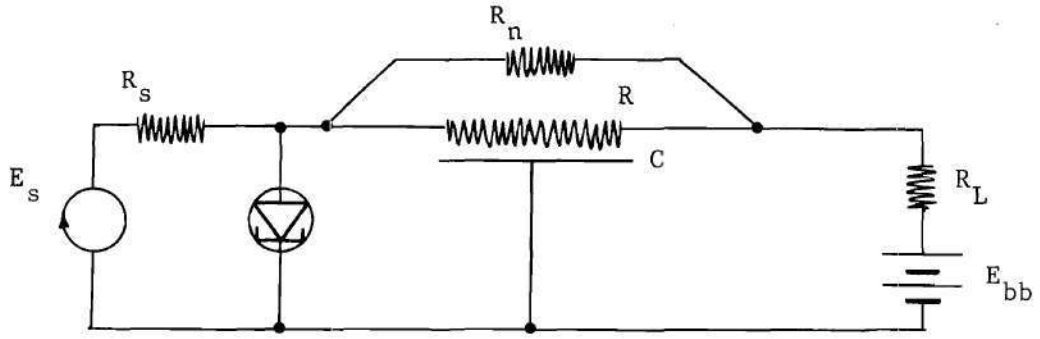

(a) The Transmission I Amplifier.

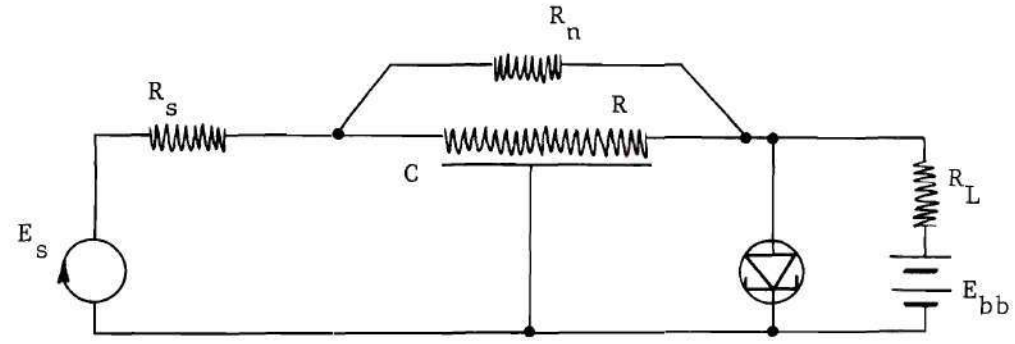

(b) The Transmission II Amplifier.

Figure 4.28 The Transmission Amplifier Configurations.

Transmission amplifiers as well. As in the case of the Series amplifiers, the reciprocity of the Transmission amplifier configurations ensures the symmetry of form between the analytical description of the two types. The Transmission I configuration will receive greatest attention in the work presented here, but it should be kept in mind that a simultaneous analysis of the Transmission II configuration is being carried out provided that R_s and R_L are interchanged everywhere in the analysis. This will be pointed out in detail when a design example is presented later. Since the line of attack in the analysis of the Transmission amplifiers follows that of the preceding sections exactly, only the results will be

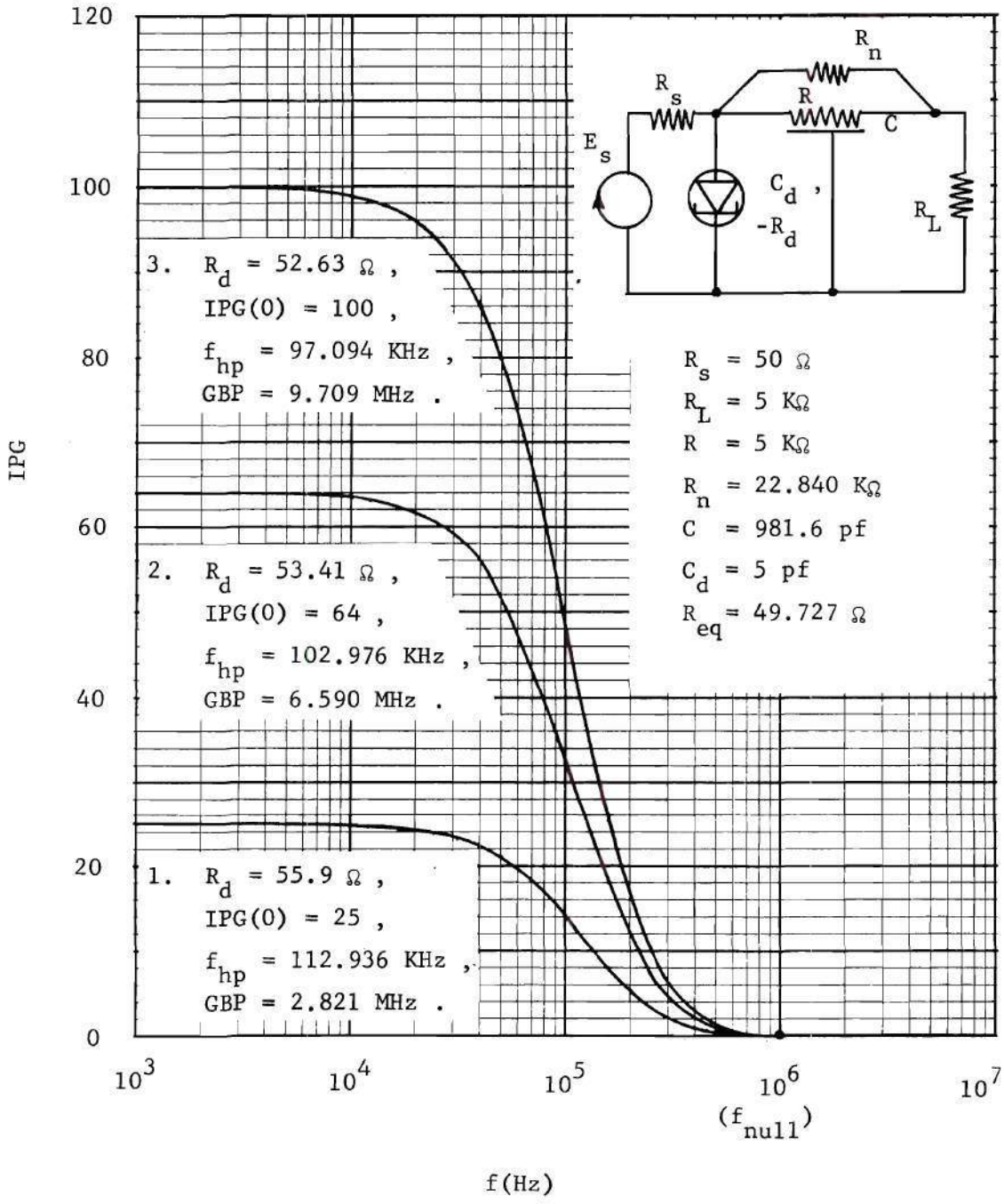

Figure 4.29 Typical IPG-Frequency Response Curves for the Transmission I Amplifier.

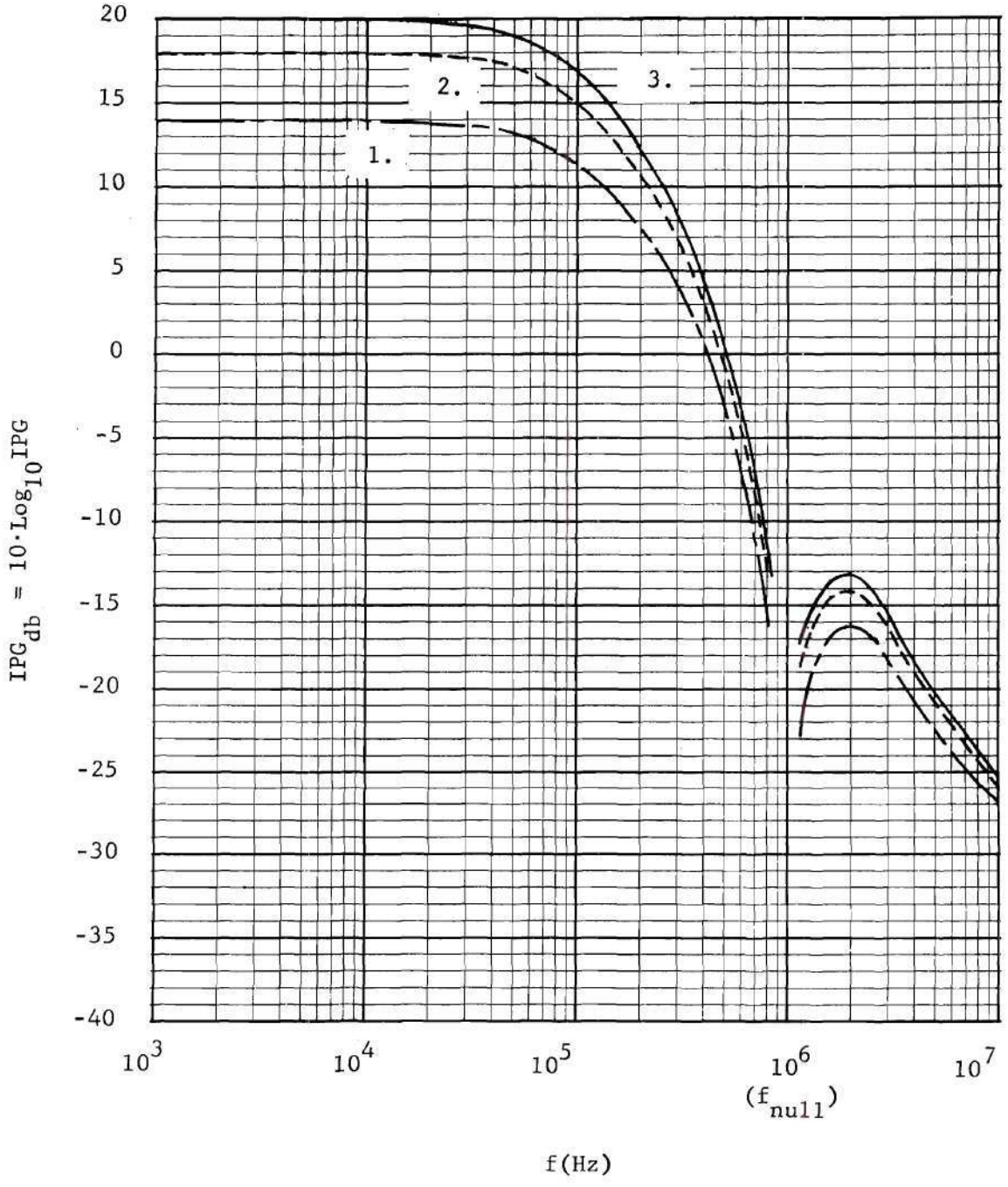

Figure 4.30 The IPG-Frequency Response Curves of Figure 4.29 in Decibels.

given here. If, at any point, there is a salient feature characteristic of the Transmission configurations, it will be discussed fully. Otherwise, the results given here can be arrived at by exactly the same approach taken in the preceding sections.

Some typical response curves are shown in Figures 4.29 and 4.30. Again, we see the same type of gain-bandwidth behavior as witnessed in the previous sections. It has likewise been shown that the PBGA of Transmission I amplifier may be made arbitrarily large, and there is no upper bound on the GBP of the Transmission I amplifier.

With the same techniques, approximations, and general definitions used previously, the normalized half-power frequency and normalized gain-bandwidth product are found to be

$$(f_{hp})_N \underset{\text{Trans. I}}{\cong} \frac{[(a+1) + (0.8204)(a+1)ab]}{\left[K[a + (0.8204)a^2b + (0.22435)a^3b^2] + [(0.44013)(a+1)ab + (0.13673)(a+1)a^2b^2]\right]}, \quad (4.159)$$

and

$$(GBP)_N = K^2 \cdot (f_{hp})_N = IPG(0) \cdot (f_{hp})_N, \quad (4.160)$$
$$\text{Trans. I}$$

where

$$K \overset{\Delta}{=} \sqrt{IPG(0)}. \quad (4.161)$$

Families of curves constructed from (4.159) and (4.160) are shown in Figures 4.31 and 4.32 for selected values of the parameters a and b.

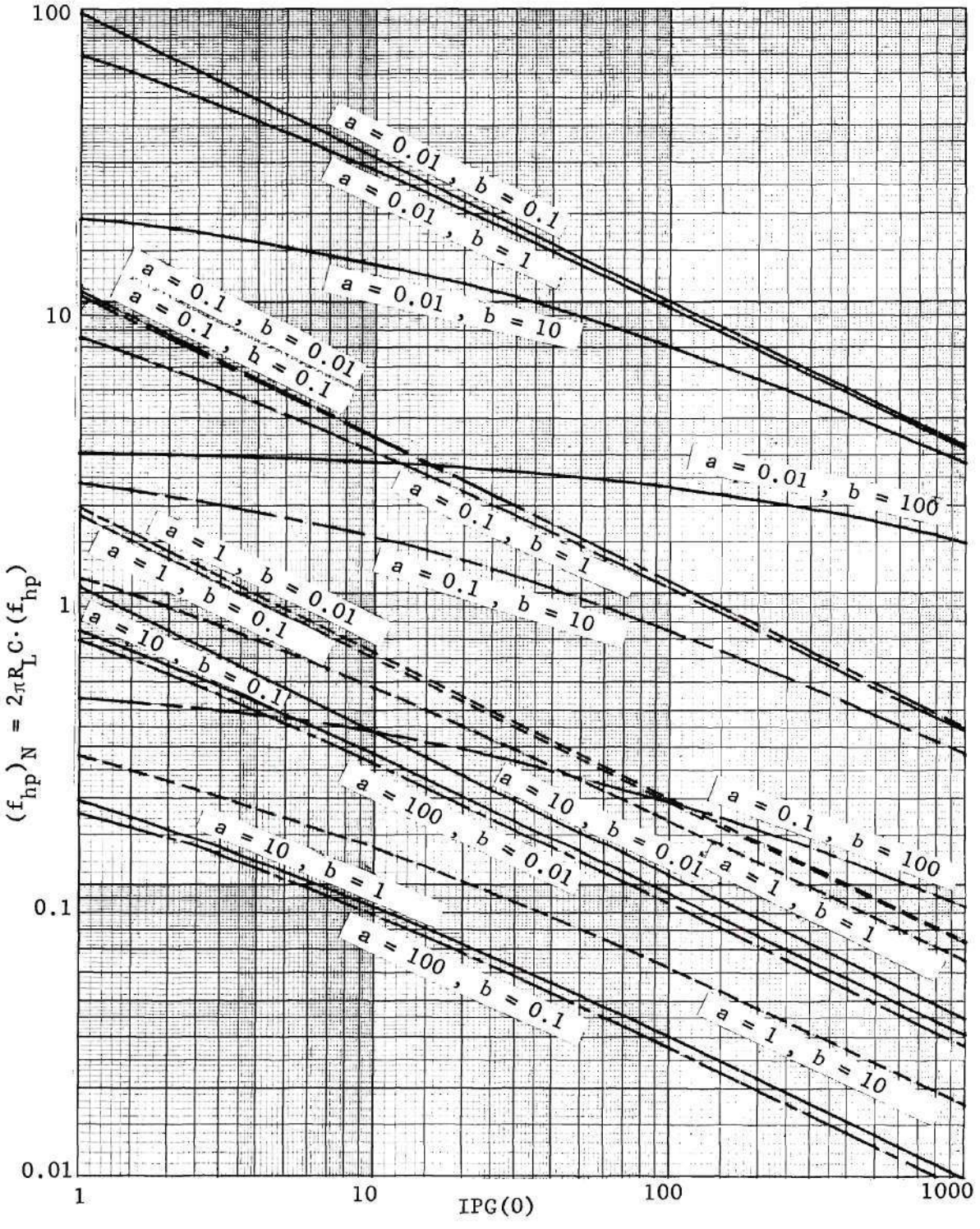

Figure 4.31 Normalized Half-Power Frequency vs. IPG(0) for the Transmission Amplifier(s).

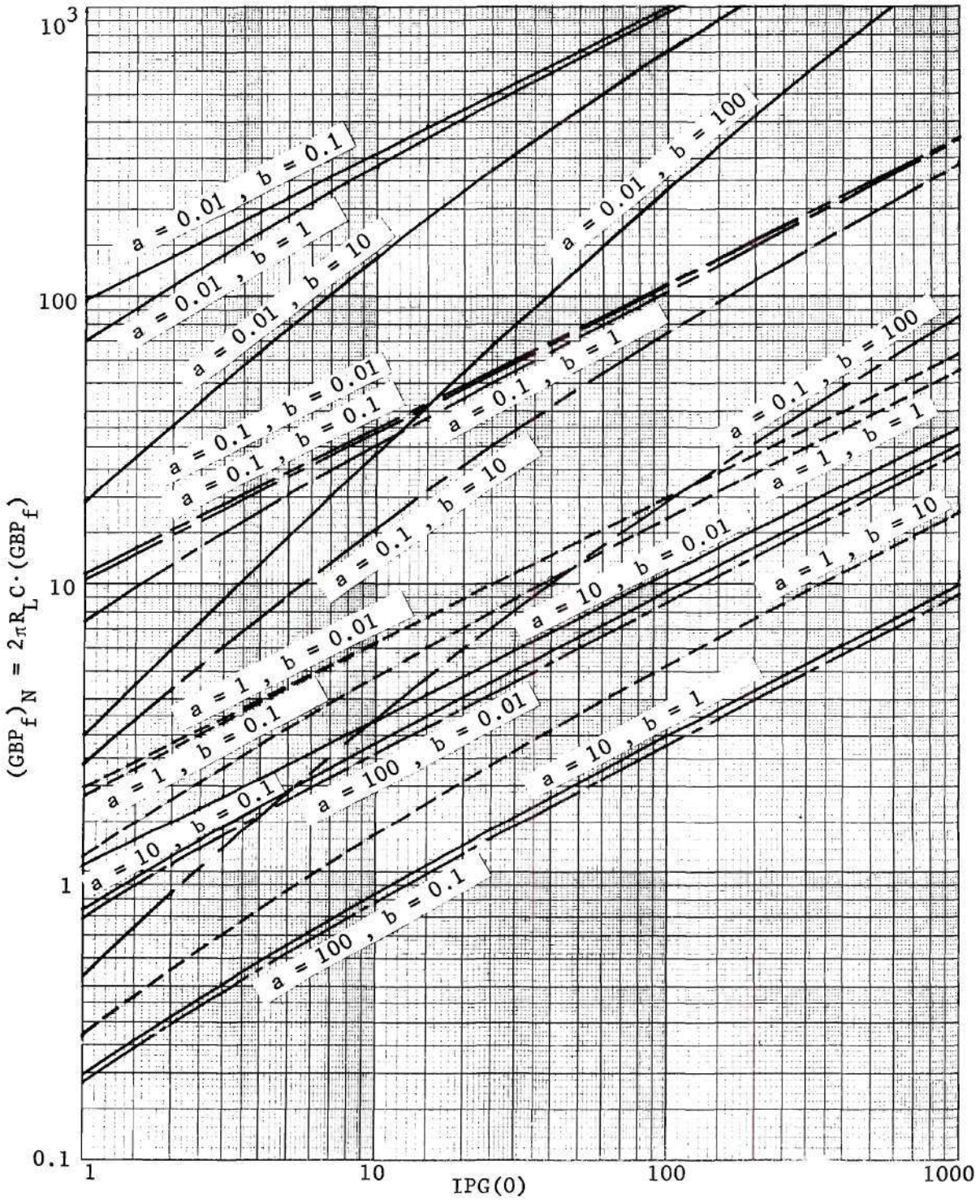

Figure 4.32 Normalized Gain-Bandwidth Product vs. IPG(0) for the Transmission Amplifier(s).

Rewriting (4.159) as a function of b yields

$$(f_{hp})_N \underset{\text{Trans. I}}{\simeq} \frac{[(0.8204)a(a+1)]b + [(a+1)]}{\left[\begin{array}{l}[(0.22435)a^3K + (0.13673)a^2(a+1)]b^2 \\ + [(0.8204)a^2K + (0.44013)a(a+1)]b + [aK]\end{array}\right]}, \qquad (4.162)$$

which is of the form

$$(f_{hp})_N = \frac{Pb + Q}{Ab^2 + Bb + C}, \qquad (4.163)$$

where the indicated coefficients are all positive. The general shape of the graph of (4.163) is shown in Figure 4.33. Families of this graph for selected values of IPG(0) and the parameter a are shown plotted to logarithmic scales in Figures G.1, G.2, and G.3 of Appendix G.

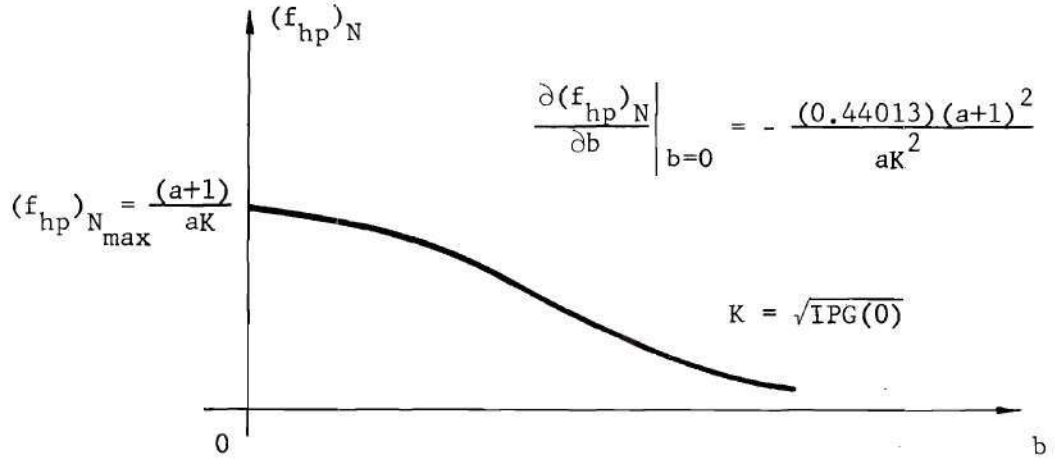

Figure 4.33 Normalized Half-Power Frequency vs. b for the Transmission I Amplifier.

In the study of the <u>frequency ratio</u>, δ, for the Transmission I configuration, we again have

$$(f_{null})_N = \frac{30.8364}{ab} \ , \tag{4.164}$$

so that, using (4.162), the frequency ratio as a function of the design parameter b is

$$\delta_{\text{Trans. I}} \cong \frac{[(0.8204)a(a+1)]b^2 + [(a+1)]b}{\left[\begin{array}{l}[(6.91814)a^2K + (4.21626)a(a+1)]b^2 \\ + [(30.8364)K] + [(25.29818)aK \\ + (13.57202)(a+1)]b\end{array}\right]} \ . \tag{4.165}$$

This is of the form

$$\delta = \frac{Nb^2 + Mb}{Db^2 + Eb + F} \ , \tag{4.166}$$

where the indicated coefficients are all positive. The general shape of the graph of (4.166) is shown in Figure 4.34. The frequency ratio approaches its maximum value asymptotically for increasing values of

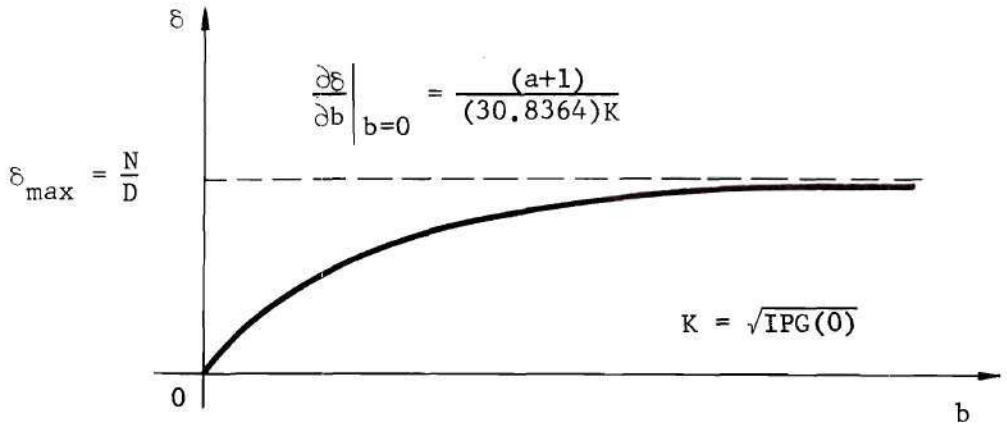

Figure 4.34 Frequency Ratio vs. b for the Transmission I Amplifier.

the parameter b, and

$$\delta_{max} = \lim_{b \to +\infty} = \frac{N}{D} = \frac{(0.8204)a(a+1)}{(6.91814)a^2K + (4.21626)a(a+1)} , \qquad (4.167)$$

where $K = \sqrt{IPG(0)}$, and the coefficients N and D are taken from (4.165). Thus, for any specified values of IPG(0) and the resistance ratio a, the frequency ratio has a least upper bound of

$$1.u.b.\left(\delta_{Trans.I}\right) = \frac{(0.8204)}{(4.21626)} = 0.19458 . \qquad (4.168)$$

Families of curves constructed from (4.165), for selected values of IPG(0) and the parameter a, are shown in Figures G.4, G.5, and G.6 of Appendix G.

Design Considerations

For the Transmission I amplifier, the stability criterion is

$$R_d > R_{eq} = \frac{R_s[(0.8204)R + R_L]}{R_s + (0.8204)R + R_L} , \qquad (4.169)$$

which, in terms of the design parameters a and b, may be expressed as

$$R_d > R_{eq} = \frac{a[(0.8204)ab + 1]\, R_L}{[(a+1) + (0.8204)ab]} . \qquad (4.170)$$

For a specified value of $IPG(0) = K^2$, the required value of diode resistance is

$$R_d = \frac{K\, R_s[(0.8204)R + R_L]}{K[R_s + (0.8204)R + R_L] - (R_s + R_L)} , \qquad (4.171)$$

which, in terms of the parameters a and b, can be written as

$$R_d = \frac{Ka[(0.8204)ab+1]\ R_L}{K[(a+1) + (0.8204)ab] - (a+1)} \quad . \tag{4.172}$$

Inspection of (4.170) in terms of (4.172) shows that the stability criterion is always satisfied if the diode resistance is chosen via (4.172). The <u>percent stability margin</u>, Λ, defined by

$$R_d = (1 + \frac{\Lambda}{100})\ R_{eq} \tag{4.173}$$

may be expressed, via (4.170) and (4.172), as

$$\underset{\text{Trans. I}}{\Lambda} = \frac{100(a+1)}{[(K-1)(a+1) + K(0.8204)ab]} \quad . \tag{4.174}$$

From (4.174) it is apparent that

$$\underset{\text{Trans. I}}{\Lambda} \leq \frac{100}{(K-1)} \quad , \tag{4.175}$$

where the equality holds only when b = 0. From (4.175), we get the inherent gain-stability limitation of the Transmission I amplifier as

$$\underset{\text{Trans. I}}{IPG(0)} \overset{\Delta}{=} K^2 \leq (\frac{100}{\Lambda} + 1)^2 \quad . \tag{4.176}$$

It is worth noting at this point that <u>the gain-stability limitation of the Transmission amplifier is identical to that found for the Reflection amplifier, and comparison of the three amplifier types (Reflection, Series, Transmission) shows the Series type to be more critical in its</u>

operation. That is, for a given value of gain, the maximum stability margin attainable in the Series configuration will be less than that achievable in either the Reflection or Transmission configuration. This is obvious upon comparing (4.175), (4.150), and (4.86).

Considering Λ as a function of the parameter b, we get from (4.174)

$$\frac{\partial \Lambda}{\partial b} = - \frac{(82.04)a(a+1)K}{[(K-1)(a+1) + K(0.8204)ab]^2} , \qquad (4.177)$$

and the general shape of the graph of (4.174) is shown in Figure 4.35. Families of this curve, for selected values of IPG(0) and the parameter a, are given in Figures G.7, G.8, and G.9 of Appendix G.

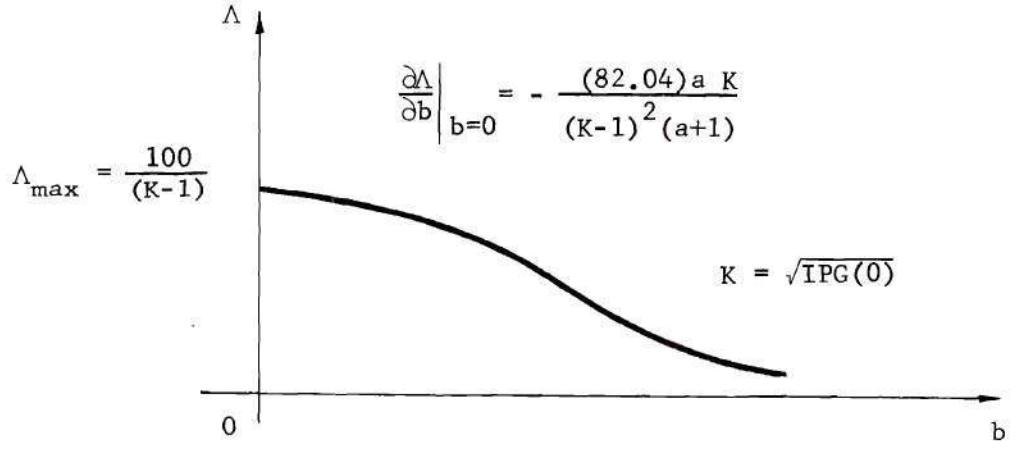

Figure 4.35 Percent Stability Margin vs. b for the Transmission I Amplifier.

All of the practical limitations discussed for the Reflection amplifier are applicable to the Transmission amplifiers. One additional point that should be noted, however, is that the opposing nature of the

frequency ratio and the percent stability margin, when considered as functions of b, might necessitate some compromise in the design. Specifically, the frequency ratio is an increasing function of b while the stability margin is a decreasing function of b. From the graphs of these functions given in Appendix G, however, it is observed that (for a specified gain) we can make b large in order to achieve large frequency ratios and still maintain acceptable stability margins if the parameter a is small. Thus, the Transmission I amplifier is best suited for those situations in which R_s is much smaller than R_L.

Design Example and Experimental Results

As an example of the design procedure for the Transmission type amplifiers, let us consider the following problem: A Transmission amplifier is desired that will operate between source and load terminations of 41 K ohms and 410 ohms, respectively, while providing an IPG of 100 (20 db) in the passband with a half-power bandwidth of 10.5 KHz. At the same time, it is desired to achieve a frequqncy ratio as large as possible consistent with a realistic choice for the stability margin.

The source and load terminations fix the parameter a at 100, and since the specified IPG(0) is 100, the curves of Figures G.3, G.6, and G.9 serve as the basis for the design. Inspection of Figure G.9 shows that, for a = 100, the stability margin falls off rapidly for values of b greater than 0.1. As a rule-of-thumb, it is difficult to maintain a stable bias point if the stability margin is less than about 10 per cent, and this dictates that the parameter b should be restricted to values equal to or less than about 0.1. Simultaneous consideration of Figures G.3, G.6, and G.9 shows that a compromise must be made in fixing the value

of b. If b is fixed at 0.1, then

$$(f_{hp})_N \cong 0.027,$$

$$\delta \cong 0.009,$$

and

$$\Lambda \cong 10 .$$

Thus, a reasonable value is achieved for the stability margin, but the frequency ratio is such that the separation between f_{hp} and f_{null} is over two decades. In addition, the value of $(f_{hp})_N$ is so low that the required line capacitance is computed to be

$$C = \frac{(f_{hp})_N}{2\pi R_L \cdot f_0}$$

$$= \frac{0.027}{(6.28318)(410)(10.5\text{x}10^3)}$$

$$= 0.998 \text{ nf} \quad , \qquad (4.178)$$

and this value is low enough that it may be difficult to achieve reliably. Another factor that must be considered is the magnitude of the required negative resistance. For IPG(0) = 100(K=10), a = 100, and b = 0.1, the required R_d is calculated from (4.172) to be

$$R_d = \frac{Ka[(0.8204)ab + 1] R_L}{K[(a+1) + (0.8204)ab] - (a+1)}$$

$$= \frac{(10)(100)[8.204 + 1] R_L}{10[101 + 8.204] - (101)}$$

$$= (9.28721)\ R_L$$

$$= (9.28721)(410)$$

$$= 3807.75\ \Omega\ , \qquad (4.179)$$

which is totally unrealistic. If the parameter b is reduced to 0.01, then

$$(f_{hp})_N \cong 0.088\ ,$$

$$\delta \cong 0.0028\ ,$$

and

$$\Lambda \cong 11\ .$$

Thus, the reduction in b achieves the slightly higher stability margin of 11 per cent, and the required line capacitance is now computed to be

$$C = \frac{(f_{hp})_N}{2\pi R_L\ f_0}$$

$$= \frac{0.088}{(6.28318)(410)(10.5\times10^3)}$$

$$= 3.253\ \text{nf}\ , \qquad (4.180)$$

which is a more reasonable value. The required negative resistance is now calculated from (4.172) to be

$$R_d = \frac{Ka[(0.8204)ab + 1]\ R_L}{K[(a+1) + (0.8204)ab] - (a+1)}$$

$$= (1.98472)\ R_L$$

$$= (1.98472)(410)$$

$$= 813.735\ \Omega \qquad (4.181)$$

which is also unrealistic. In addition, the frequency ratio has been further reduced to about one third of its initial value which is just the opposite of what is desired, i.e. an increased value of frequency ratio. Thus, it seems that, no matter how we are willing to compromise in the choice of the parameter b, one or more of the network parameters must take on an unrealistic value in order to meet the design specifications. This is a discouraging state of affairs until one realizes that there is a fundamental fault in all of the preliminary design calculations above. They were made for a Transmission I amplifier. In the previous section dealing with design considerations it was pointed out that the Transmission I configuration is best suited for those cases where R_s is much smaller than R_L. The case at hand (R_s = 41KΩ, R_L = 410Ω) hardly fits this description, and the unrealistic values calculated above are a manifestation of this fact. From the symmetry-of-form property it follows that the Transmission II configuration is best suited for those situations where R_s is much larger than R_L. Since the specifications in the original design problem call for a source termination that is 100 times larger than the load termination, the Transmission II configuration is the proper choice here. The first task in the design, therefore, is to modify the preceding analysis so that it applies to the Transmission II configuration.

Fortunately, all of the previously developed design formulas and curves hold for the Transmission II configuration if R_s and R_L are interchanged everywhere in the analysis.* This symmetry of form was mentioned earlier, and it is a direct consequence of the reciprocity of these amplifiers. For the Transmission II configuration, the following changes are made: The design parameters a and b, originally defined by (4.125) and (4.126), are now given by the modified definitions

$$R_L = a\, R_s, \tag{4.182}$$

and

$$R = b\, R_L = ab\, R_s\ . \tag{4.183}$$

If the derivation of $(f_{hp})_N$ is carried out, we find that (4.159) and Figures 4.31 and 4.32 are still valid (provided the normalization factor is interpreted as $2\pi R_s C$ instead of $2\pi R_L C$). Likewise, (4.162) and Figures G.1, G.2, and G.3 are applicable with the modified normalization factor. It is also found that, with the proper normalization factor of $2\pi R_s C$, (4.164) and (4.165) are valid exactly as they are. Hence, the curves of Figures G.4, G.5, and G.6 are applicable without further modification. The modified forms of (4.170) and (4.172) become

$$R_d > R_{eq} = \frac{a[(0.8204)ab + 1]\, R_s}{[(a+1) + (0.8204)\ ab]}\ , \tag{4.184}$$

---

* There is a single exception to this statement that will be discussed in detail.

and

$$R_d = \frac{Ka[(0.8204)ab + 1]\, R_s}{K[(a+1) + (0.8204)ab] - (a+1)} \cdot \tag{4.185}$$

The stability margin is universally defined by (4.173), and we see that, using (4.184) and (4.185), we arrive at exactly the same expression for Λ given by (4.174). Hence, the gain-stability limitation for the Transmission II configuration is precisely the same as that for the Transmission I configuration, and the curves of Figures G.7, G.8, and G.9 apply without further modification.* With these points in mind, the design can now be carried out.

For the case at hand, the modified value of the parameter a becomes 0.01, and the curves of Figures G.3, G.6, and G.9 serve as the basis of the design. If b is chosen as 27.6, then

$$(f_{hp})_N \cong 4.75 ,$$

$$\delta \cong 0.043 ,$$

and

$$\Lambda \cong 8.9 .$$

Since $(f_{hp})_N$ is now defined as

$$(f_{hp})_N \overset{\Delta}{=} 2\pi R_s C \cdot (f_{hp}) , \tag{4.186}$$

---

* All of these properties similarly hold for the Series II configuration and the design curves of Appendix F.

the required line capacitance is computed as

$$C = \frac{(f_{hp})_N}{2\pi R_s \cdot f_0}$$

$$= \frac{4.75}{(6.28318)(41\text{x}10^3)(10.5\text{x}10^3)}$$

$$= 1.756 \text{ nf} . \qquad (4.187)$$

The new value of frequency ratio is considerably improved over those reached in the initial design attempts, and the slightly reduced value for the stability margin is a consequence of the compromise that must be made between high frequency ratio and high stability margin. With a gain as high as 100 a slightly more critical stability problem is to be expected. The required line resistance is now given by

$$R = b\, R_L$$

$$= (27.6)(410)$$

$$= 11.316 \text{ K}\Omega , \qquad (4.188)$$

and the required nulling resistor, R_n, is given by

$$R_n = (4.56814)\, R$$

$$= (4.56814)(11.316 \text{ K}\Omega)$$

$$= 51.693 \text{ K}\Omega . \qquad (4.189)$$

The required negative resistance is computed from (4.185) as

$$R_d = \frac{Ka[(0.8204)ab + 1]\, R_s}{K[(a+1) + (0.8204)ab] - (a+1)}$$

$$= (0.010814)\, R_s$$

$$= (0.010814)(41 \times 10^3)$$

$$= 442.857\ \Omega\ , \qquad (4.190)$$

and this value may be realized physically.

The model transmission line fabricated for this example achieved the parameter values

$$R = 11.310\ K\Omega\ ,$$

and

$$C = 1.77\ nf\ .$$

The null resistance, R_n, was measured to be 51.666 KΩ, and a Hoffman 1N2928 tunnel diode biased at approximately 120 mv furnished the required negative resistance. Again, the fine adjustment of the bias and value of IPG(0) was made by adjusting the low-frequency voltage amplification via (4.104) so that

$$|A_v(0)| = \frac{K\, R_L}{R_s + R_L}\ . \qquad (4.191)$$

It should be noted that (4.104) was used directly without any interchange of R_s and R_L. Since (4.104) is derived for the general amplifier configuration of Figure 4.16, it is invariant. Thus, (4.191) applies for the Transmission II as well as the Transmission I configuration, and (4.191) is the single exception in the use of the symmetry-of-form

property in describing the Transmission II configuration.* The modified design parameter a, defined by (4.182), can be substituted in (4.191), however, so that for the Transmission II configuration we have

$$|A_v(0)| = \frac{a\,K}{(a+1)} \quad . \tag{4.192}$$

For the case at hand, a = 0.01 and K = 10, and the bias was finely adjusted so that the low-frequency voltage amplification had a magnitude of

$$|A_v(0)| = \frac{(0.01)(10)}{(1.01)} = 0.099 \ ,$$

and the bias was then maintained throughout the measurement of the frequency response.

The resulting frequency response is shown in Figure 4.36. The solid curve represents the theoretically predicted response (based on the chosen parameter values) calculated via the exact gain expression given in Appendix D. Superimposed are points representing the experimental measurements made on the prototype amplifier. The exactly calculated value of f_{hp} based on the chosen set of parameters was 12.33 KHz which was 17 per cent higher than the design goal of 10.5 KHz. The measured value of f_{hp} was 13.1 KHz which was 24 per cent higher than the design goal. The value of the frequency ratio achieved experimentally was 0.05343 based on the measured value of f_{hp} and the line parameters. This was 24.2 per cent higher than the value 0.0430 predicted by the design curve of Figure G.6.

---

* This point also applies to the Series I and II configurations.

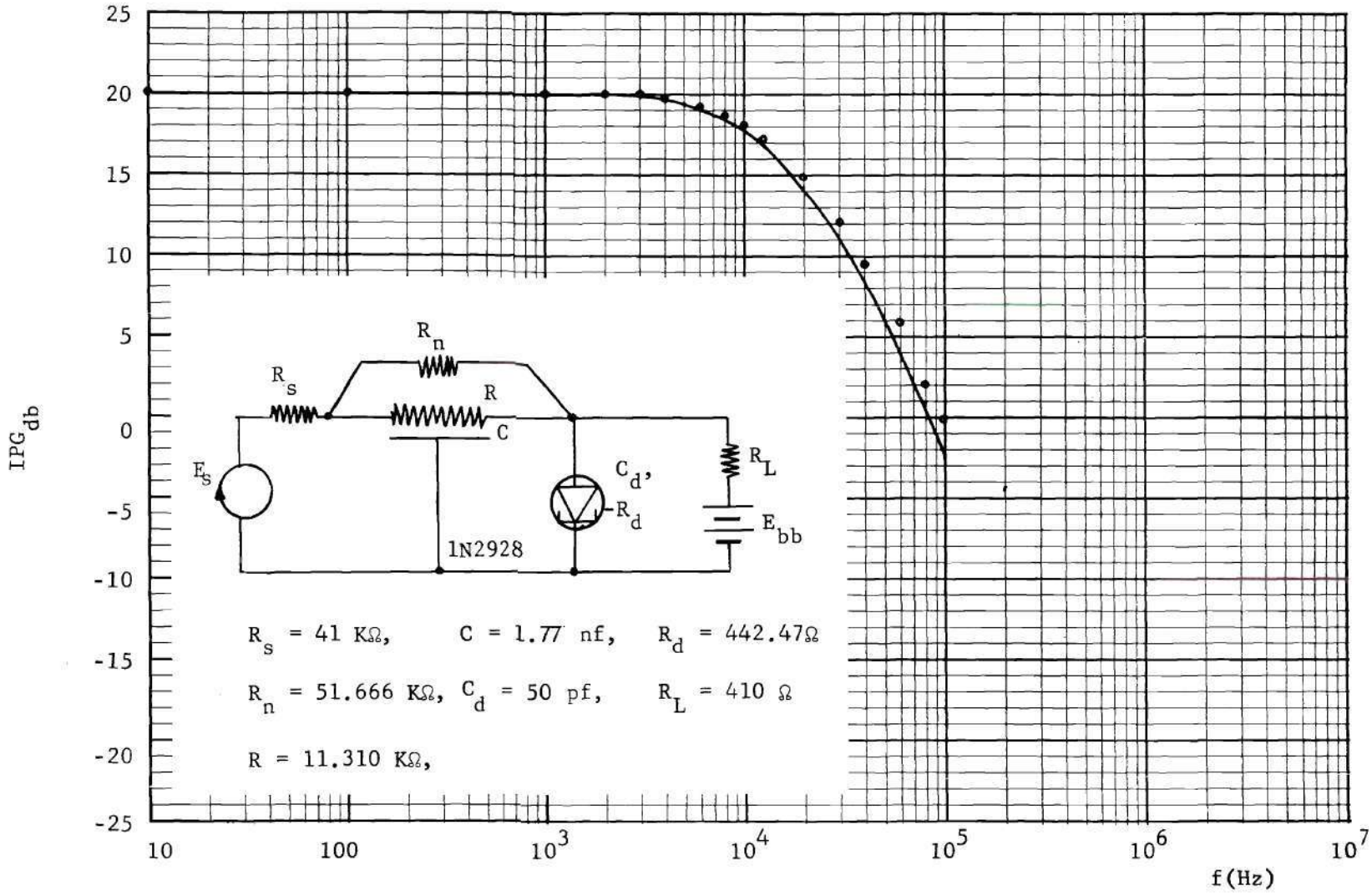

Figure 4.36 IPG-Frequency Response of Prototype Transmission II Amplifier.

The experimental results of this example were not as favorable as those presented earlier, but since the design curves of Figures G.3 and G.6 are based on approximate expressions it is not surprising that the correlation varies between experimental and theoretical results. There are two sources of error in this case that can have significant effect on the results. The first source of error is that the method of measuring the effective line capacitance is very sensitive to small variations in the nulling resistance and thus subject to significant error. The second source of error in this case is that the line capacitance is relatively small, and it is likely that in the derivation of the approximation for f_{hp} the assumptions made about dropping certain terms are beginning to break down. At any rate, the expressions derived for f_{hp} and δ are approximations and as such are subject to limitations in the range of parameter values that can be used to any specified degree of accuracy. The approximate expressions for f_{hp} and δ do serve their intended purpose, however, in that they do give the network designer preliminary design information from which he can make a few reiterative calculations to arrive at his design goal.

CHAPTER V

SUMMARY, CONCLUSIONS, AND RECOMMENDATIONS

It has been the purpose of this investigation to develop an overall theory for and to demonstrate the feasibility of certain base-band negative-resistance amplifier configurations that utilize a single tunnel diode in conjunction with a uniformly distributed RC transmission line. The problem was conceived in terms of the monolithic integrated circuit technology which is presently receiving much attention by research workers, and the practical details and limitations encountered in this thesis are specifically related to this type of circuit morphology. The areas of the investigation on which greatest attention was focused were the stability criteria for the amplifier configurations, their gain-bandwidth properties, and the techniques and considerations involved in their practical design together with experimental verification of the analytical results.

Background material was given in Chapter II describing the construction of the uniformly-distributed RC transmission line and methods of modeling it. The line, shown symbolically in Figure 5.1, was then discussed regarding its two-port parameters and nulling properties. The coupling network for the proposed amplifier configurations was chosen to be either the RC line section of Figure 5.1 or the null network of Figure 5.2 which realizes a real-frequency transmission zero at the frequency f_n. The insertion power gain (IPG) used to describe the

performance of the amplifiers was defined as shown in Figure 5.3, and the proposed amplifier configurations were defined as shown in Figure 5.4.

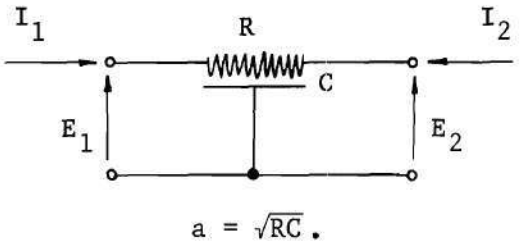

$a = \sqrt{RC}$.

$$z_{11} = z_{22} = \frac{R}{(a\sqrt{s})} \cdot \cosh(a\sqrt{s}).$$

$$z_{12} = z_{21} = \frac{R}{(a\sqrt{s})} \cdot \frac{1}{\sinh(a\sqrt{s})} .$$

Figure 5.1 The Uniform RC Transmission Line.

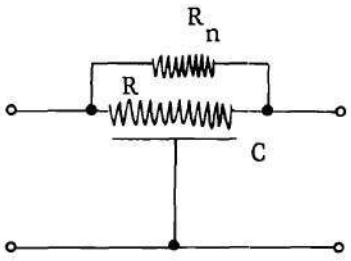

Null Resistor: $R_n = 4.56814\ R.$

Null Frequency: $f_n = \frac{4.90775}{RC}$.

Figure 5.2 RC Transmission Line Null Network.

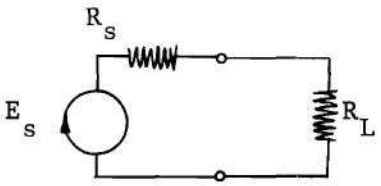

(a) Source connected directly to load. (Power to load = P_{LO}.)

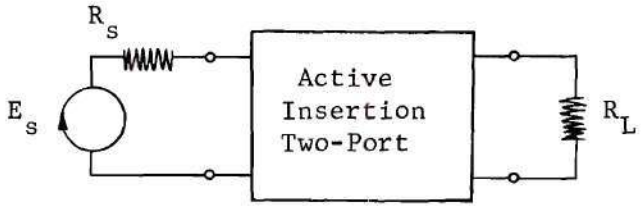

(b) Active two-port inserted between source and load. (Power to load = P_{LA}.)

$$IPG \triangleq P_{LA}/P_{LO} .$$

Figure 5.3 Definition of Insertion Power Gain (IPG).

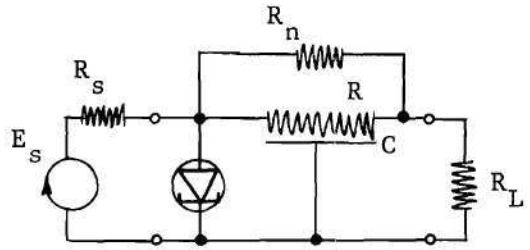

(a) Transmission I Amplifier.

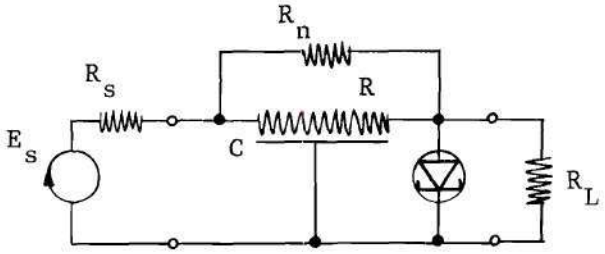

(b) Transmission II Amplifier.

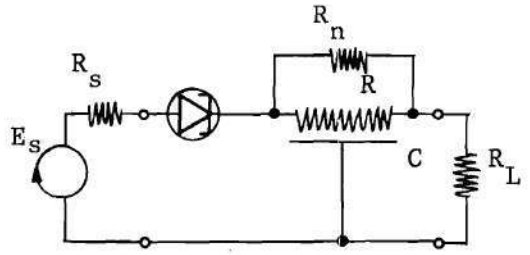

(c) Series I Amplifier.

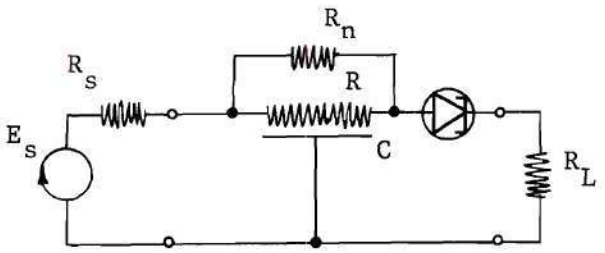

(d) Series II Amplifier.

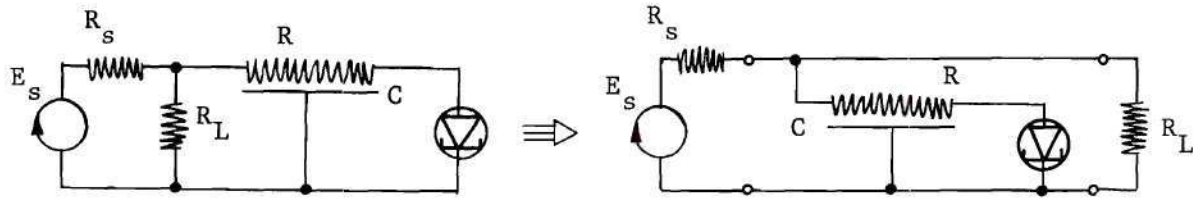

(e) Reflection Amplifier.

Figure 5.4 The Amplifier Configurations Utilizing a Single Tunnel Diode in Conjunction With a Uniformly-Distributed RC Transmission Line.

Chapter III dealt with the stability criteria of the amplifier configurations on both a static (bias) and dynamic (signal) basis. The relationship between the method of coupling and the bias stability was discussed in detail with the following conclusion:

> For the same degree of bias stability, a directly-coupled amplifier will exhibit higher gain for the signal components than a capacitance-coupled amplifier, and the gain exhibited by the directly-coupled amplifier will be maximum for the given degree of bias stability.

For this reason, directly-coupled configurations were employed throughout the investigation. With the aid of a theorem due to Mitra [13] the signal stability criteria were established with the following results:

> The bias and signal stability criteria are identical, and stabilizing the DC operating point stabilizes the circuit in a signal sense as well.

> A fundamental limitation exists in these negative-resistance amplifiers in that there is a trade-off between the conditions of high signal gain and high stability margin, where stability is taken to mean total (both static and dynamic) stability.

A summary of the stability criteria for the various configurations is:

Reflection: $$R_d > R + \frac{R_s R_L}{R_s + R_L} \quad , \tag{5.1}$$

Series I: $$R_d > R_s + R_p + R_L \quad , \tag{5.2}$$

Series II: $$R_d > R_s + R_p + R_L \quad , \tag{5.3}$$

Transmission I: $$R_d > \frac{R_s (R_p + R_L)}{R_s + R_p + R_L} \quad , \tag{5.4}$$

and

$$\text{Transmission II:} \qquad R_d > \frac{R_L(R_p+R_s)}{R_s+R_p+R_L} \quad , \tag{5.5}$$

where

$$R_p = \frac{RR_n}{R+R_n} = 0.8204\ R \quad , \tag{5.6}$$

and R_d is the magnitude of the negative resistance furnished by the tunnel diode.

> From the results given above, it is concluded that the most general form of the stability criteria is $R_d > R_{eq}$, where R_{eq} is the equivalent DC resistance of the circuit external to the tunnel diode.

Chapter IV dealt with the gain-bandwidth properties and design techniques associated with the various amplifier configurations. In an effort to establish a least upper bound on the realizable gain-bandwidth product of these amplifiers, the following conclusion was reached:

> The gain-bandwidth product of these negative-resistance amplifiers can, theoretically, be made arbitrarily large. This result is of limited practical value, however, because unbounded gain-bandwidth products can be achieved only for high-gain narrow-band operation, and in practice the previously mentioned gain-stability limitation will prevent the realization of arbitrarily large gain values.

The basic question concerning the gain-bandwidth properties was then cast in the two forms:

1.) For a specified value of DC gain, IPG(0), what are the maximum values of the half-power frequency, f_{hp}, and the gain-bandwidth product, GBP?

or

2.) For a specified value of half-power frequency, f_{hp}, what are the maximum values of IPG(0) and GBP?

These questions were answered by deriving approximate expressions relating f_{hp}, GBP, and IPG(0) for each of the amplifier configurations. The results were presented in graphical form for various sets of circuit parameters and, as such, served as valuable aids in the design of the amplifiers.

In addition a stability margin, Λ, was defined by the relation

$$R_d = (1 + \frac{\Lambda}{100})\, R_{eq} \quad . \tag{5.7}$$

where R_d and R_{eq} are defined above. Since the general form of the stability criteria is $R_d > R_{eq}$, we see that the value of Λ is the percentage by which $R_d > R_{eq}$. The gain-stability limitations for the amplifier configurations were found to be:

Reflection: $$IPG(0) \leq (\frac{100}{\Lambda} + 1)^2 \quad , \tag{5.8}$$

Series I, II: $$IPG(0) \leq (\frac{100}{\Lambda})^2 \quad , \tag{5.9}$$

and

Transmission I, II: $$IPG(0) \leq (\frac{100}{\Lambda} + 1)^2 \quad , \tag{5.10}$$

where IPG(0) is the DC value of the insertion power gain. Thus, we see that for a stability margin of ten per cent ($\Lambda = 10$) the maximum realizable gain for the Reflection and Transmission configurations is 121 (20.8 db), and it is 100 (20 db) for the Series configurations. In

practice, the minimum value of Λ that may be used is on the order of 10, and we may draw the following conclusions:

> The Reflection and Transmission configurations have an identical gain-stability limitation, and it is less severe than that for the Series configurations.

> As a rule-of-thumb, the practical minimum value for the stability margin is on the order of ten per cent, and the resulting maximum realizable gain is on the order of 20 db.

For the Series and Transmission amplifiers (whose geometry permits the realization of a real-frequency transmission zero in the gain expression) a study was made of the rapidity of cutoff outside their passbands. The cutoff properties were investigated in terms of a frequency ratio defined as

$$\delta \triangleq \frac{f_{hp}}{f_{null}} , \tag{5.11}$$

where f_{hp} is the half-power frequency, and f_{null} is the frequency of the transmission zero in the IPG-frequency response. With a frequency ratio of unity defined as the ideal case, a least upper bound was found for each of these amplifiers to be:

$$\text{Series I, II:} \qquad \text{l. u. b. } [\delta] = 0.07368 , \tag{5.12}$$

and

$$\text{Transmission I, II:} \quad \text{l. u. b. } [\delta] = 0.19458 . \tag{5.13}$$

> Thus, it was found that the Transmission configurations can be made to exhibit the most rapid cutoff above the half-power frequency.

Design considerations were made with regard to stability margin, rapidity of cutoff, and the values required of the circuit parameters to meet specified values of f_{hp} and IPG(0) [with specified values of R_s and R_L]. These considerations led to the following conclusions:

> The Reflection amplifier is best suited to those situations where $R_s \leq R_L$ and the overall impedance level is low.
>
> The Series I configuration is best suited to those situations where $R_s \gg R_L$ and the overall impedance level is low.
>
> The Series II configuration is best suited to those situations where $R_s \ll R_L$ and the overall impedance level is low.
>
> The Transmission I configuration is best suited to those situations where $R_s \ll R_L$.
>
> The Transmission II configuration is best suited to those situations where $R_s \gg R_L$.

As verification of the analytical results of the investigation, a design example was worked out for three of the amplifier configurations. In general the correlation between theory and experiment was favorable, and the feasibility of these amplifiers was demonstrated.

There are several extensions of this investigation that might be worthy of future research. The most obvious and natural extension, of course, is the analysis of amplifiers with the RC line reoriented so that band-pass, or high-pass gain response is achieved. Another facet worthy of investigation is that of employing tapered RC lines such as those whose parameters are distributed linearly, exponentially or

trigonometrically. The frequency characteristics of such amplifiers would certainly be interesting and worthy of research effort. In addition, the use of inductance in shaping the frequency response of these lumped/distributed-parameter amplifiers would be an important contribution to the theory. Admittedly, the foregoing investigation was specifically intended for the strictly RC case of monolithic integrated circuit morphologies, but as the state-of-the-art advances a method of realizing suitable integrated inductors must surely be in the offing. In that event, the analysis of the lumped/distributed RLC case would be a valuable contribution to this growing area of research. There would be a formidable problem, however, in predicting stability criteria for this case. The presence of inductance would rule out the use of Mitra's theorem, and it would be very difficult to make general statements about the natural frequencies of a circuit containing lumped and distributed R, L, and C and a negative resistance. It might be that computer-oriented numerical procedures would have to be employed to search for the natural frequencies, but the results of such an investigation could prove both interesting and useful.

APPENDICES

APPENDIX A

INSERTION POWER GAIN OF THE REFLECTION AMPLIFIER

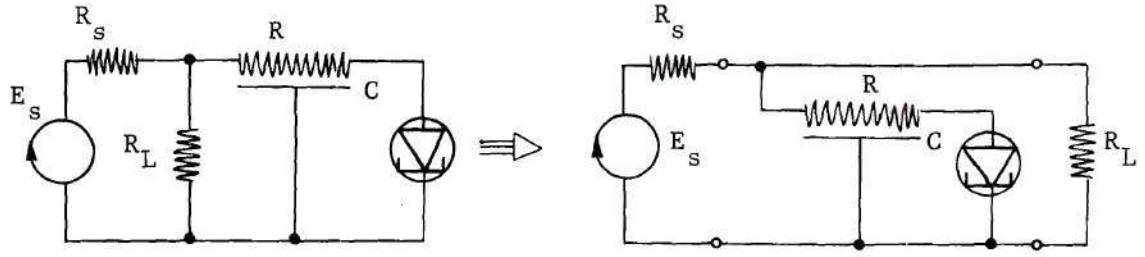

Figure A.1 The Reflection Amplifier (Standard Configuration).

The insertion power gain (IPG) of the Reflection amplifier shown in Figure A.1 is

$$IPG = (R_s + R_L)^2 \left| \frac{y_{11} + Y_d}{R_s R_L (y_{11} Y_d + |y|) + (R_s + R_L)(y_{11} + Y_d)} \right|^2_{s=j\omega}$$

$$= \left| \frac{y_{11} + Y_d}{R_x (y_{11} Y_d + |y|) + y_{11} + Y_d} \right|^2_{s=j\omega} , \qquad (A.1)$$

where

$$R_x = \frac{R_s R_L}{R_s + R_L} , \qquad (A.2)$$

$$y_{11} = \frac{(a\sqrt{s})}{R} \frac{\cosh(a\sqrt{s})}{\sinh(a\sqrt{s})} , \qquad (A.3)$$

$$|y| = \frac{(a\sqrt{s})^2}{R^2} \quad , \tag{A.4}$$

$$Y_d = C_d s - G_d \quad , \tag{A.5}$$

and

$$a = \sqrt{RC} \, . \tag{A.6}$$

For $s=j\omega$ we have

$$a\sqrt{s}\Big|_{s=j\omega} = a\sqrt{j\omega} = A + jA \quad , \tag{A.7}$$

where

$$A = \sqrt{\frac{\omega RC}{2}} \quad . \tag{A.8}$$

Equation (A.1) then takes the form

$$IPG = \frac{N_r^2 + N_i^2}{D_r^2 + D_i^2} \quad , \tag{A.9}$$

where

$$N_r = A(\cosh A \cos A - \sinh A \sin A) - \frac{2C_d}{C} A^2 \cosh A \sin A - RG_d \sinh A \cos A \, , \tag{A.10}$$

$$N_i = A(\cosh A \cos A + \sinh A \sin A) + \frac{2C_d}{C} A^2 \sinh A \cos A - RG_d \cosh A \sin A , \quad (A.11)$$

$$D_r = -\frac{2R_x C_d}{RC} A^3(\cosh A \cos A + \sinh A \sin A) + (1 - G_d R_x) A(\cosh A \cos A - \sinh A \sin A) - 2\left(\frac{R_x}{R} + \frac{C_d}{C}\right) A^2(\cosh A \sin A) - RG_d \sinh A \cos A , \quad (A.12)$$

and

$$D_i = \frac{2R_x C_d}{RC} A^3(\cosh A \cos A - \sinh A \sin A) + (1 - G_d R_x) A(\cosh A \cos A + \sinh A \sin A) + 2\left(\frac{R_x}{R} + \frac{C_d}{C}\right) A^2(\sinh A \cos A) - RG_d \cosh A \sin A . \quad (A.13)$$

At zero frequency, the insertion power gain is

$$IPG(0) = \left(\frac{R_d - R}{R_d - R_{eq}}\right)^2 , \quad (A.14)$$

where

$$R_{eq} = R + R_x . \quad (A.15)$$

APPENDIX B

PBGA PROPERTY OF THE REFLECTION AMPLIFIER

The insertion power gain of the Reflection amplifier is of the form

$$IPG = g(\omega, G_d) = f\left(\sqrt{\frac{\omega RC}{2}}\ ,\ G_d\right) = f(A, G_d)\ . \tag{B.1}$$

If G_d takes on the limiting value G_{eq}, then we have the resulting upper-limit gain function, i.e.,

$$\lim_{G_d \to G_{eq}} (IPG) = g(\omega, G_{eq}) = f(A, G_{eq})\ . \tag{B.2}$$

The PBGA of the upper-limit gain function is

$$PBGA = \int_{\omega=0}^{\omega=\omega_{hp}} g(\omega, G_{eq})\ d\omega \tag{B.3}$$

As shown in Appendix A, the insertion power gain is more conveniently written as a function of $A = \sqrt{\omega RC/2}$ rather than ω. Rewriting equation (B.3) in terms of the function $f(A, G_{eq})$ and making the proper change of variable yields

$$PBGA = \frac{4}{RC} \int_{A=0}^{A=A_{hp}} A \cdot f(A, G_{eq})\ dA = \frac{4}{RC} \int_{A=0}^{A=A_{hp}} F(A)\ dA, \tag{B.4}$$

where

$$f(A,G_{eq}) = \left.\frac{N_r^2+N_i^2}{D_r^2+D_i^2}\right|_{G_d=G_{eq}} = \frac{f_N(A)}{f_D(A)} \quad , \tag{B.5}$$

$$F(A) = A \cdot f(A,G_{eq}) = \frac{A(N_r^2+N_i^2)}{(D_r^2+D_i^2)} = \frac{A \cdot f_N(A)}{f_D(A)} \quad , \tag{B.6}$$

and the terms N_r, N_i, D_r, and D_i are given in equations (A.10), (A.11), (A.12), and (A.13) of Appendix A. At this point, it is convenient to investigate the behavior of both the upper-limit gain function, $f(A,G_{eq})$, and the function F(A), as A approaches zero. From this point on, $G_d \equiv G_{eq}$.

Inspection of equations (A.10), (A.11), (A.12), and (A.13) shows that

$$\lim_{A\to 0} N_r = \lim_{A\to 0} N_i = \lim_{A\to 0} D_r = \lim_{A\to 0} D_i = 0 \quad , \tag{B.7}$$

and therefore

$$\lim_{A\to 0} f(A,G_{eq}) = \frac{\lim_{A\to 0} f_N(A)}{\lim_{A\to 0} f_D(A)} \tag{B.8}$$

assumes the indeterminate form 0/0 necessitating the use of L'Hospital's rule. Differentiating we have

$$f_N'(A) = 2N_rN_r' + 2N_iN_i' \quad , \tag{B.9}$$

and

$$f_D'(A) = 2D_rD_r' + 2D_iD_i' \quad , \tag{B.10}$$

from which it is obvious

$$\lim_{A\to 0} f_N'(A) = 0 \quad , \tag{B.11}$$

and

$$\lim_{A\to 0} f_D'(A) = 0 \quad . \tag{B.12}$$

A second differentiation yields

$$f_N''(A) = 2[N_r N_r'' + (N_r')^2 + N_i N_i'' + (N_i')^2] \quad , \tag{B.13}$$

and

$$f_D''(A) = 2[D_r D_r'' + (D_r')^2 + D_i D_i'' + (D_i')^2] \quad . \tag{B.14}$$

Therefore

$$\lim_{A\to 0} f_N''(A) = 2\left[\left(\lim_{A\to 0} N_r'\right)^2 + \left(\lim_{A\to 0} N_i'\right)^2\right] \quad , \tag{B.15}$$

and

$$\lim_{A\to 0} f_D''(A) = 2\left[\left(\lim_{A\to 0} D_r'\right)^2 + \left(\lim_{A\to 0} D_i'\right)^2\right] \quad . \tag{B.16}$$

Computing N_r' from equation (A.10) and taking the limit yields

$$\lim_{A\to 0} N_r' = (1 - RG_{eq}) \quad . \tag{B.17}$$

Likewise, computing N_i' from equation (A.11) and taking the limit

yields

$$\lim_{A\to 0} N_i' = (1 - RG_{eq}) \ . \tag{B.18}$$

Thus, from (B.15), we get

$$\lim_{A\to 0} f_N''(A) = 4(1 - RG_{eq})^2 \ . \tag{B.19}$$

Computing D_r' from equation (A.12) and taking the limit yields

$$\lim_{A\to 0} D_r' = 1 - G_{eq}(R_x+R) = 1 - G_{eq}R_{eq} = 0 \ . \tag{B.20}$$

Likewise, computing D_i' from equation (A.13) and taking the limit yields

$$\lim_{A\to 0} D_i' = 1 - G_{eq}(R_x+R) = 1 - G_{eq}R_{eq} = 0 \ . \tag{B.21}$$

Thus, from (B.16) we get

$$\lim_{A\to 0} f_D''(A) = 0 \ . \tag{B.22}$$

The final result for the limit of (B.8) is then

$$\lim_{A\to 0} f(A,G_{eq}) = \frac{\lim_{A\to 0} f_N''(A)}{\lim_{A\to 0} f_D''(A)} = +\infty \ . \tag{B.23}$$

Now, investigating the function $F(A) = A\cdot f_N(A)/f_D(A)$ in light of the foregoing development, it is obvious that L'Hospital's rule yields an indeterminate form until the ratio is formed with the limits of <u>third</u>

derivatives, i.e.

$$[A \cdot f_N(A)]''' = A \cdot f_N'''(A) + 3 f_N''(A) , \tag{B.24}$$

and

$$f_D'''(A) = 2[D_r D_r''' + D_r'' D_r' + 2D_r' D_r'' + D_i D_i''' + D_i'' D_i' + 2D_i' D_i''] , \tag{B.25}$$

so that

$$\lim_{A\to 0} [A \cdot f_N(A)]''' = 3[\lim_{A\to 0} f_N''(A)] = 12(1 - RG_{eq})^2 , \tag{B.26}$$

and

$$\lim_{A\to 0} f_D'''(A) = 0 . \tag{B.27}$$

The final result from L'Hospital's rule is then

$$\lim_{A\to 0} F(A) = \frac{\lim_{A\to 0}[A \cdot f_N(A)]'''}{\lim_{A\to 0} f_D'''(A)} = +\infty . \tag{B.28}$$

From the definition of the upper-limit gain function in equation (B.2) and the fact that $A = \sqrt{\omega RC/2}$, it is obvious that

$$\lim_{A\to 0} f(A, G_{eq}) = +\infty \iff \lim_{\omega\to 0} g(\omega, G_{eq}) = +\infty , \tag{B.29}$$

indicating that the upper-limit gain function (in either of its forms)

is unbounded as the frequency goes to zero. The limits of (B.28) and (B.29) likewise indicate that the PBGA associated with the upper-limit gain function must be found from a gain-integral [either (B.3) or (B.4)] which is improper since the integrand is unbounded at the lower limit of integration. The question of convergence naturally arises at this point, and it is convenient to make use of the following [14]:

$$\left.\begin{array}{l} \underline{\text{Theorem}}: \quad \text{If } F(A) \in C, \quad \text{where} \quad 0 < A \leqq A_{hp}\,, \\ \text{and} \qquad \lim_{A\to 0}\,[A\cdot F(A)] = K \ (\text{or } \pm\infty) \neq 0, \\ \text{then} \qquad \int_{A=0}^{A=A_{hp}} F(A)\,dA \quad \text{diverges.} \end{array}\right\} \tag{B.30}$$

In order to test the gain-integral of (B.4) we must now investigate the

$$\lim_{A\to 0}[A\cdot F(A)] = \lim_{A\to 0}\left[A^2\,\frac{f_N(A)}{f_D(A)}\right]. \tag{B.31}$$

From previous work and some additional differentiation it is found that L'Hospital's rule yields an indeterminate form until the ratio of fourth derivatives is used, i.e.,

$$\lim_{A\to 0}[A\cdot F(A)] = \frac{\lim_{A\to 0}\,[A^2 f_N(A)]^{(4)}}{\lim_{A\to 0} f_D^{(4)}(A)}\,, \tag{B.32}$$

where

$$\lim_{A\to 0}[A^2\cdot f_N(A)]^{(4)} = 12 \lim_{A\to 0} f_N''(A) = 48(1 - RG_{eq})^2, \tag{B.33}$$

and

$$\lim_{A\to 0} f_D^{(4)}(A) = 6\left[\left(\lim_{A\to 0} D_r''\right)^2 + \left(\lim_{A\to 0} D_i''\right)^2\right] . \qquad (B.34)$$

Computing D_r'' from equation (A.12) and taking the limit yields

$$\lim_{A\to 0} D_r'' = 0 . \qquad (B.35)$$

Likewise, computing D_i'' from equation (A.13) and taking the limit yields

$$\lim_{A\to 0} D_i'' = 0 . \qquad (B.36)$$

Thus, from (B.34) we get

$$\lim_{A\to 0} f_D^{(4)}(A) = 0 . \qquad (B.37)$$

The final result for the limit of (B.32) is then

$$\lim_{A\to 0}[A\cdot F(A)] = +\infty , \qquad (B.38)$$

and from the theorem of (B.30) we see that the gain integral of (B.4) diverges. Hence, <u>the PBGA associated with the upper-limit gain function is unbounded.</u>

APPENDIX C

INSERTION POWER GAIN OF THE SERIES AMPLIFIERS

Series I Amplifier

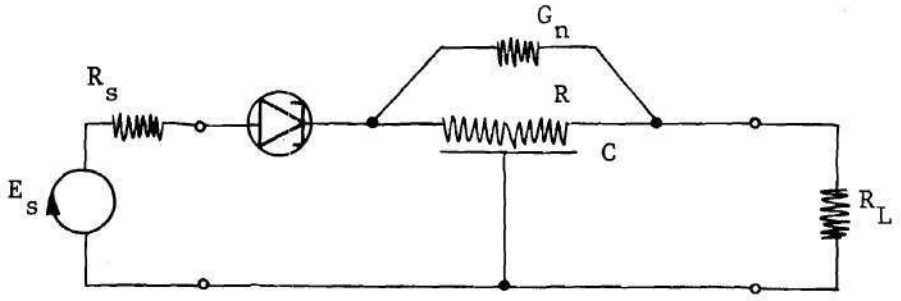

Figure C.1 The Series I Amplifier .

The insertion power gain (IPG) of the Series I amplifier shown in Figure C.1 is

$$IPG = (R_s+R_L)^2 \left| \frac{Y_d(-y_{12}+G_n)}{R_L(R_sY_d+1)|y| + (JY_d+K)y_{11} + L(R_sY_d+1)y_{12} + MY_d + G_n} \right|^2_{s=j\omega} \qquad (C.1)$$

where

$$y_{11} = \frac{(a\sqrt{s})}{R} \cdot \frac{\cosh(a\sqrt{s})}{\sinh(a\sqrt{s})} \quad , \qquad (C.2)$$

$$y_{12} = -\frac{(a\sqrt{s})}{R} \cdot \frac{1}{\sinh(a\sqrt{s})} \quad , \qquad (C.3)$$

$$|y| = \frac{(a\sqrt{s})^2}{R^2} \quad , \qquad (C.4)$$

$$Y_d = C_d s - G_d \ , \tag{C.5}$$

$$J = 2G_n R_s R_L + R_s + R_L \ , \tag{C.6}$$

$$K = 2G_n R_L + 1 \ , \tag{C.7}$$

$$L = 2G_n R_L \ , \tag{C.8}$$

$$M = G_n R_s + G_n R_L + 1 \ , \tag{C.9}$$

and

$$a = \sqrt{RC} \ . \tag{C.10}$$

For $s=j\omega$ we have

$$a\sqrt{s}\Big|_{s=j\omega} = a\sqrt{j\omega} = A + jA \ , \tag{C.11}$$

where

$$A = \sqrt{\frac{\omega RC}{2}} \ . \tag{C.12}$$

Equation (C.1) then takes the form

$$IPG = (R_s+R_L)^2 \left(\frac{N_r^{\,2} + N_i^{\,2}}{D_r^{\,2} + D_i^{\,2}} \right) , \tag{C.13}$$

where

$$N_r = - A(\omega C_d + G_d) - G_n R(\omega C_d \ \text{coshA sinA} + G_d \ \text{sinhA cosA}), \tag{C.14}$$

$$N_i = A(\omega C_d - G_d)$$

$$+ G_n R(\omega C_d \sinh A \cos A - G_d \cosh A \sin A) , \qquad (C.15)$$

$$D_r = -\omega C R_L [(1-G_d R_s) \cosh A \sin A + \omega C_d R_s \sinh A \cos A]$$

$$+A[(K-G_d J)(\cosh A \cos A - \sinh A \sin A)$$

$$-\omega C_d J(\cosh A \cos A + \sinh A \sin A)]$$

$$-LA[(1-G_d R_s) - \omega C_d R_s]$$

$$+ R[(G_n-G_d M) \sinh A \cos A - \omega C_d M \cosh A \sin A] , \qquad (C.16)$$

and

$$D_i = \omega C R_L [(1-G_d R_s) \sinh A \cos A - \omega C_d R_s \cosh A \sin A]$$

$$+ A[(K-G_d J)(\cosh A \cos A + \sinh A \sin A)$$

$$+\omega C_d J (\cosh A \cos A - \sinh A \sin A)] .$$

$$- LA[(1-G_d R_s) + \omega C_d R_s]$$

$$+ R[(G_n-G_d M) \cosh A \sin A + \omega C_d M \sinh A \cos A] . \qquad (C.17)$$

At zero frequency, the insertion power gain is

$$IPG(0) = \frac{(R_s + R_L)^2}{(R_d - R_{eq})^2} , \qquad (C.18)$$

where

$$R_{eq} = R_s + R_L + \frac{R_n R}{R_n + R} \quad . \tag{C.19}$$

Series II Amplifier

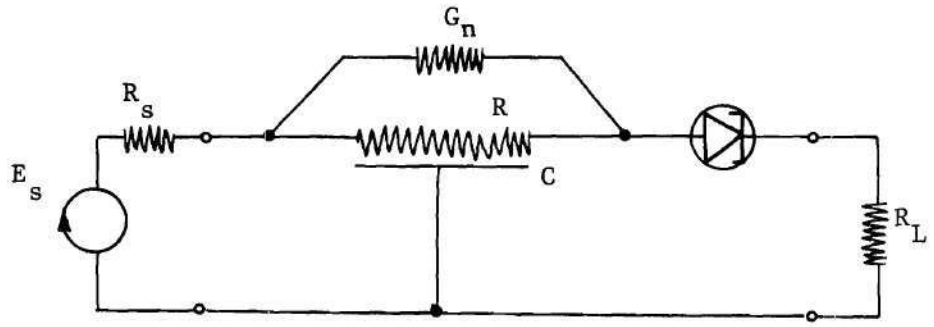

Figure C.2 The Series II Amplifier.

The insertion power gain of the Series II amplifier is the same as that given above for the Series I amplifier with R_s everywhere replaced by R_L and R_L everywhere replaced by R_s. That is,

$$IPG\Big|_{\text{Series II}} = (IPG)_{\text{Series I}}\Big|_{\substack{R_s \to R_L \\ R_L \to R_s}} \quad . \tag{C.20}$$

APPENDIX D

INSERTION POWER GAIN OF THE TRANSMISSION AMPLIFIERS

Transmission I Amplifier

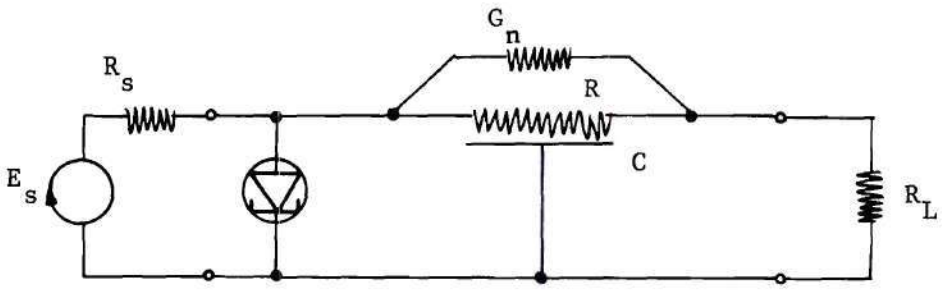

Figure D.1 The Transmission I Amplifier.

The insertion power gain (IPG) of the Transmission I amplifier shown in Figure D.1 is

$$IPG = (R_s+R_L)^2 \left| \frac{-y_{12} + G}{R_s R_L[Y_d(y_{11}+G_n) + 2G_n(y_{11}+y_{12}) + |y|] + R_s(Y_d+y_{11}+G_n) + R_L(y_{11}+G_n) + 1} \right|^2_{s=j\omega} , \quad (D.1)$$

where

$$y_{11} = \frac{(a\sqrt{s})}{R} \cdot \frac{\cosh(a\sqrt{s})}{\sinh(a\sqrt{s})} , \quad (D.2)$$

$$y_{12} = -\frac{(a\sqrt{s})}{R} \cdot \frac{1}{\sinh(a\sqrt{s})} , \quad (D.3)$$

$$|y| = \frac{(a\sqrt{s})^2}{R^2} , \tag{D.4}$$

$$Y_d = C_d s - G_d , \tag{D.5}$$

and

$$a = \sqrt{RC} . \tag{D.6}$$

For $s=j\omega$ we have

$$a\sqrt{s}\Big|_{s=j\omega} = a\sqrt{j\omega} = A + jA , \tag{D.7}$$

where

$$A = \sqrt{\frac{\omega RC}{2}} . \tag{D.8}$$

Equation (D.1) then takes the form

$$IPG = (R_s+R_L)^2 \left(\frac{N_r^2 + N_i^2}{D_r^2 + D_i^2} \right) , \tag{D.9}$$

where

$$N_r = AR + G_n R^2 \sinh A \cos A, \tag{D.10}$$

and

$$N_i = AR + G_n R^2 \cosh A \sin A . \tag{D.11}$$

The denominator terms are

$$D_r = (P_r A - MA^3)\ \text{coshA cosA}$$
$$- (P_r A + MA^3)\ \text{sinhA sinA} - KA$$
$$+ Q_r\ \text{sinhA cosA} ,$$
$$- NA^2\ \text{coshA sinA} , \qquad (D.12)$$

and

$$D_i = (P_r A + MA^3)\ \text{coshA cosA}$$
$$+ (P_r A - MA^3)\ \text{sinhA sinA} - KA$$
$$+ Q_r\ \text{coshA sinA}$$
$$+ NA^2\ \text{sinhA cosA} , \qquad (D.13)$$

where

$$P_r = 2G_n R_s R R_L + R(R_s + R_L) - G_d R_s R R_L , \qquad (D.14)$$

$$M = 2C_d R_s R_L / C , \qquad (D.15)$$

$$K = 2G_n R_s R R_L , \qquad (D.16)$$

$$Q_r = R^2 + G_n R^2 (R_s + R_L) - G_d R^2 R_s (G_n R_L + 1) , \qquad (D.17)$$

and

$$N = 2R_s R_L + 2C_d R R_s (G_n R_L + 1)/C . \qquad (D.18)$$

At zero frequency, the insertion power gain is

$$IPG(0) = \frac{(R_s+R_L)^2 R_d^2}{(R_s+R_p+R_L)^2 (R_d-R_{eq})^2} , \qquad (D.19)$$

where

$$R_P = \frac{RR_n}{R+R_n} , \qquad (D.20)$$

and

$$R_{eq} = \frac{R_s(R_p+R_L)}{(R_s+R_p+R_L)} . \qquad (D.21)$$

Transmission II Amplifier

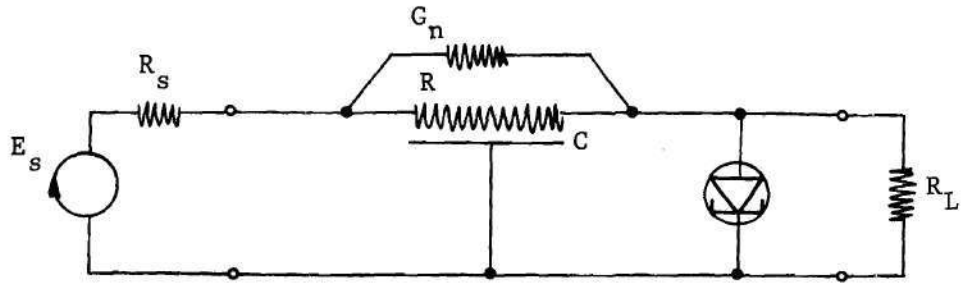

Figure D.2 The Transmission II Amplifier.

The insertion power gain of the Transmission II amplifier is the same as that given above for the Transmission I amplifier with R_s everywhere replaced by R_L and R_L everywhere replaced by R_s. That is,

$$IPG\Big|_{Trans.II} = (IPG)_{Trans.I}\Big|_{\substack{R_s \to R_L \\ R_L \to R_s}} . \qquad (D.22)$$

APPENDIX E

DESIGN CURVES FOR THE REFLECTION AMPLIFIER

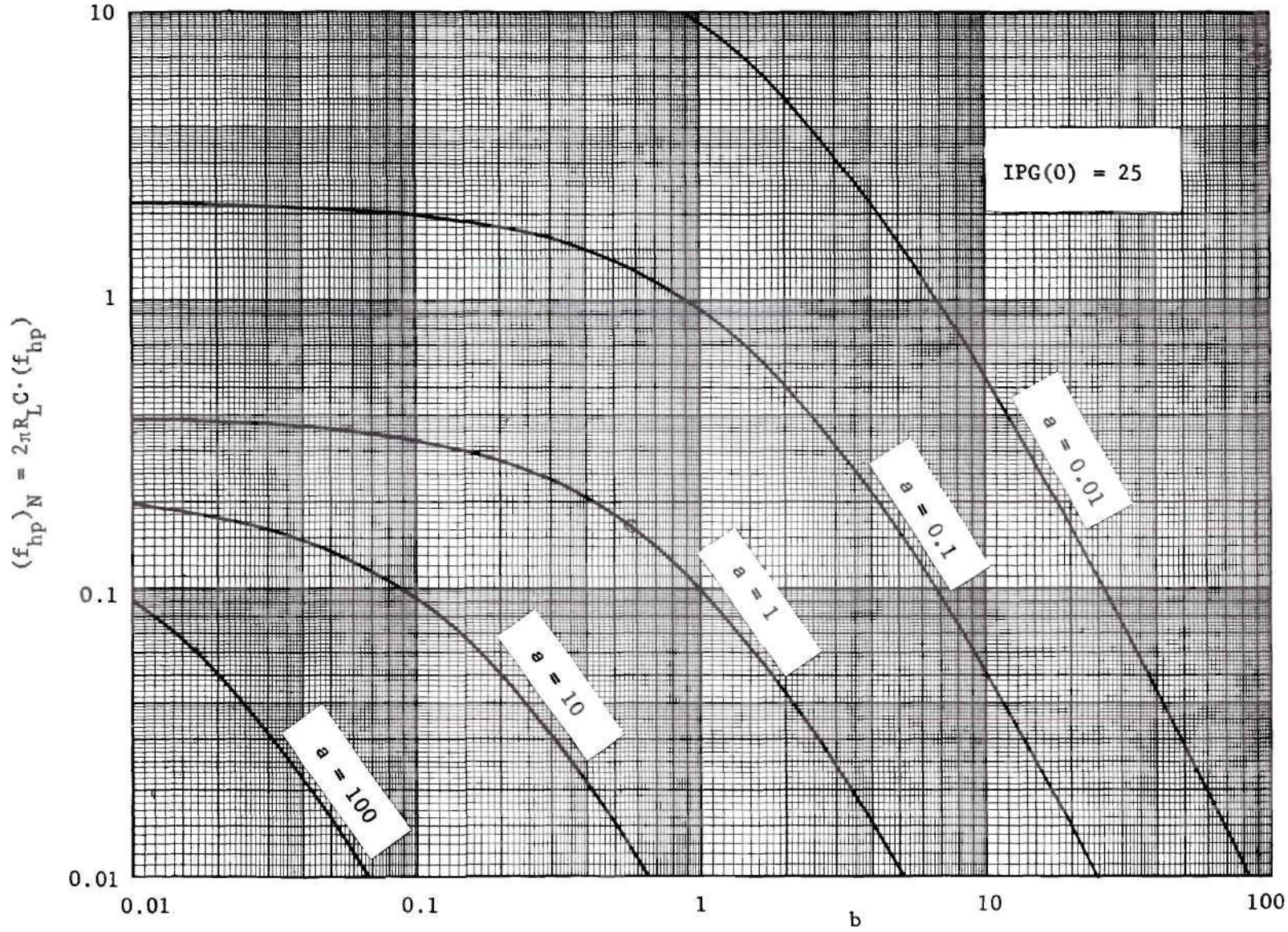

Figure E.1 Normalized Half-Power Frequency vs. b for the Reflection Amplifier.

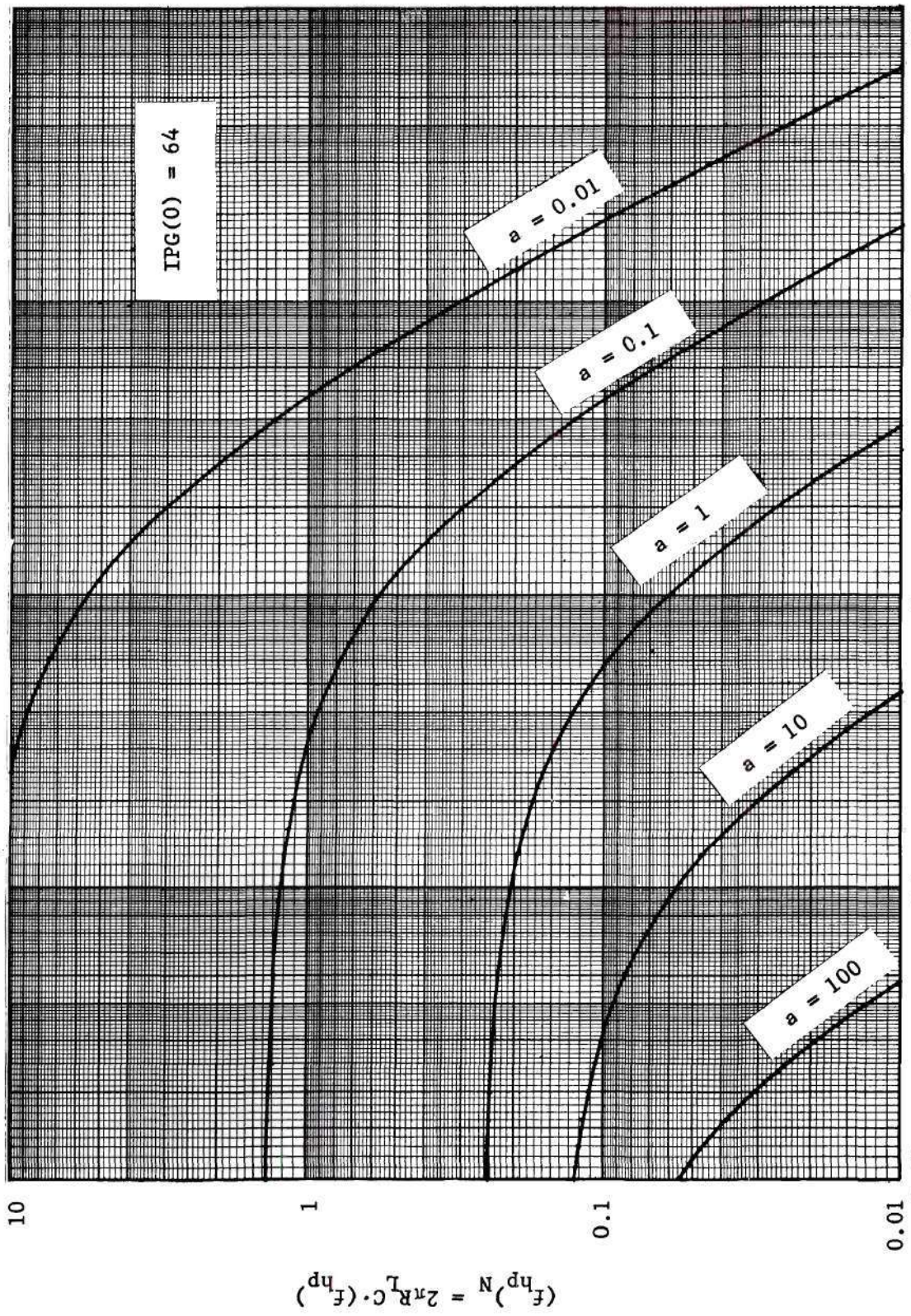

Figure E.2 Normalized Half-Power Frequency vs. b for the Reflection Amplifier.

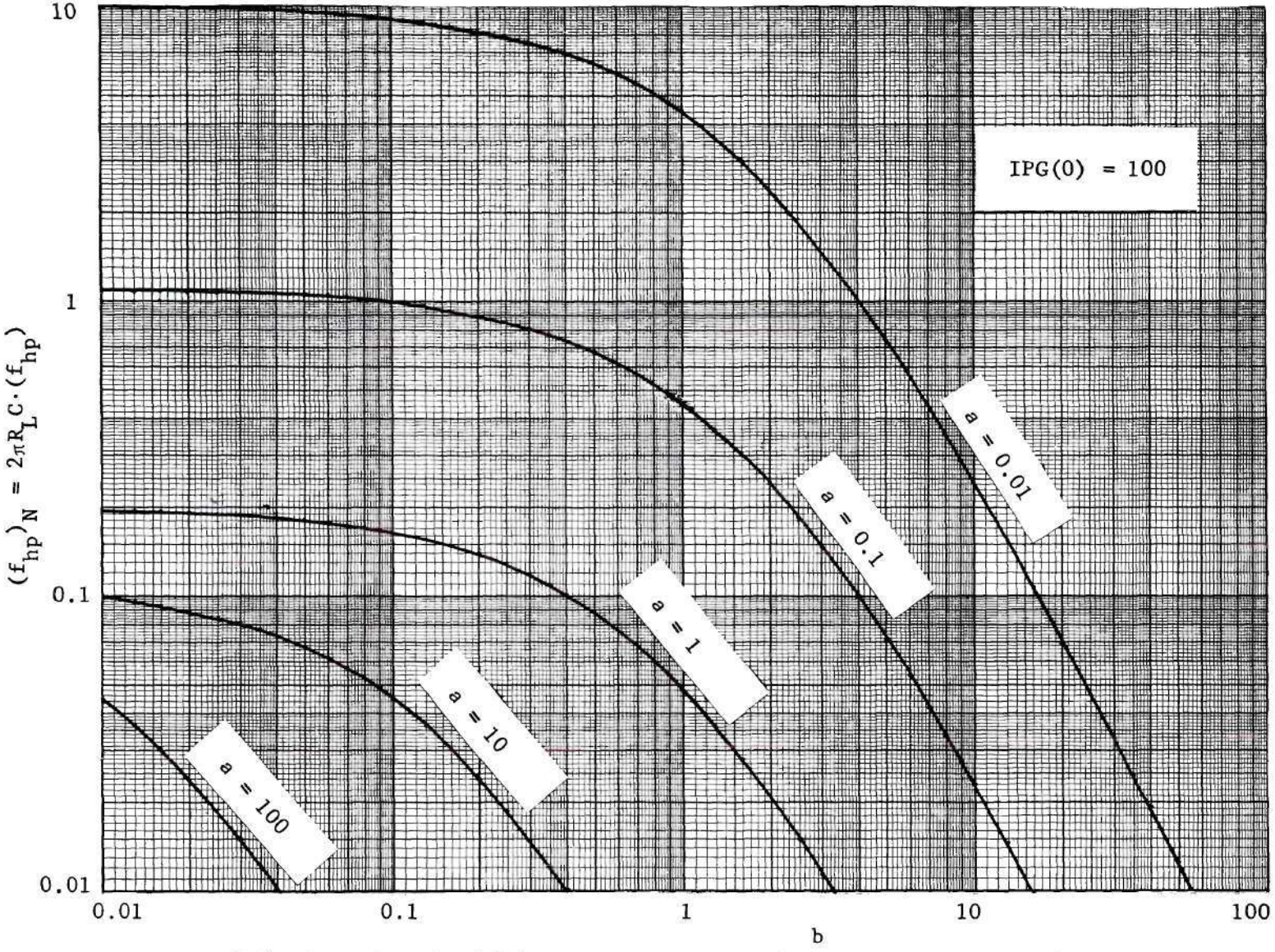

Figure E.3 Normalized Half-Power Frequency vs. b for the Reflection Amplifier.

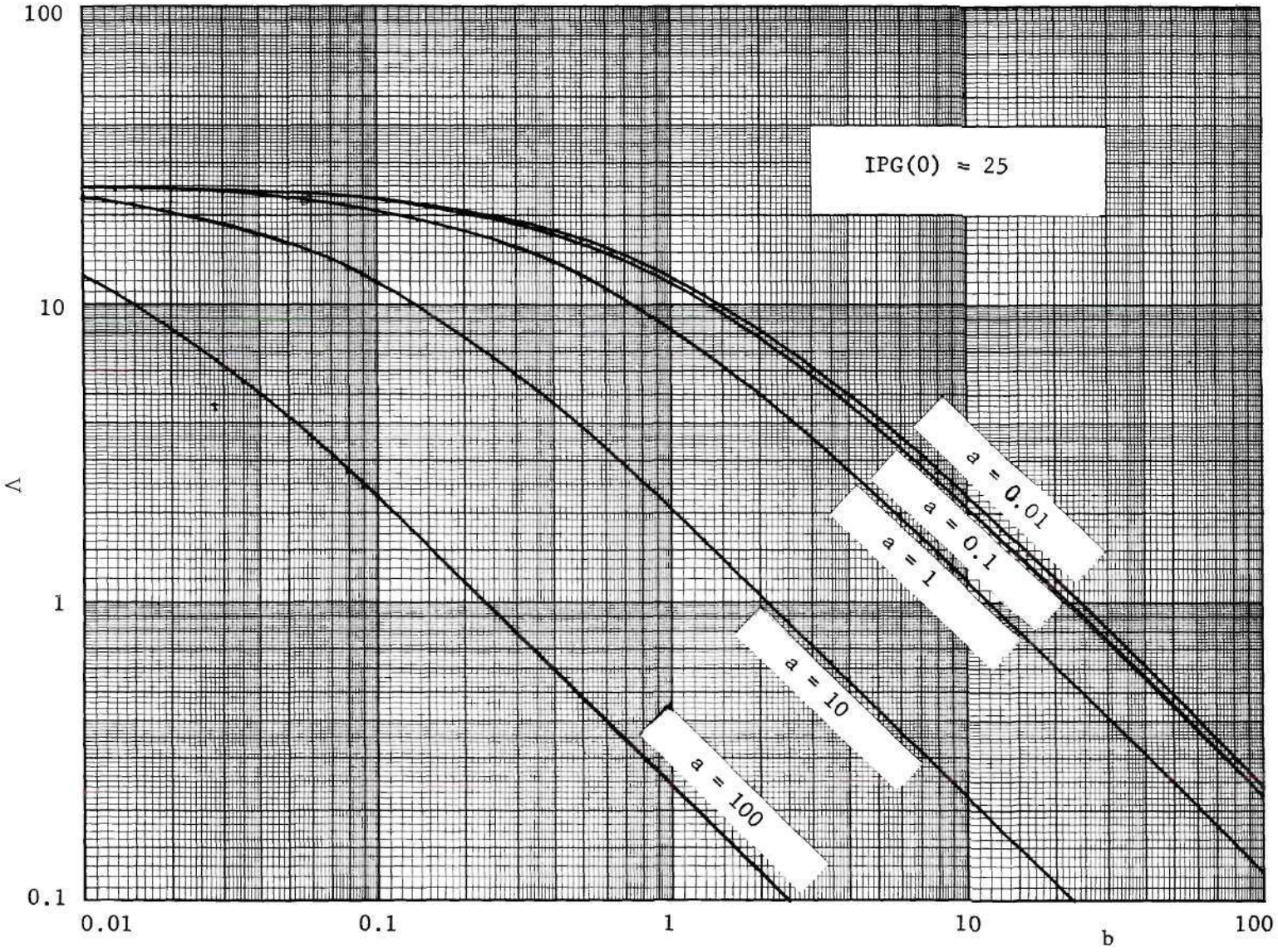

Figure E.4 Percent Stability Margin vs. b for the Reflection Amplifier.

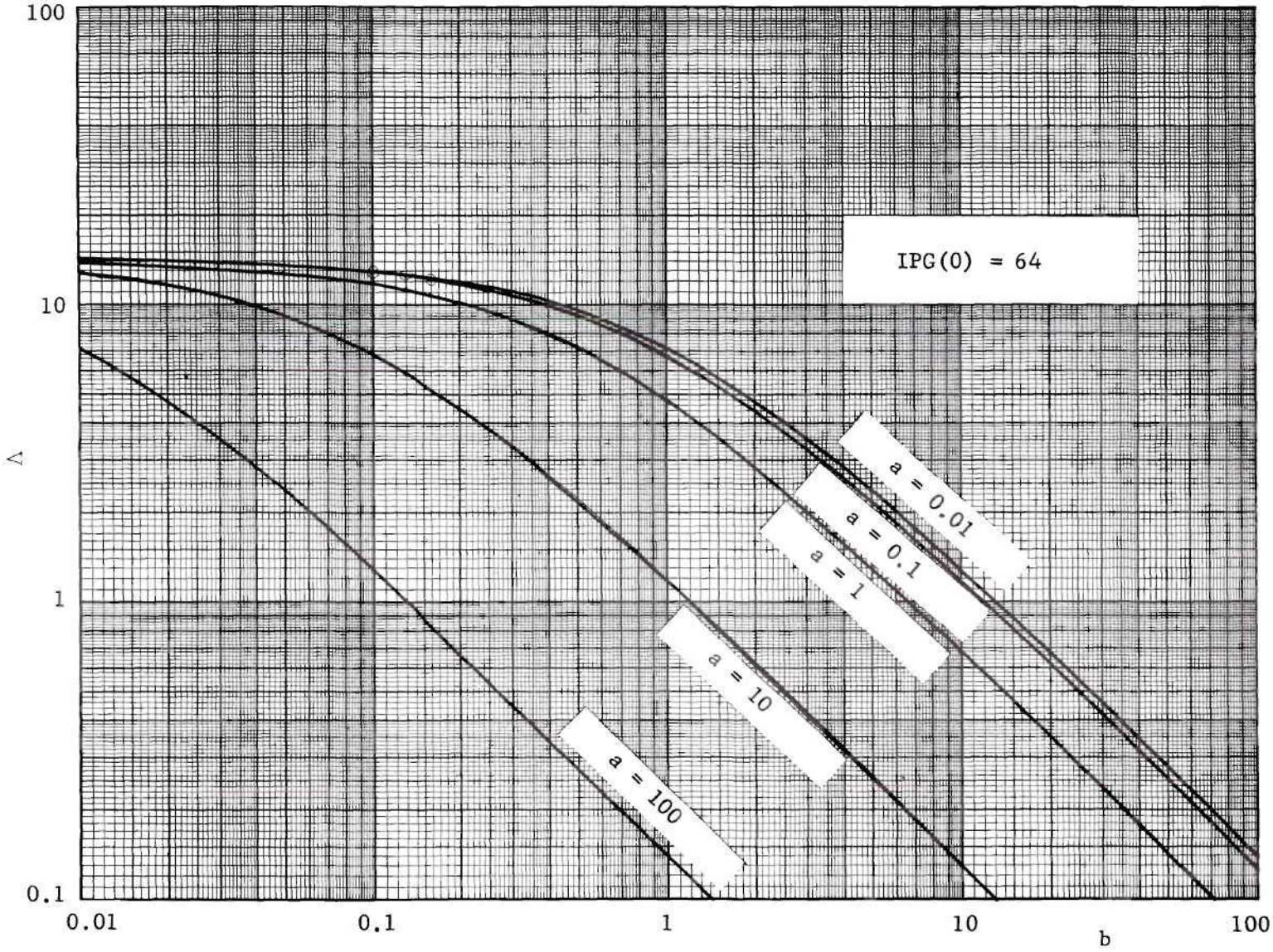

Figure E.5 Percent Stability Margin vs. b for the Reflection Amplifier.

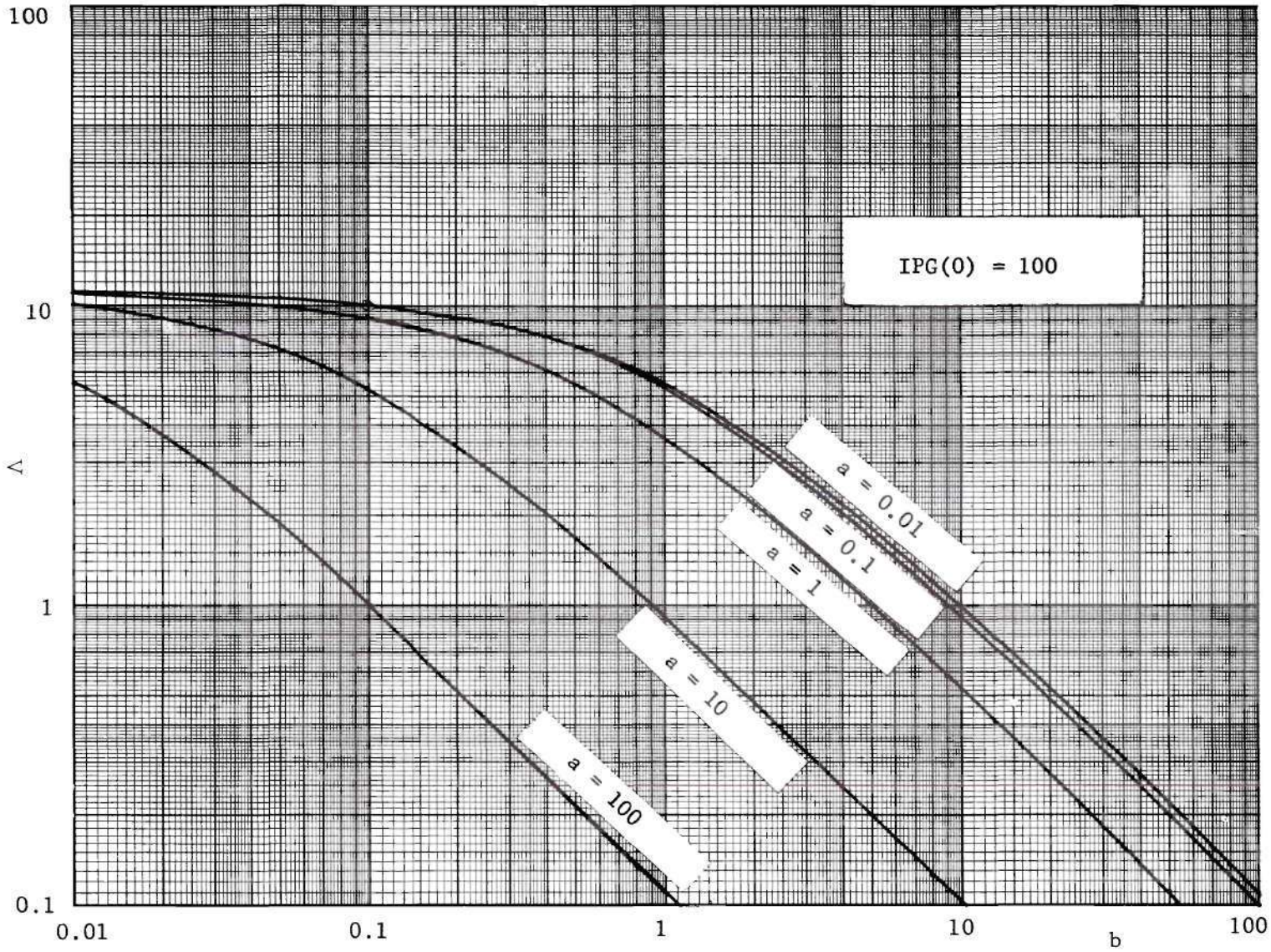

Figure E.6 Percent Stability Margin vs. b for the Reflection Amplifier.

APPENDIX F

DESIGN CURVES FOR THE SERIES AMPLIFIERS

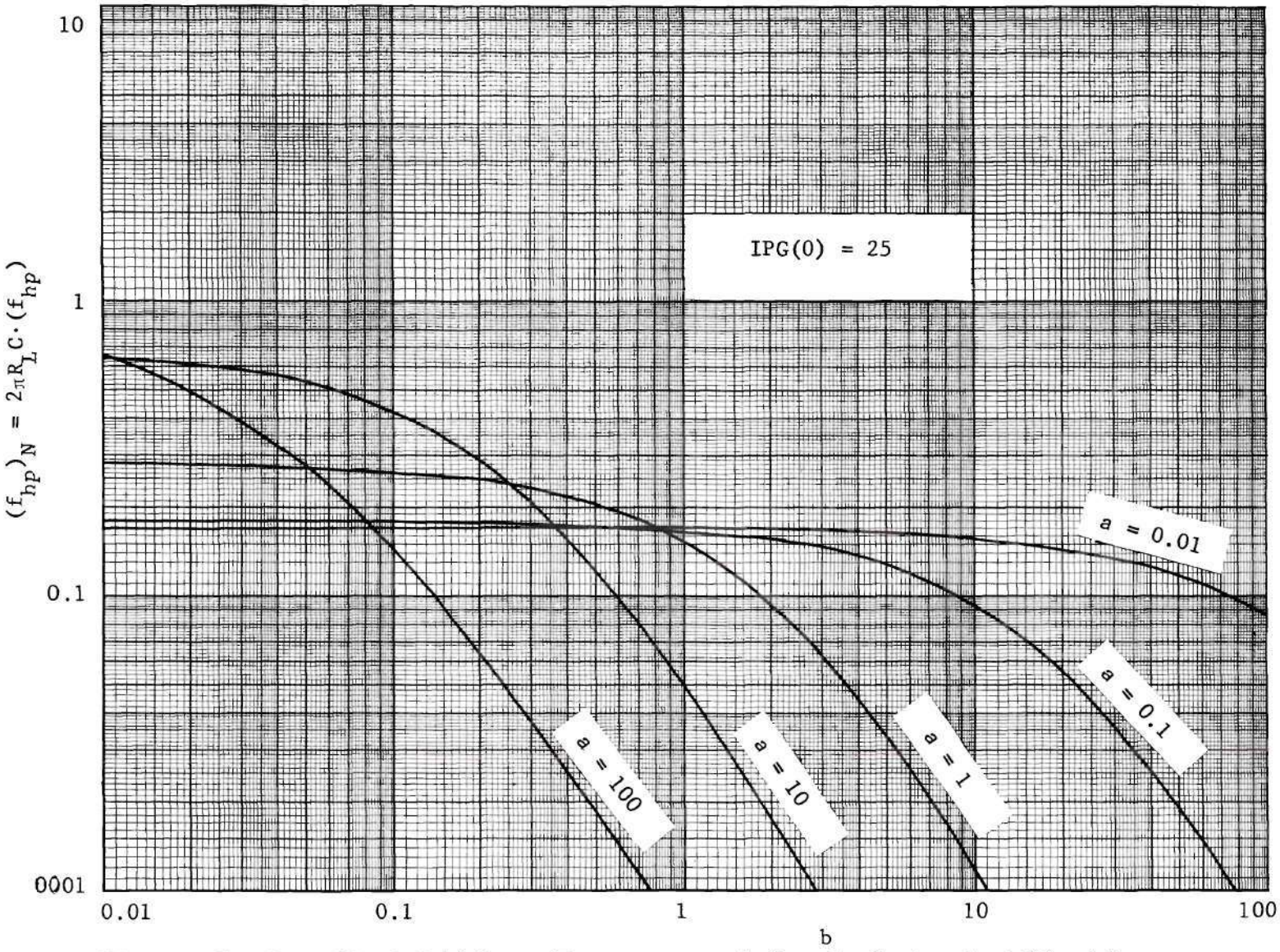

Figure F.1 Normalized Half-Power Frequency vs. b for the Series Amplifier(s).

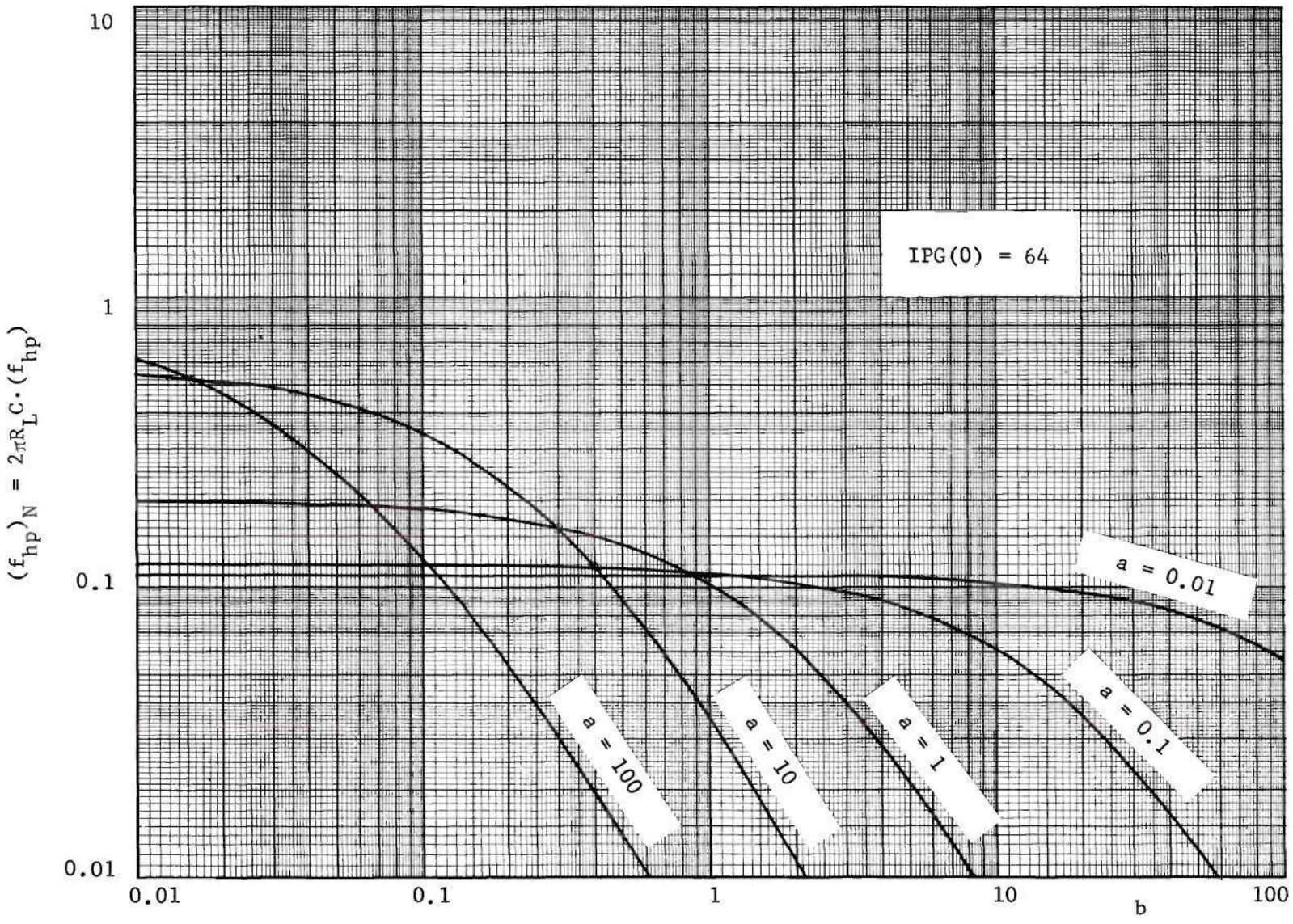

Figure F.2 Normalized Half-Power Frequency vs. b for the Series Amplifier(s).

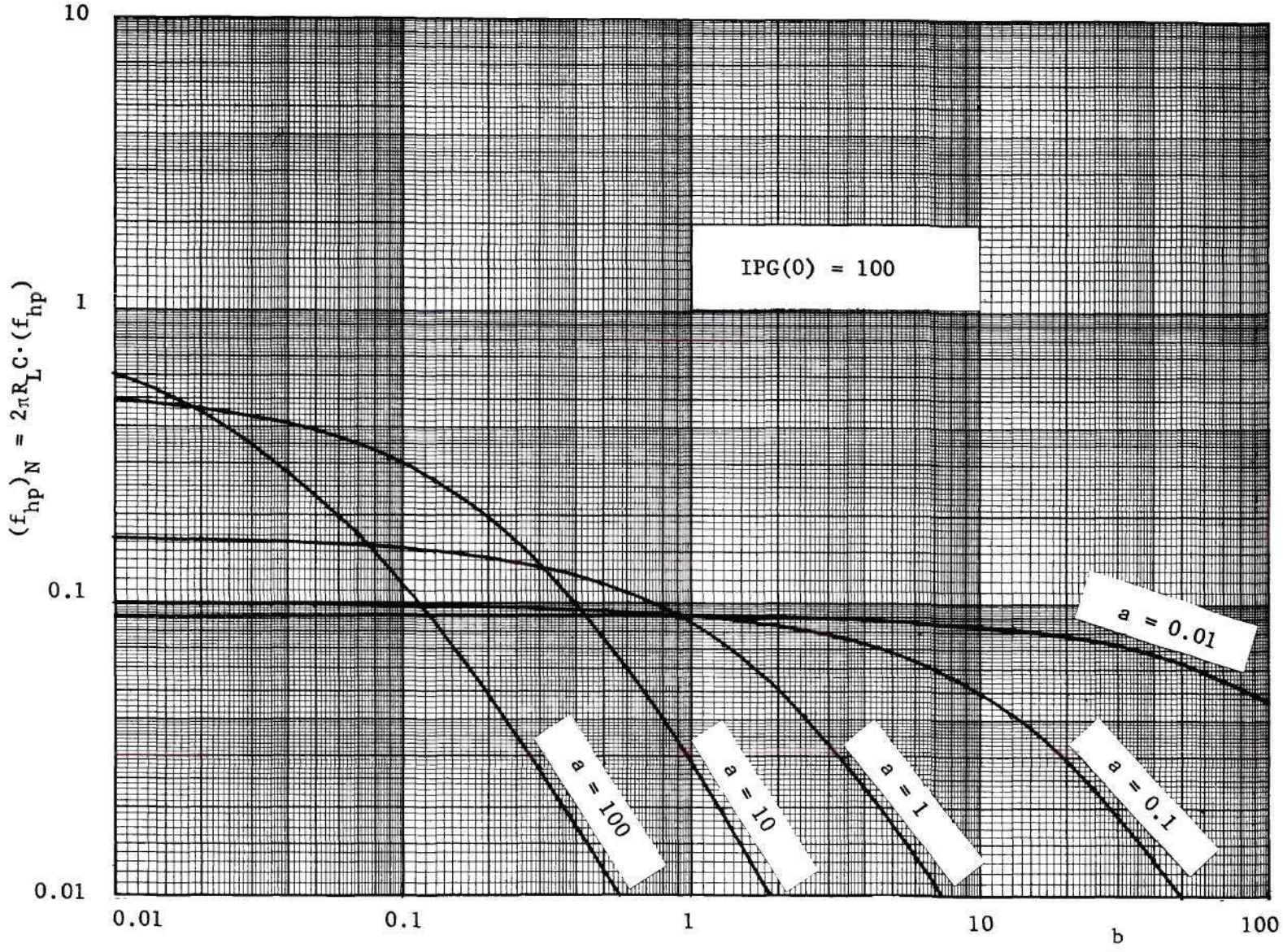

Figure F.3 Normalized Half-Power Frequency vs. b for the Series Amplifier(s).

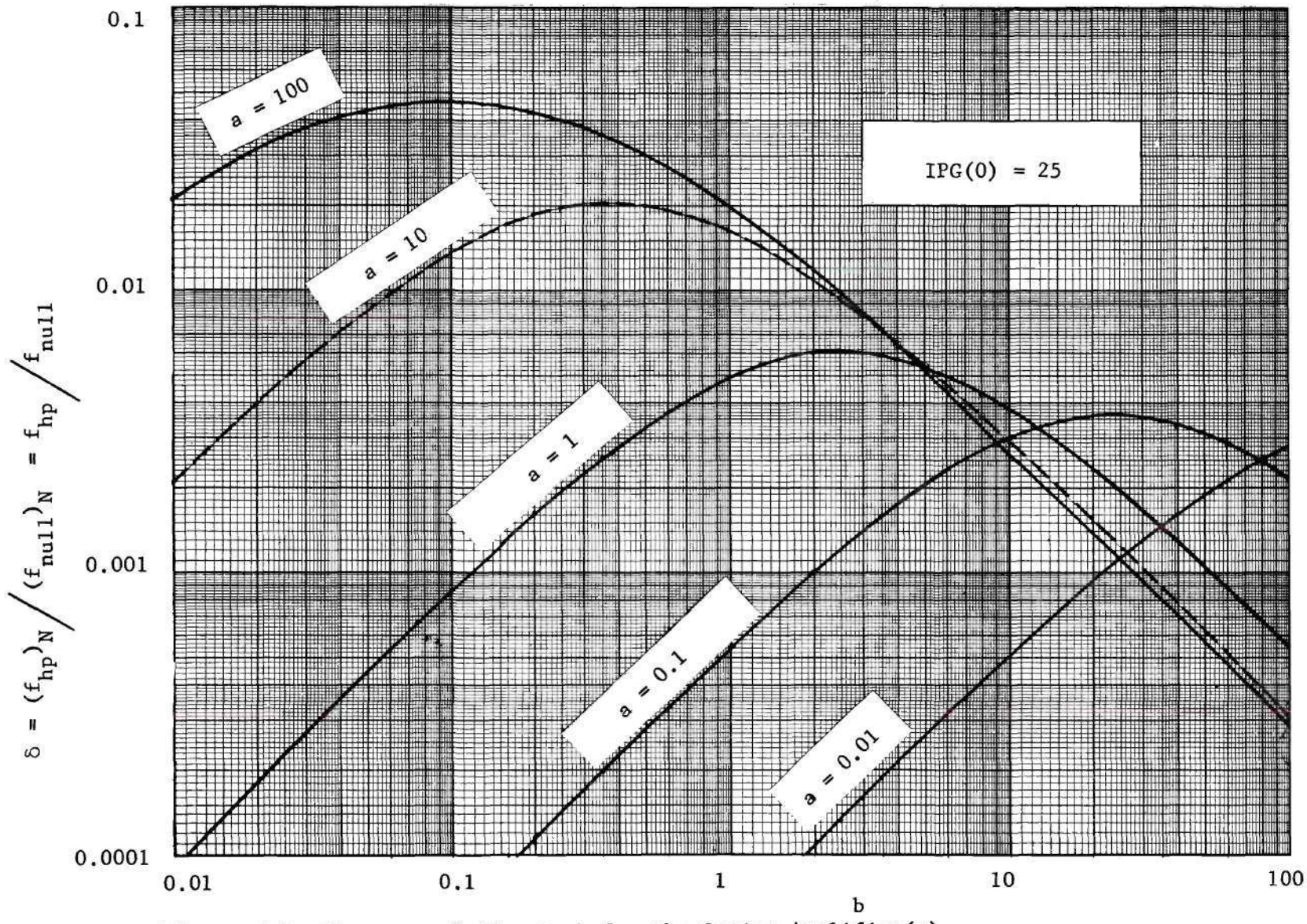

Figure F.4 Frequency Ratio vs. b for the Series Amplifier(s).

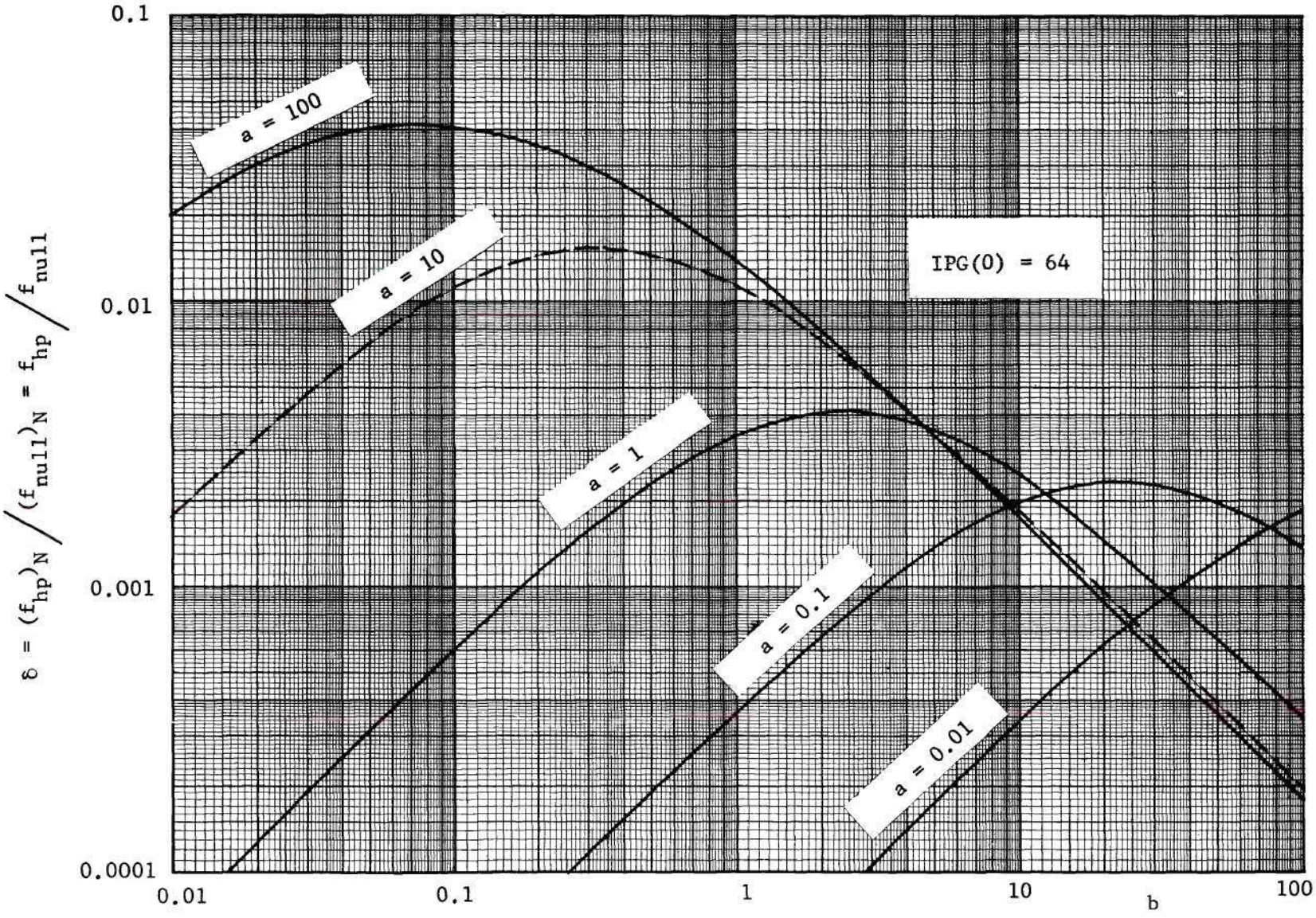

Figure F.5 Frequency Ratio vs. b for the Series Amplifier(s).

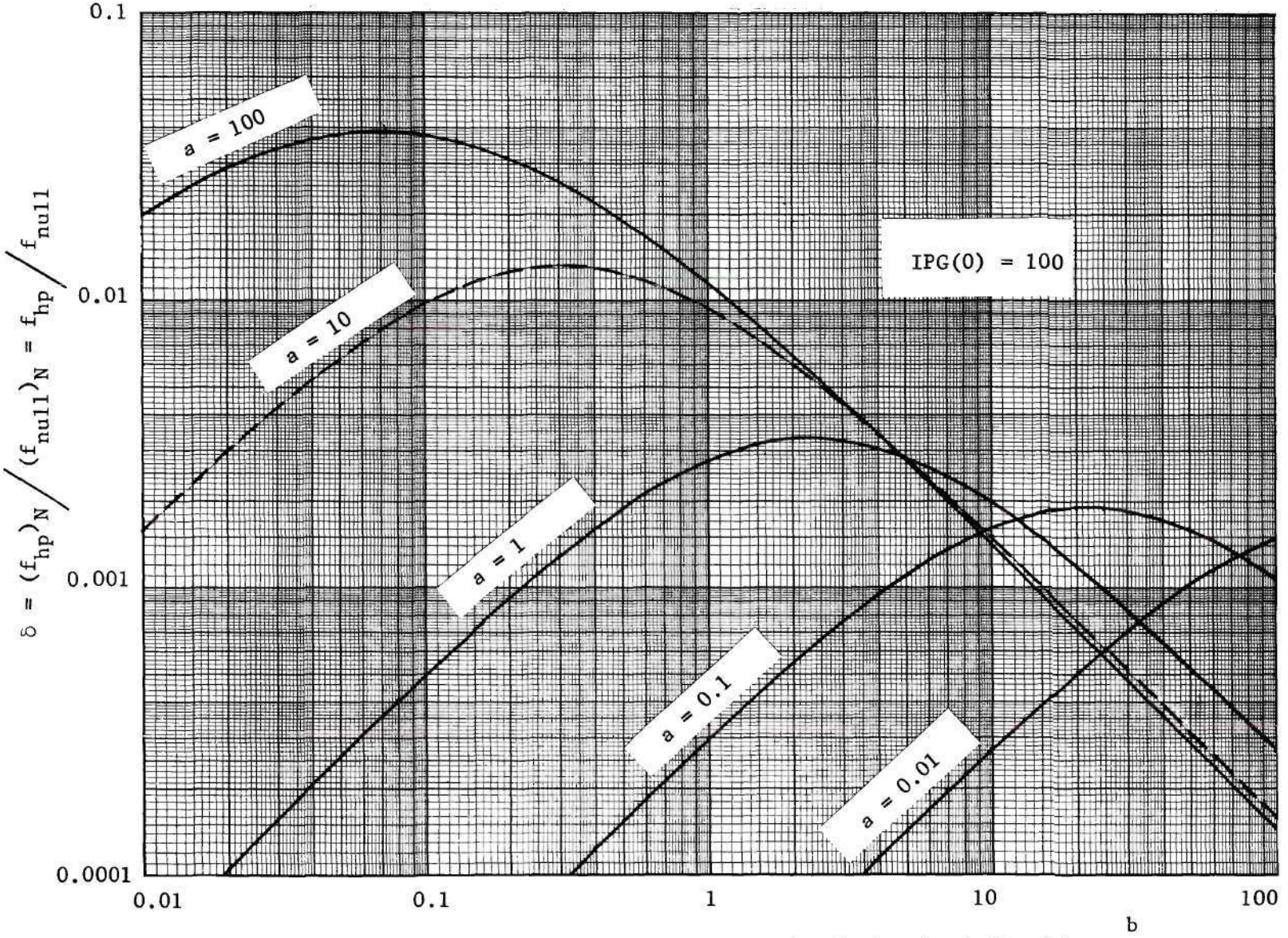

Figure F.6 Frequency Ratio vs. b for the Series Amplifier(s).

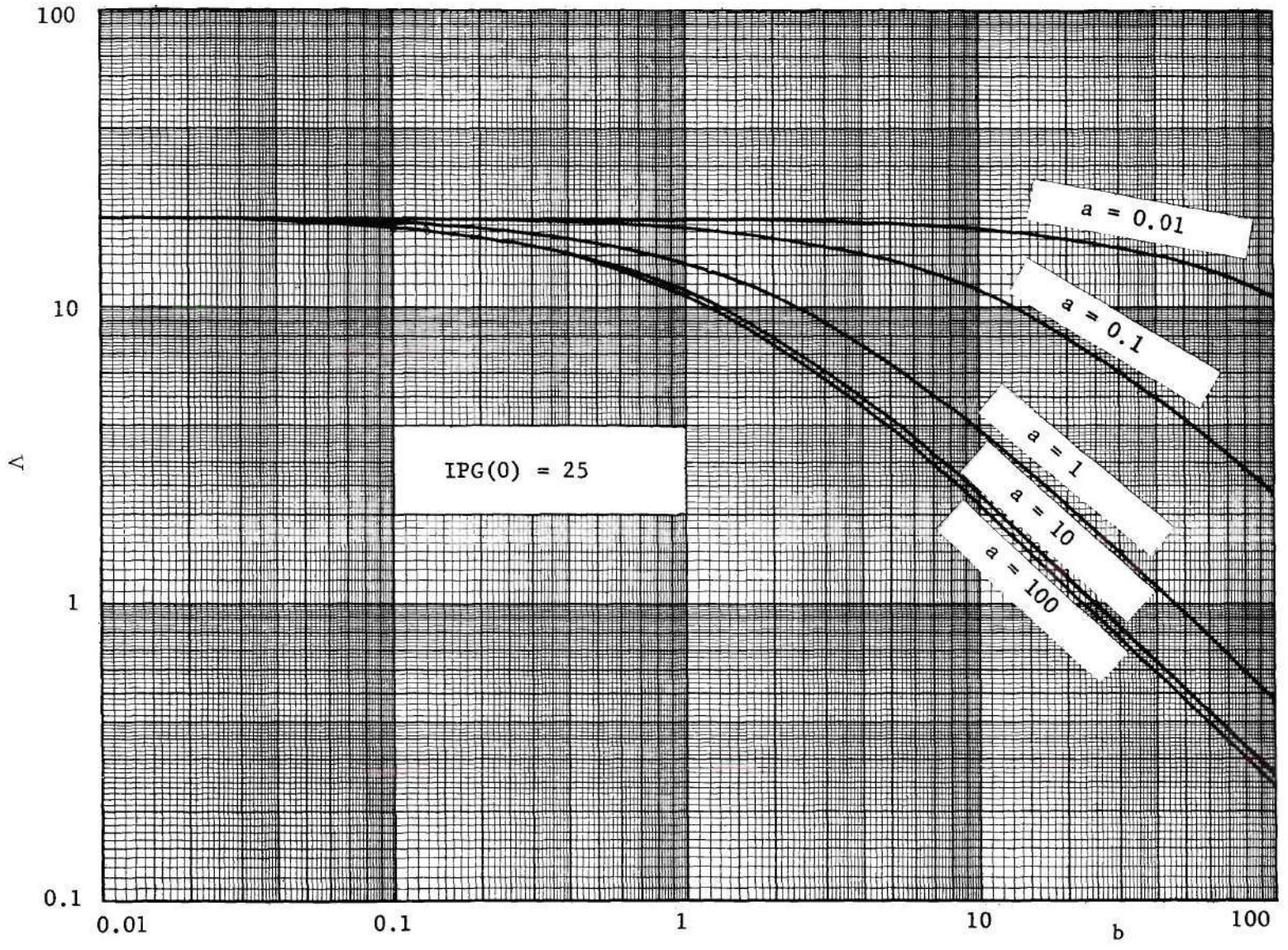

Figure F.7 Percent Stability Margin vs. b for the Series Amplifier(s).

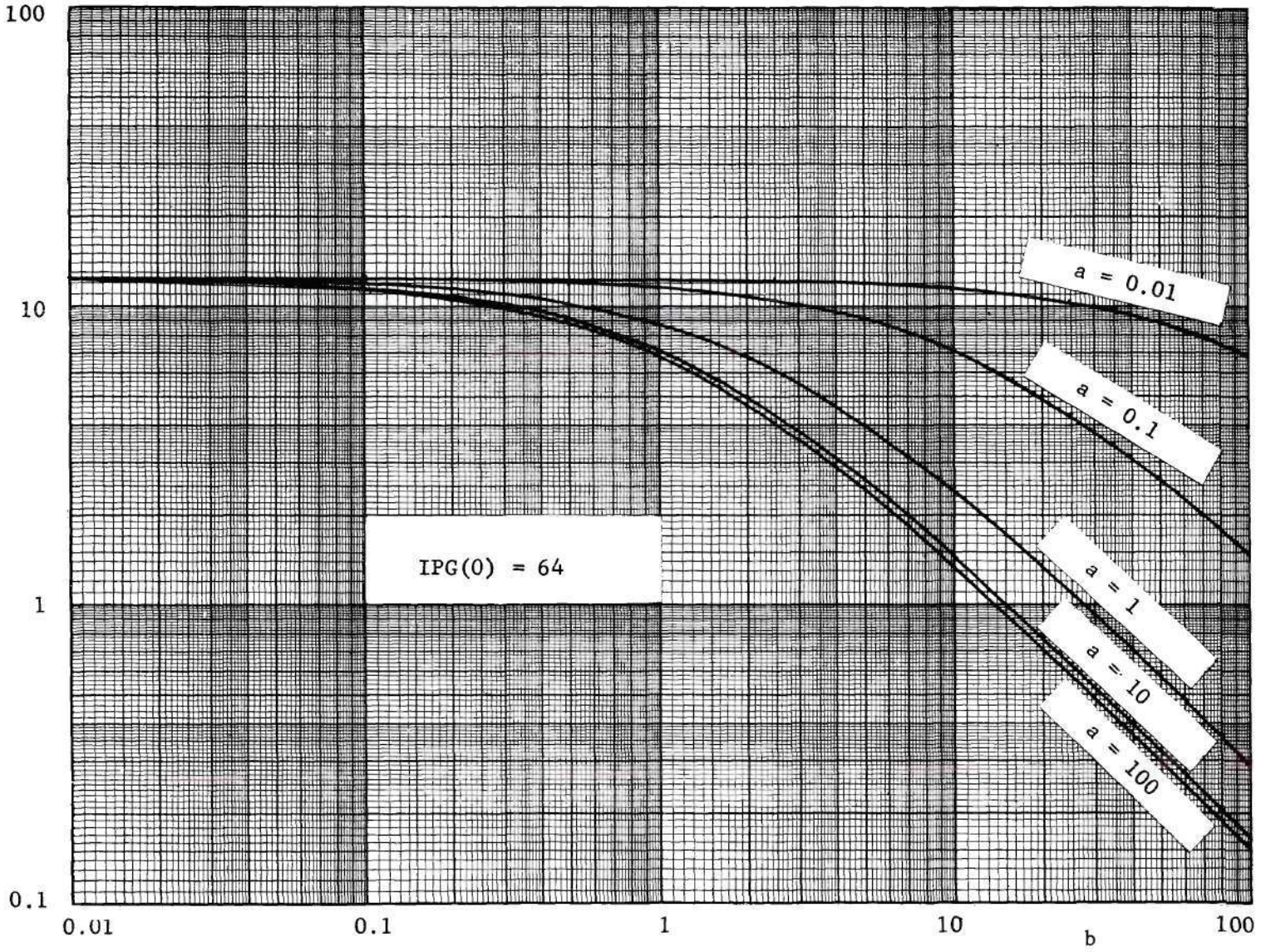

Figure F.8 Percent Stability Margin vs. b for the Series Amplifier(s).

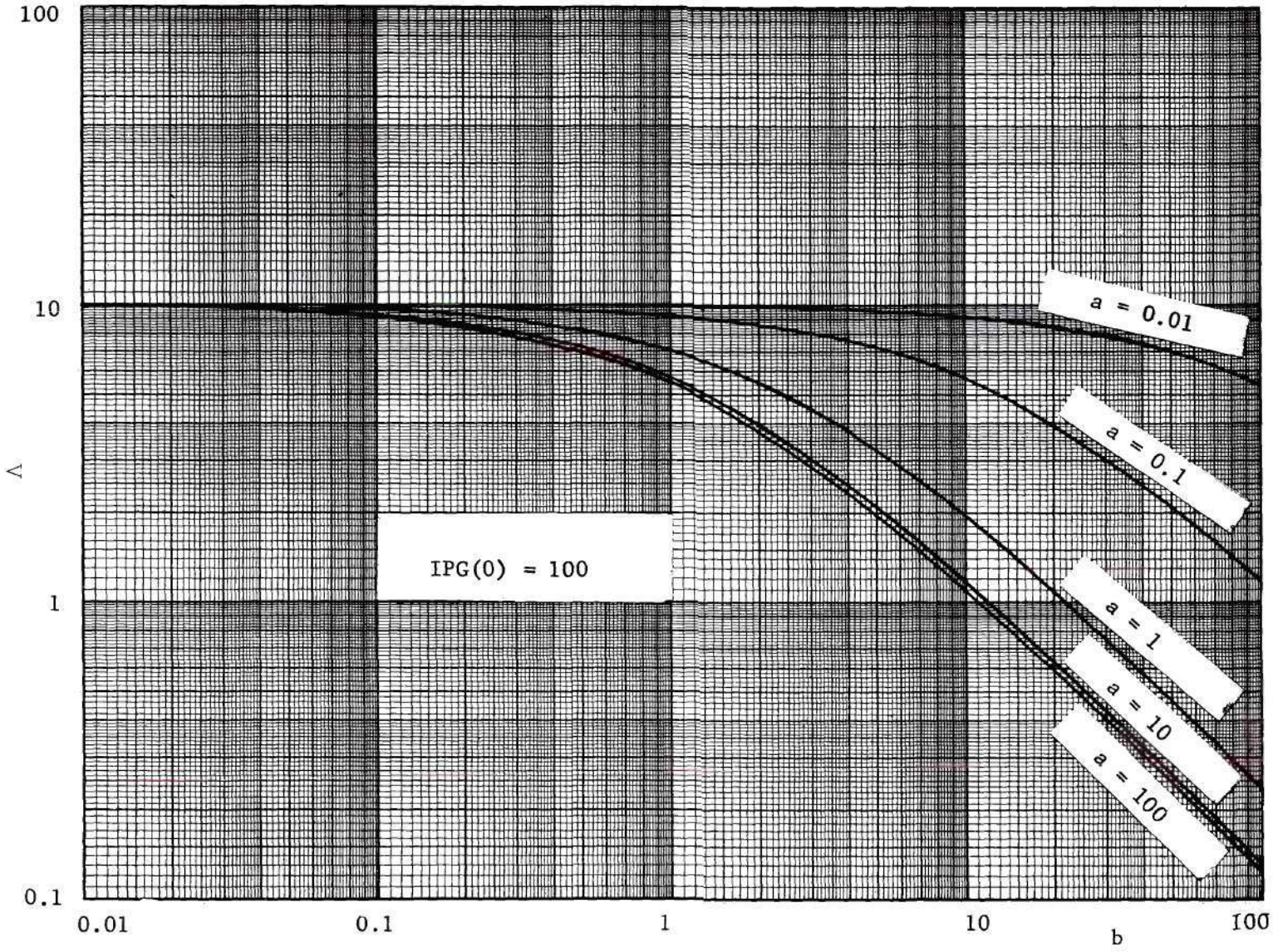

Figure F.9 Percent Stability Margin vs. b for the Series Amplifier(s).

APPENDIX G

DESIGN CURVES FOR THE TRANSMISSION AMPLIFIERS

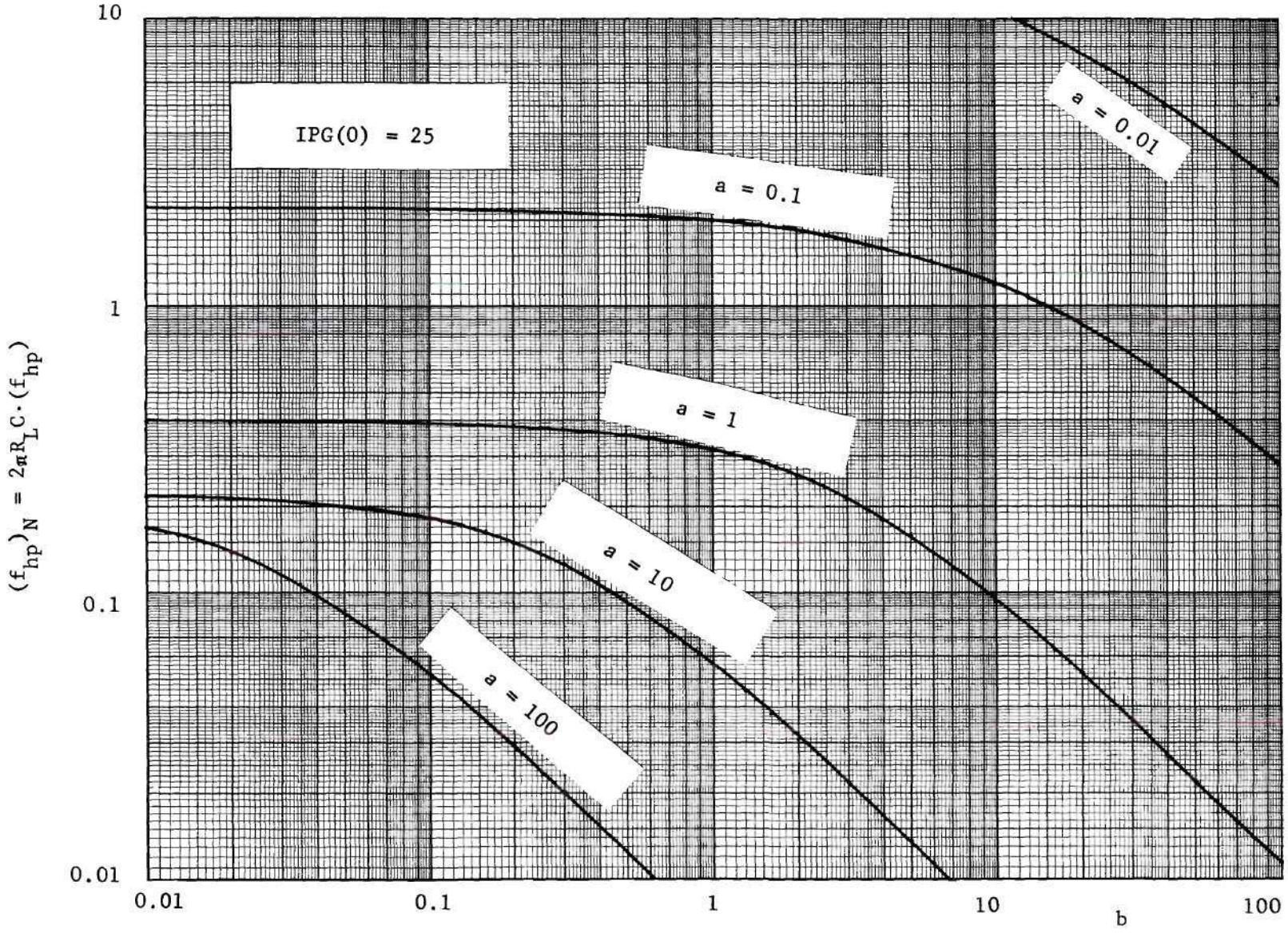

Figure G.1 Normalized Half-Power Frequency vs. b for the Transmission Amplifier(s).

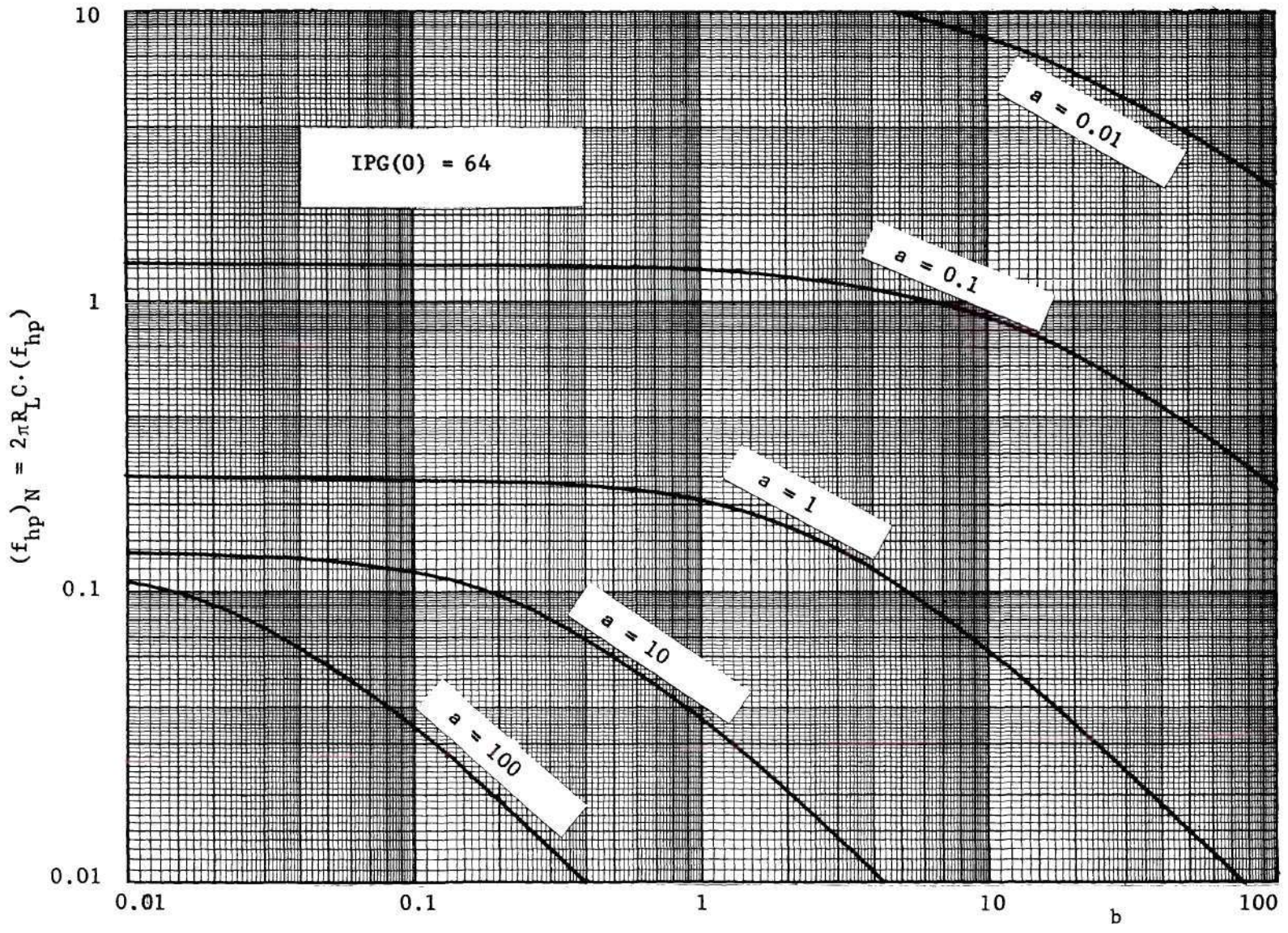

Figure G.2 Normalized Half-Power Frequency vs. b for the Transmission Amplifier(s).

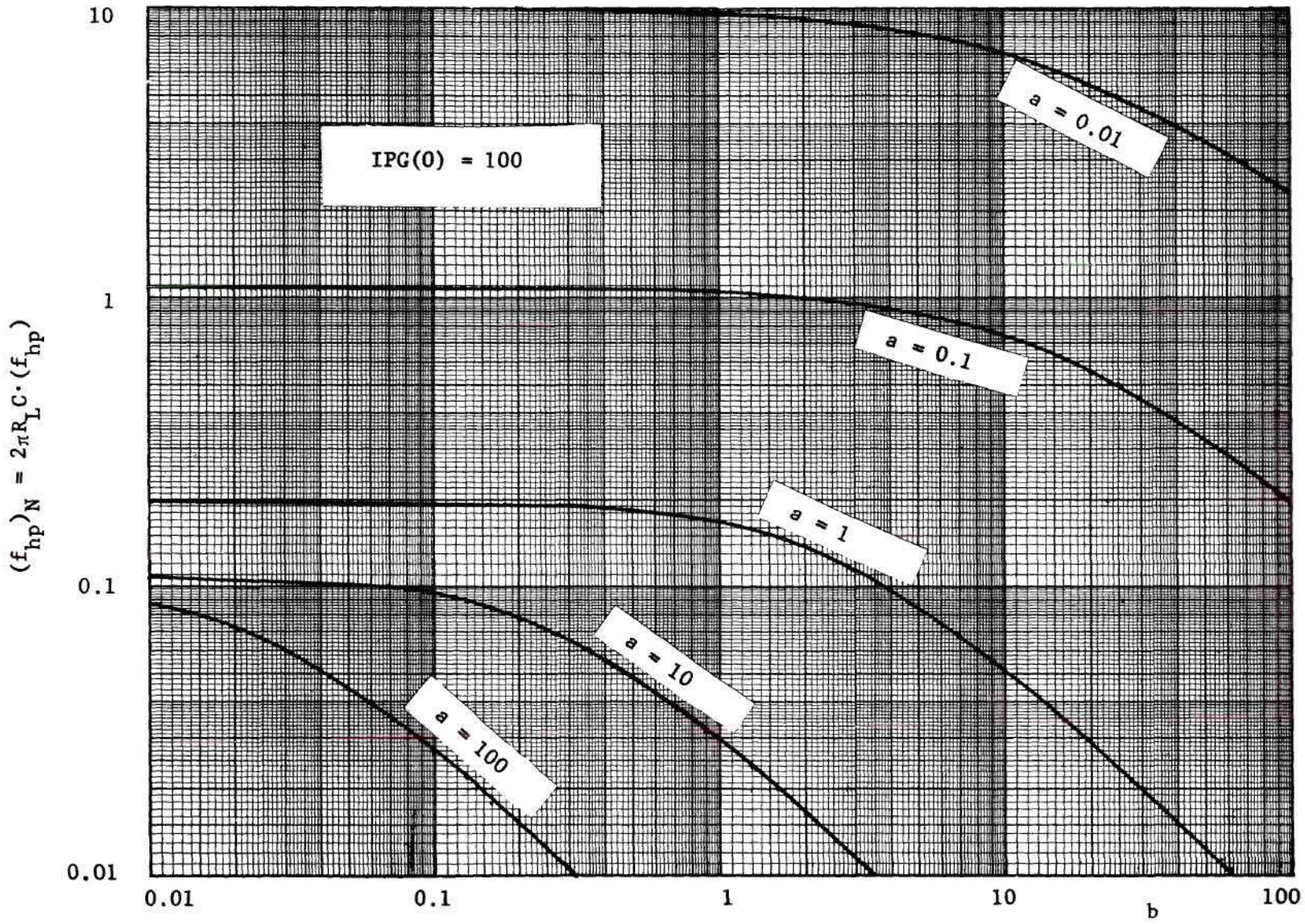

Figure G.3 Normalized Half-Power Frequency vs. b for the Transmission Amplifier(s).

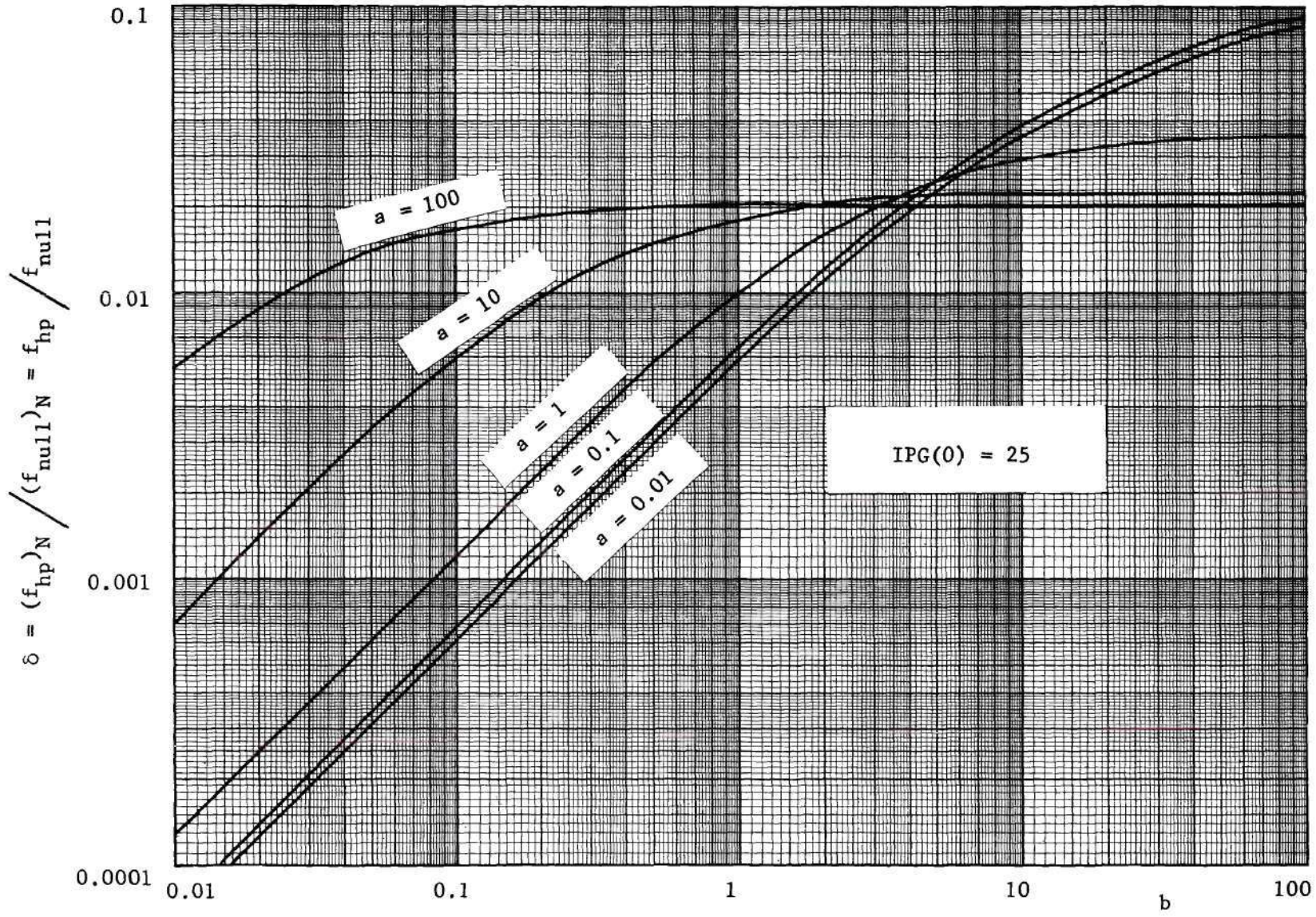

Figure G.4 Frequency Ratio vs. b for the Transmission Amplifier(s).

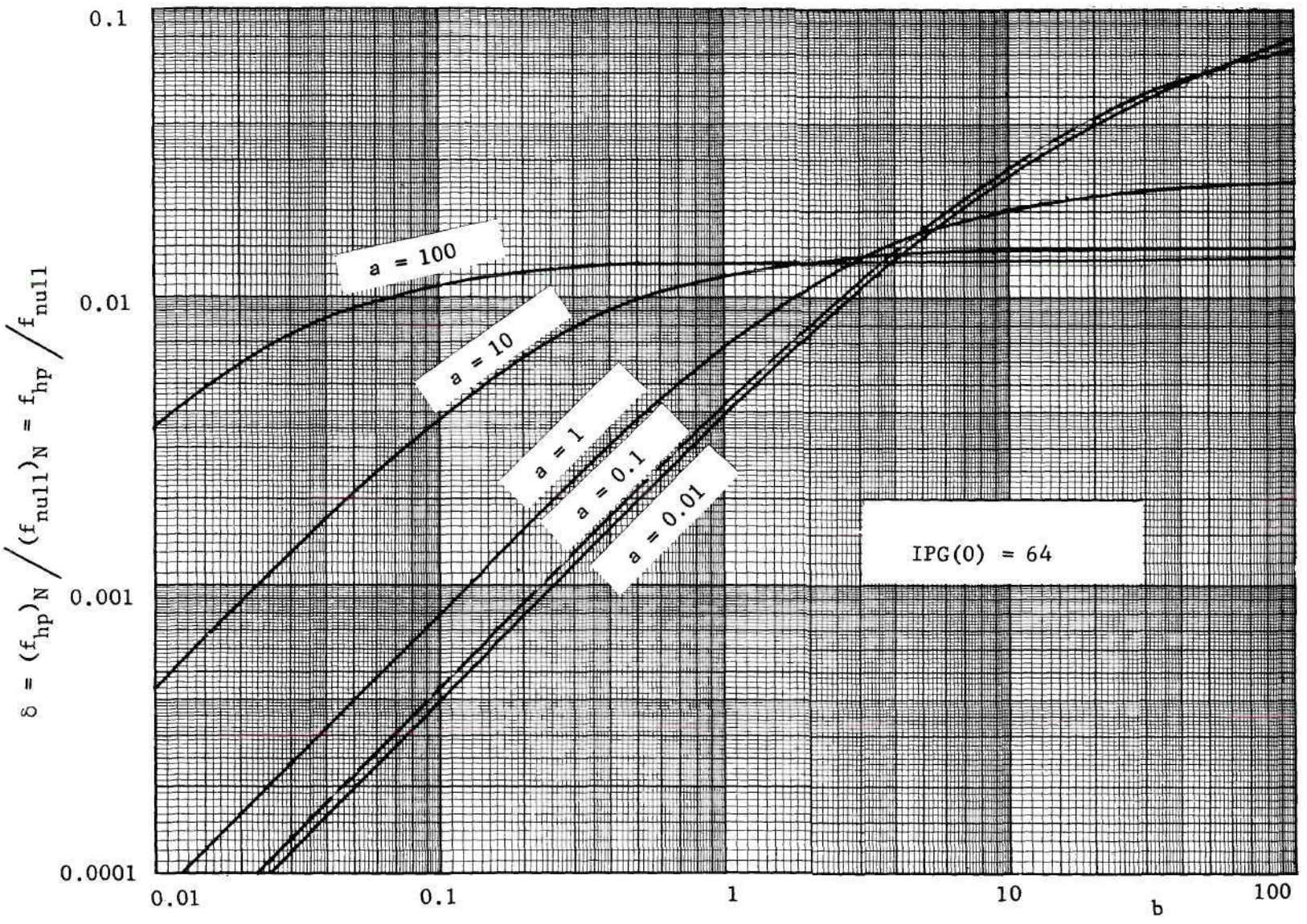

Figure G.5 Frequency Ratio vs. b for the Transmission Amplifier(s).

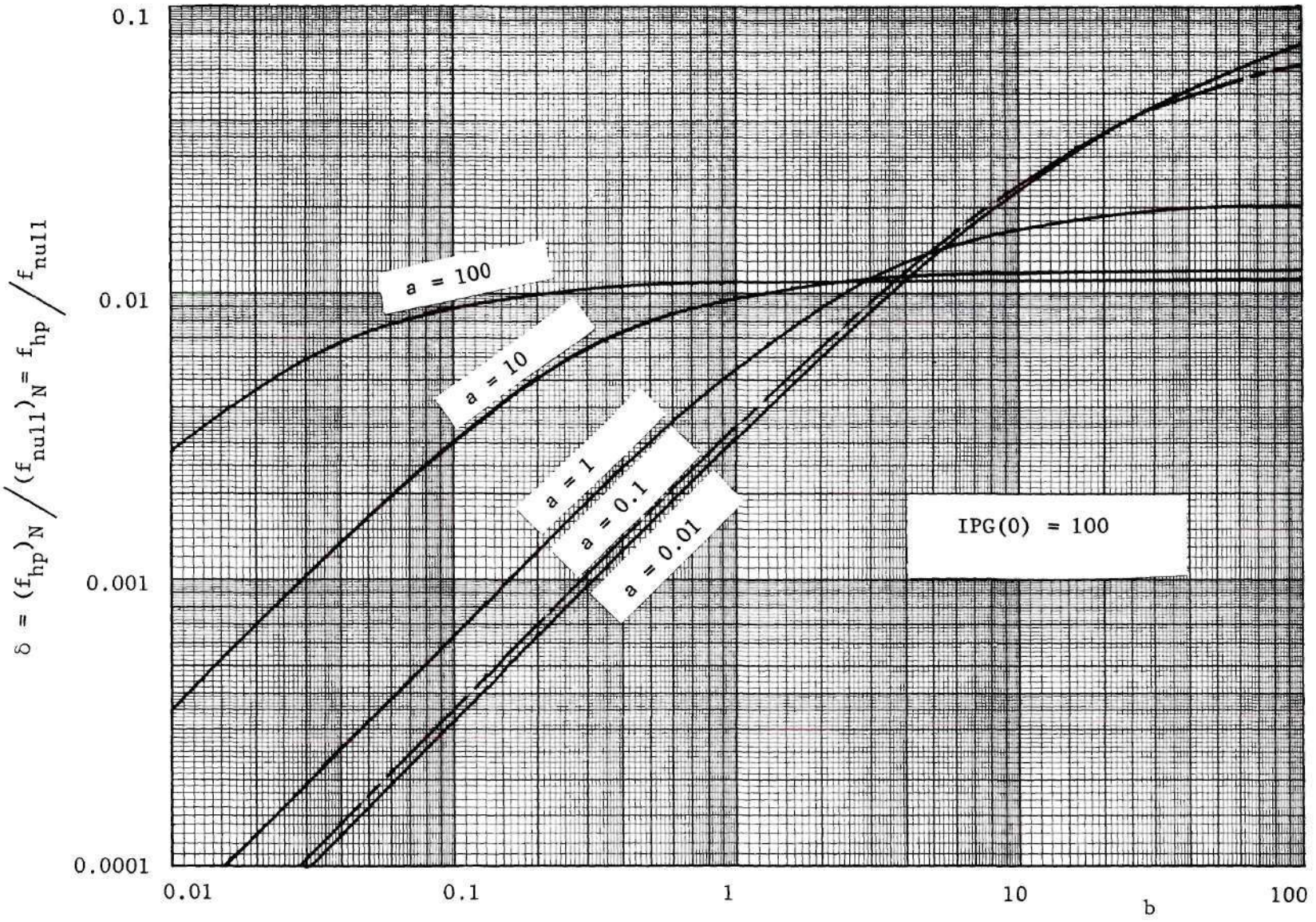

Figure G.6 Frequency Ratio vs. b for the Transmission Amplifier(s).

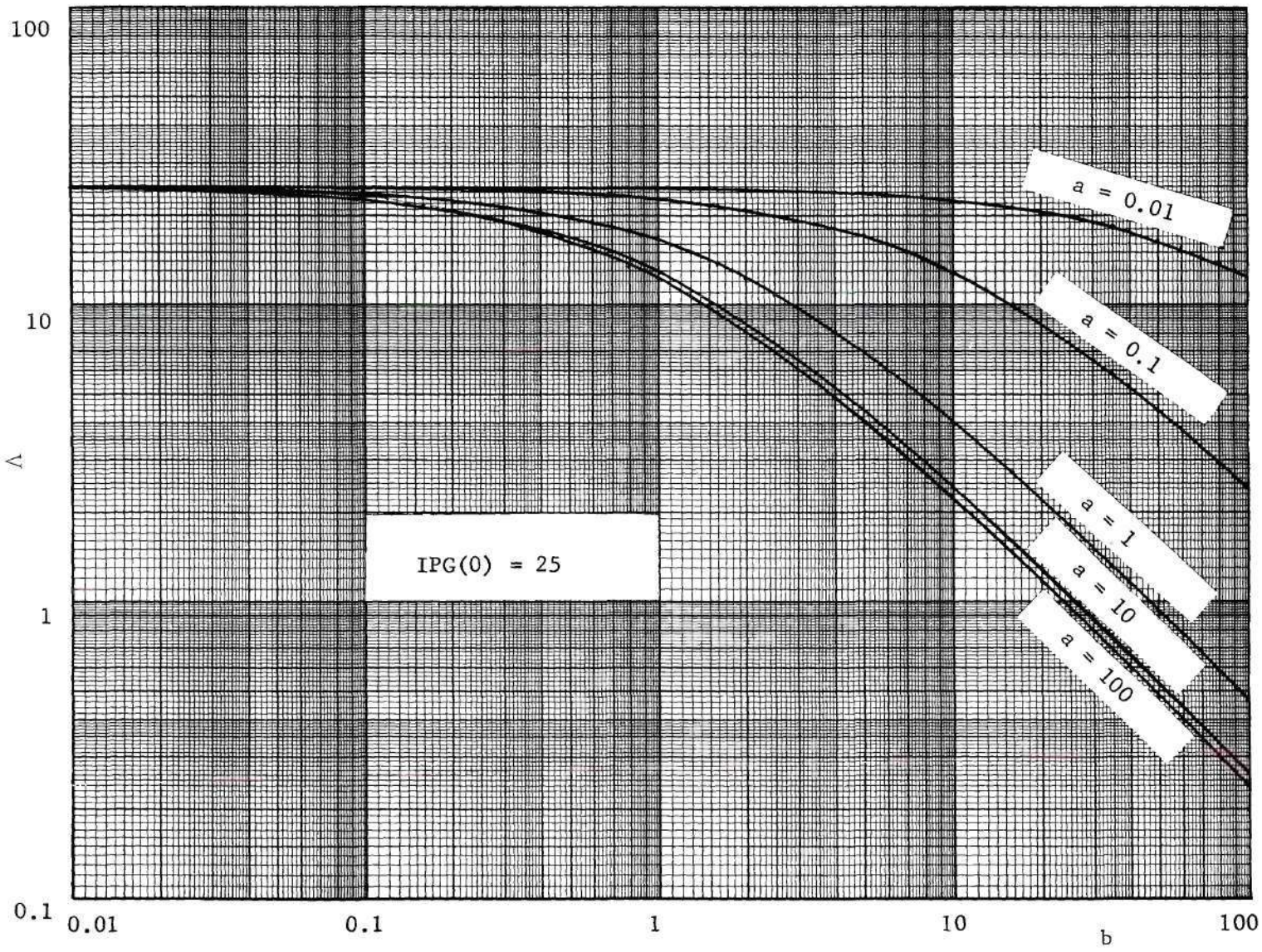

Figure G.7 Percent Stability Margin vs. b for the Transmission Amplifier(s).

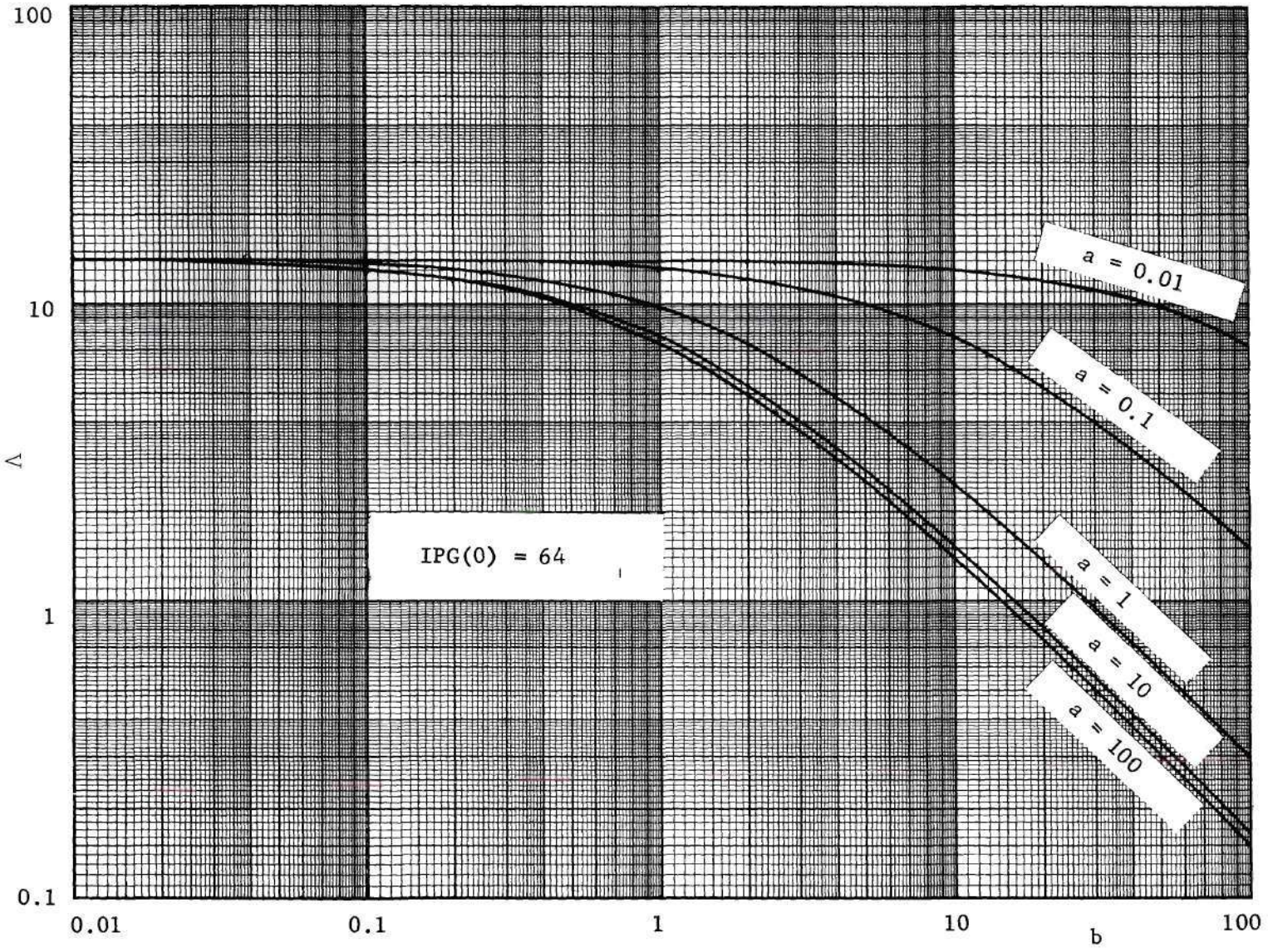

Figure G.8 Percent Stability Margin vs. b for the Transmission Amplifier(s).

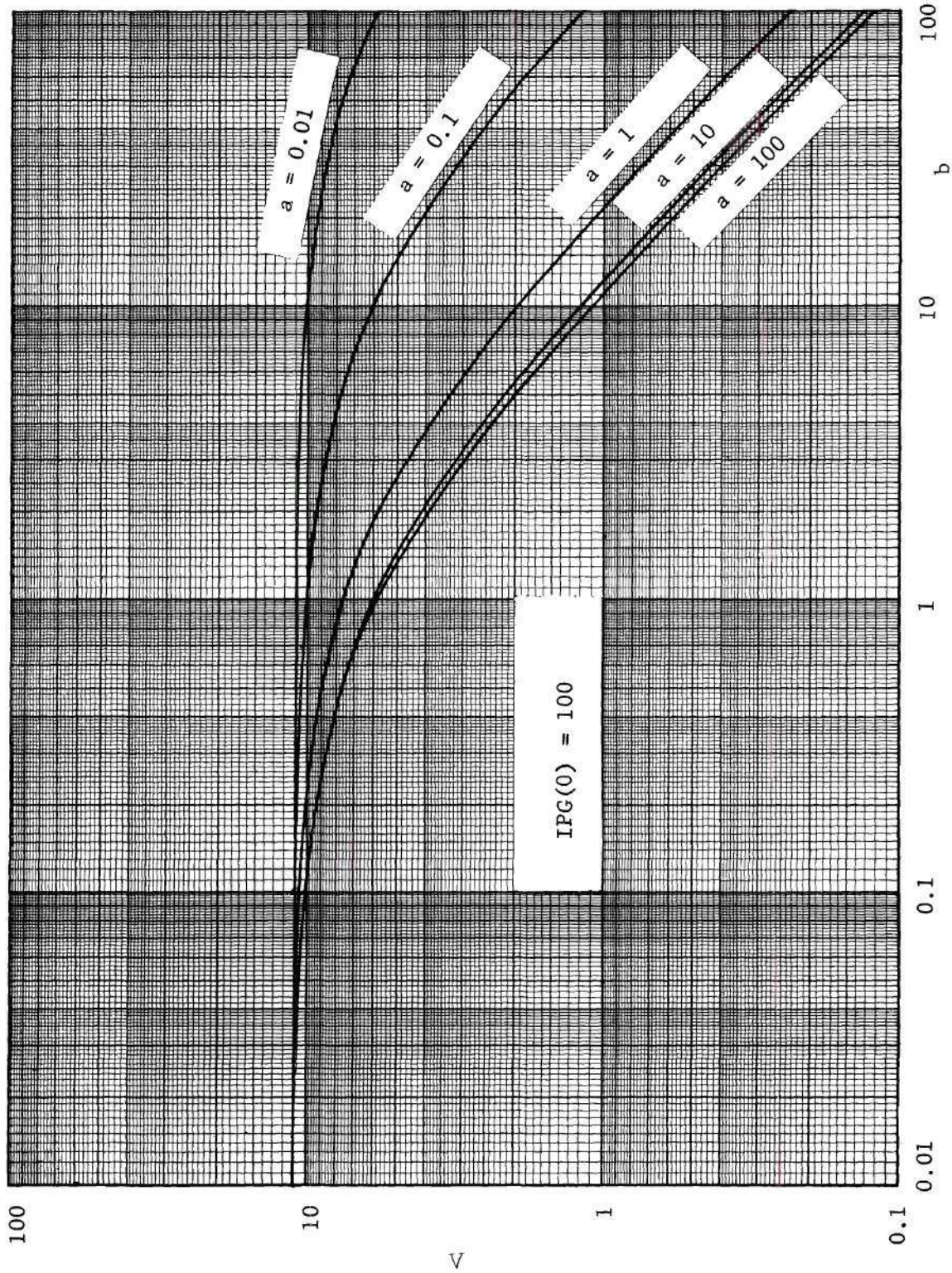

Figure G.9 Percent Stability Margin vs. b for the Transmission Amplifier(s).

BIBLIOGRAPHY

[1] Kaufman, W. M., "Theory of a Monolithic Null Device and Some Novel Circuits," Proceedings of the Institute of Radio Engineers, Vol. 48, No. 9, pp. 1540-1545, September 1960.

[2] Su, K. L., "The Trigonometric RC Transmission Lines," IEEE International Convention Record, Vol. 11, Part 2, pp. 43-55, 1963.

[3] Su, K. L., "Hyperbolic RC Transmission Lines," Electronics Letters, Vol. 1, pp. 59-60, May 1965.

[4] Googe, J. M., "The Analysis of the Double-Kelvin Transmission Line and Some Applications," Ph.D. Thesis, Georgia Institute of Technology, Atlanta, Georgia, February 1963.

[5] Chow, W. F., Principles of Tunnel Diode Circuits, John Wiley and Sons, Inc., New York, 1964.

[6] Mitra, S. K., "The Realizability of Tunnel-Diode-RC Networks," Journal of the Franklin Institute, Vol. 275, No. 3, March 1963.

[7] Ibid.

[8] Smilen, L. I. and D. C. Youla, "Optimum Negative-Resistance Amplifiers," Symposium on Active Networks and Feedback Systems, Polytechnic Institute of Brooklyn, April 19-21, 1960.

[9] Wyndrum, R. W., "The Exact Synthesis of Distributed RC Networks," Technical Report 400-76, School of Electrical Engineering, New York University, New York, May 1963.

[10] Holland, L., Thin Film Microelectronics, John Wiley and Sons, Inc., New York, 1965.

[11] Ibid.

[12] Ibid.

[13] Mitra, op. cit.

[14] Widder, D. V., Advanced Calculus, 2nd Ed., Prentice-Hall, Englewood Cliffs, New Jersey, July 1964.

VITA

Robert David Shults was born in Atlanta, Georgia, on November 23, 1937. He is the son of Wilbur Dotry Shults and Eva Katherine Jones Shults. He is married to the former Maxine Ann Sneider of Atlanta, Georgia, and has one child.

He attended grammar schools in Greenville, South Carolina, and Atlanta, Georgia, and graduated from Roosevelt High School of Atlanta, Georgia, in 1955. In 1960 and 1963, he received the B.E.E. and M.S.E.E. degrees, respectively, from the Georgia Institute of Technology, and in 1964 was given the M. A. Ferst Award by the Georgia Tech Chapter of Sigma Xi for his Master's thesis research.

From September, 1961, to August, 1963, he was an Instructor in the School of Electrical Engineering at Georgia Tech, and from September, 1963, to December, 1964, he held a NASA Traineeship. In January, 1965, he rejoined the staff of the School of Electrical Engineering as a Graduate Research/Teaching Assistant, and from September, 1966, to June, 1967, he held the position of Instructor in the School of Electrical Engineering. He is presently employed by the Research Division of Scientific-Atlanta, Inc.